ERDC/EL TR-08-10

US Army Corps
of Engineers®
Engineer Research and
Development Center

System-Wide Water Resources Program

Use of Coupled Eutrophication and Network Models for Examination of Fisheries and Eutrophication Processes

Carl F. Cerco and Dorothy H. Tillman

March 2008

Environmental Laboratory

System-Wide Water Resources Program

ERDC/EL TR-08-10
March 2008

Use of Coupled Eutrophication and Network Models for Examination of Fisheries and Eutrophication Processes

Carl F. Cerco and Dorothy H. Tillman

Environmental Laboratory
U.S. Army Engineer Research and Development Center
3909 Halls Ferry Road
Vicksburg, MS 39180-6199

Prepared for U.S. Army Corps of Engineers
Washington, DC 20314-1000

Under System-Wide Water Resources Program

Abstract: The Corps of Engineers Integrated Compartment Water Quality Model (CE-QUAL-ICM or simply ICM) was designed to be a flexible, widely applicable eutrophication model. Ecopath with Ecosim (EWE) is a freely distributed network model supported by the Fisheries Centre, University of British Columbia. This study aimed to develop a coupling between the two models so that they could be used, in combination, to address management questions concerning the effects of nutrient load reductions on fisheries and the effects of fisheries management on primary producers. Specific objectives included: 1) comparing ICM and Ecopath representations of contemporary conditions in three regions of Chesapeake Bay; 2) comparing ICM and Ecopath representations of conditions in mid Chesapeake Bay following nutrient load reductions to levels consistent with the 1950s; and 3) comparing ICM and Ecopath representations of conditions in three regions of Chesapeake Bay resulting from increased grazing on phytoplankton by menhaden. Corresponding quantities in the two models were identified, and an ICM postprocessor was developed to facilitate the exchange of information between the two models. Significant differences were noted between the two model representations of contemporary primary production, benthic invertebrate biomass, and sediment-water organic carbon exchange. Substitution of ICM computed primary production from a 90% nutrient reduction scenario, intended to simulate loads in the 1950s, into Ecopath indicated that some higher trophic level groups (i.e., blue crab, white perch, spot, croaker, hogchoker, and catfish) cannot be supported without adjustments to their prey biomasses and diet compositions. Results of a similar procedure, intended to simulate enhanced menhaden grazing, did not require a reduction in biomasses of higher trophic levels.

Contents

Figures and Tables

Figures

Tables

Preface

This report was prepared by Dr. Carl F. Cerco and Dorothy H. Tillman, Water Quality and Contaminant Modeling Branch (WQCMB), Environmental Laboratory (EL), U.S. Army Engineer Research and Development Center (ERDC), Vicksburg, MS.

Funding was provided by the System-Wide Water Resources Program (SWWRP) under the Ecological Modeling Focus Area. For more information on SWWRP, please consult *https://swwrp.usace.army.mil/* or contact SWWRP Program Manager Dr. Steven L. Ashby at *Steven.L.Ashby@usace.army.mil*. This study was facilitated by Dr. Barry Payne, Aquatic Ecology and Endangered Species Branch, EL.

The report was prepared under the general supervision of Dr. Barry Bunch, Chief, WQCMB; Dr. Michael Passmore, Deputy Director, EL; and Dr. Beth Fleming, Director, EL.

The Commander and Executive Director of ERDC is COL Richard B. Jenkins. The Director is Dr. James R. Houston.

1 Introduction

The management of water quality is usually based on a "bottom up" approach. That is, nutrient loads are reduced with the intention of limiting the excess production of phytoplankton and associated effects (low dissolved oxygen, reduced water clarity, species shifts). Recent management developments focus on a "top down" approach. The "top down" approach is based on the premise that restoration of algal predators, such as oysters and menhaden, will limit excess phytoplankton production and, perhaps, substitute for costly nutrient control programs.

Guidance for nutrient control programs is frequently obtained from eutrophication models such as CE-QUAL-ICM (Cerco and Cole 1994). (No eutrophication models aimed at guiding "top down" management are readily available.) Eutrophication models provide temporal representations of carbon, nutrient, and oxygen cycling on a discrete spatial grid. These models usually represent the rate of primary production and/or phytoplankton biomass but extend no further to higher trophic levels. More complex eutrophication models incorporate organisms from higher trophic levels such as zooplankton or oysters, but the approach has its limits. The application of multiple interacting partial differential equations to describe the food web leads to numerical difficulties as well as model results that defy interpretation.

One approach to modeling the complex materials and/or energy transfers that describe interactions between higher trophic levels such as zooplankton, benthos, and fish is the network model. Network models provide complexity in representing the food web at the cost of simplicity in temporal and spatial resolution. At their basic level, they consider steady-state mass flows with little or no spatial resolution. They are equivalent to ledger sheets in which mass and/or energy flows must balance.

A combination of eutrophication and network models is required to address questions such as:

- How does management in a watershed affect fisheries harvest in adjacent water bodies?

- How does fisheries management affect water quality problems such as low dissolved oxygen?

No straightforward means of coupling the two modeling approaches is available or apparent. The present report describes the second year of a research effort to couple a spatially and temporally discrete eutrophication model with a steady-state, spatially uniform network model. The eutrophication model is CE-QUAL-ICM (Cerco and Noel 2004b). The network model is Ecopath with Ecosim, version 5 (Christensen et al. 2000).

CE-QUAL-ICM

The Corps of Engineers Integrated Compartment Water Quality Model (CE-QUAL-ICM or simply ICM) was designed to be a flexible, widely applicable eutrophication model. The version employed in the present effort (Cerco and Noel 2004b) was developed to guide the 2002 re-evaluation of nutrient control strategies for Chesapeake Bay. The model incorporates 24 state variables in the water column that form groups or cycles, including a physical group, phytoplankton and zooplankton groups, and carbon, nitrogen, phosphorus, silica, and oxygen cycles. Multiple living resource groups are incorporated as well, including benthic algae, submerged aquatic vegetation (SAV), and filter-feeding and deposit-feeding benthos.

Ecopath with Ecosim

Ecopath with Ecosim (EWE) is a freely distributed network model supported by the Fisheries Centre, University of British Columbia (Christensen et al. 2000). EWE includes both steady-state (Ecopath) and time-variable (Ecosim) components. The model was selected for use in this study because of its widespread employment in Chesapeake Bay and elsewhere. One existing application is of particular interest (Hagy 2002) and forms the basis for this study. Ecopath was employed to represent summer conditions for three regions of Chesapeake Bay characteristic of the period 1985–1999. The model was next used to illustrate conditions in the mid bay consistent with nutrient loads of the 1950s to early 1960s. The application incorporated 34 state variables, including various forms of detritus, bacteria, primary producers, zooplankton, fish, and benthic invertebrates.

Previous Results

The first year of this study (Tillman et al. 2006) was devoted to examining ICM and Ecopath and identifying commonalities or "hooks." Once identified, biomasses and rates common to the two models were compared using existing publications and software. Broadly speaking, biomasses represented in the water column by both models were comparable (within a factor of two). Larger differences were noted in other biomass components (e.g. SAV) and in some common rates (e.g. phytoplankton net production). An objective named for the second year of the study was to revisit the comparisons after developing appropriate algorithms and carefully accounting for spatial and temporal aggregation of ICM results.

Study Objectives

The study reported here had the following objectives:

- Compare ICM and Ecopath representations of contemporary conditions in three regions of Chesapeake Bay.
- Compare ICM and Ecopath representations of conditions in mid Chesapeake Bay following nutrient load reductions to levels consistent with the 1950s.
- Compare ICM and Ecopath representations of conditions in three regions of Chesapeake Bay resulting from increased grazing on phytoplankton by menhaden.

To accomplish these objectives, specific ICM algorithms and postprocessors were developed and are described here.

2 ICM Fundamentals

Major Components of the ICM Carbon Cycle

At present, the CE-QUAL-ICM model incorporates 24 state variables in the water column, including physical variables, multiple algal groups, two zooplankton groups, and multiple forms of carbon, nitrogen, phosphorus, and silica (Table 1). Correspondence between CE-QUAL-ICM and Ecopath is limited to elements of the ICM carbon cycle, since Ecopath, as implemented, is a carbon-based model. The original ICM formulation included representations of carbon cycling in the water column (Cerco and Cole 1994) and of carbon diagenesis in benthic sediments (DiToro and Fitzpatrick 1993). Net settling from water to sediments linked the carbon components of the two representations. As the model developed, modules were added to simulate submerged aquatic vegetation (SAV), benthic algae, and benthic invertebrates. Various processes linked the new modules to the original two (Figure 1). SAV leaf mortality contributed carbon to the water column, while root mortality contributed carbon to the sediments. Carbonaceous products produced by benthic algal mortality were routed to the sediments. Filter-feeding benthos grazed carbon from the water column and deposited carbon to the sediments as feces and as byproducts from predation. Deposit-feeding benthos consumed sediment carbon and returned unassimilated material and byproducts from predation.

Table 1. Water quality model state variables.

Temperature	Salinity
Fixed Solids	Freshwater Cyanobacteria
Spring Diatoms	Other (Green) Algae
Microzooplankton	Mesozooplankton
Dissolved Organic Carbon	Labile Particulate Organic Carbon
Refractory Particulate Organic Carbon	Ammonium
Nitrate+Nitrite	Dissolved Organic Nitrogen
Labile Particulate Organic Nitrogen	Refractory Particulate Organic Nitrogen
Total Phosphate	Dissolved Organic Phosphorus
Labile Particulate Organic Phosphorus	Refractory Particulate Organic Phosphorus
Chemical Oxygen Demand	Dissolved Oxygen
Dissolved Silica	Particulate Biogenic Silica

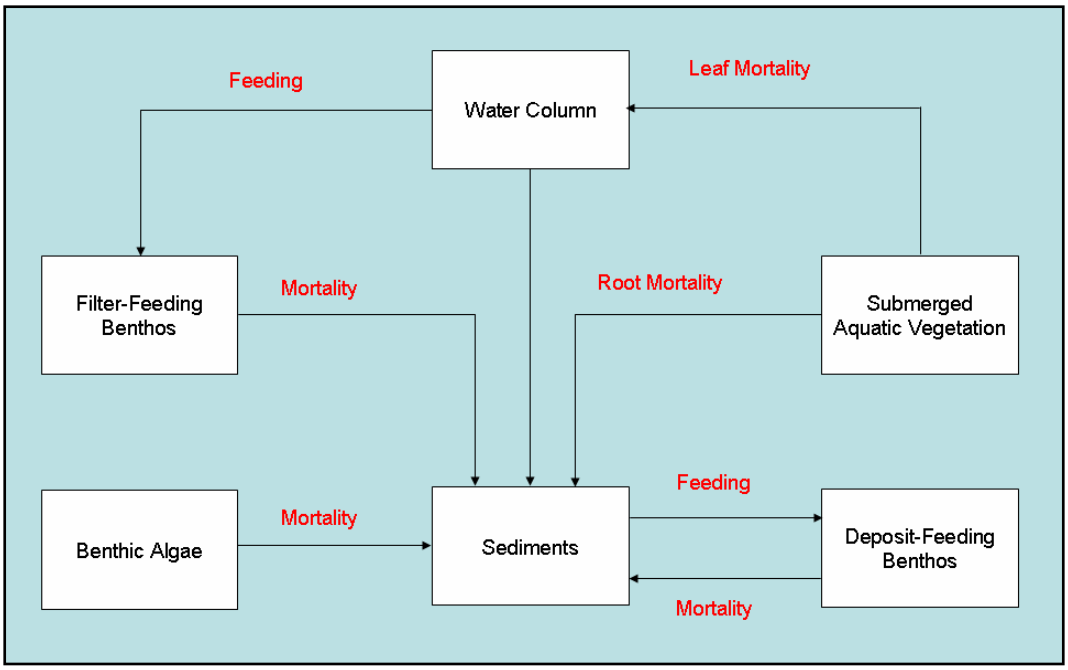

Figure 1. Major components of the ICM carbon cycle.

Conservation of Mass Equation

The CE-QUAL-ICM representation of the water column is based on the three-dimensional mass-conservation equation for a control volume. Control volumes correspond to discrete cells on a model computational grid. CE-QUAL-ICM solves, for each volume and for each state variable, the equation:

$$\frac{\delta V_j \times C_j}{\delta t} = \sum_{k=1}^{n} Q_k \times C_k + \sum_{k=1}^{n} A_k \times D_k \times \frac{\delta C}{\delta x_k} + \Sigma S_j \qquad (1)$$

in which:

V_j = volume of j^{th} control volume (m^3)
C_j = concentration in j^{th} control volume (g m^{-3})
t, x = temporal and spatial coordinates
n = number of flow faces attached to j^{th} control volume
Q_k = volumetric flow across flow face k of j^{th} control volume (m^3 s^{-1})
C_k = concentration in flow across face k (g m^{-3})
A_k = area of flow face k (m^2)
D_k = diffusion coefficient at flow face k (m^2 s^{-1})
S_j = external loads and kinetic sources and sinks in j^{th} control volume (g s^{-1}).

Solution of Equation 1 on a computer requires discretization of the continuous derivatives and specification of parameter values. The equation is solved using the QUICKEST algorithm (Leonard 1979) in the horizontal plane and a Crank-Nicolson scheme in the vertical direction. Discrete time steps, determined by computational stability requirements, are approximately 15 minutes.

Water Column State Variables

Algae

Algae are grouped into three model classes: cyanobacteria, spring diatoms, and other green algae. The grouping is based on the distinctive characteristics of each class and on the significant role they play in the ecosystem. The cyanobacteria distinguished in the model are the bloom-forming species found in the tidal, freshwater Potomac River. They are characterized as having negligible settling velocity and are subject to low predation pressure. Spring diatoms are large phytoplankton that produce an annual bloom in the saline portions of the bay and tributaries. Diatoms are distinguished by their requirement of silica as a nutrient to form cell walls. Algae that do not fall into the preceding two groups are lumped into the heading of green algae. These green algae represent the mixture that characterizes saline waters during summer and autumn and fresh waters year round. Non-bloom-forming diatoms comprise a portion of this mixture.

Zooplankton

Two zooplankton groups are considered: microzooplankton and mesozooplankton. The microzooplankton can be important predators on phytoplankton, and they are one of the prey groups for mesozooplankton. Mesozooplankton consume phytoplankton and detritus as well as microzooplankton. The mesozooplankton are an important prey resource for carnivorous finfish such as bay anchovies. Zooplankton were included in the model as a first step towards computing the effect of eutrophication management on top-level predators.

Organic Carbon

Three organic carbon state variables are considered: dissolved, labile particulate, and refractory particulate. Labile and refractory distinctions are based on the time scale of decomposition. Labile organic carbon

decomposes on a time scale of days to weeks, while refractory organic carbon requires more time. Labile organic carbon decomposes rapidly in the water column or the sediments. Refractory organic carbon decomposes slowly, primarily in the sediments, and may contribute to sediment oxygen demand years after deposition.

Nitrogen

Nitrogen is first divided into available and unavailable fractions. Available refers to its role in algal nutrition. Two available forms are considered: reduced and oxidized nitrogen. Reduced nitrogen is represented as ammonium, while nitrate and nitrite comprise the oxidized nitrogen pool. Both reduced and oxidized nitrogen are utilized to fulfill algal nutrient requirements. The primary reason for distinguishing the two is that ammonium is oxidized by nitrifying bacteria into nitrite and, subsequently, nitrate. This oxidation can be a significant sink of oxygen in the water column and sediments. Unavailable nitrogen state variables are dissolved organic nitrogen, labile particulate organic nitrogen, and refractory particulate organic nitrogen.

Phosphorus

As with nitrogen, phosphorus is first divided into available and unavailable fractions. Dissolved phosphate is the single available form. Three forms of unavailable phosphorus are considered: dissolved organic phosphorus, labile particulate organic phosphorus, and refractory particulate organic phosphorus.

Silica

Silica is divided into two state variables: dissolved silica and particulate biogenic silica. Dissolved silica is available to diatoms, while particulate biogenic silica cannot be utilized. In the model, particulate biogenic silica is produced through diatom mortality. Particulate biogenic silica undergoes dissolution to available silica or else settles to the bottom sediments.

Chemical Oxygen Demand

Chemical oxygen demand quantifies reduced substances that are oxidized by abiotic processes. The primary component of chemical oxygen demand

is sulfide released from sediments. Oxidation of sulfide to sulfate may remove substantial quantities of dissolved oxygen from the water column.

Dissolved Oxygen

Dissolved oxygen is required for the existence of higher life forms. Oxygen availability determines the distribution of organisms and the flows of energy and nutrients in an ecosystem. Dissolved oxygen is a central component of the water-quality model.

Salinity

Salinity is a conservative tracer that provides verification of the transport component of the model and facilitates examination of conservation of mass. Salinity also influences the dissolved oxygen saturation concentration and may be used in the determination of kinetics constants that differ in saline and fresh water.

Temperature

Temperature is a primary determinant of the rate of biochemical reactions. Reaction rates increase as a function of temperature, although extreme temperatures may result in the mortality of organisms and a decrease in kinetics rates.

Fixed Solids

Fixed solids are the mineral fraction of total suspended solids. Solids are considered primarily for their role in light attenuation.

The Water-Column Carbon Cycle

The principal components of the model carbon cycle (Figure 2) include:

- Phytoplankton production and excretion
- Zooplankton production and excretion
- Predation on phytoplankton
- Dissolution of particulate carbon
- Heterotrophic respiration
- Settling.

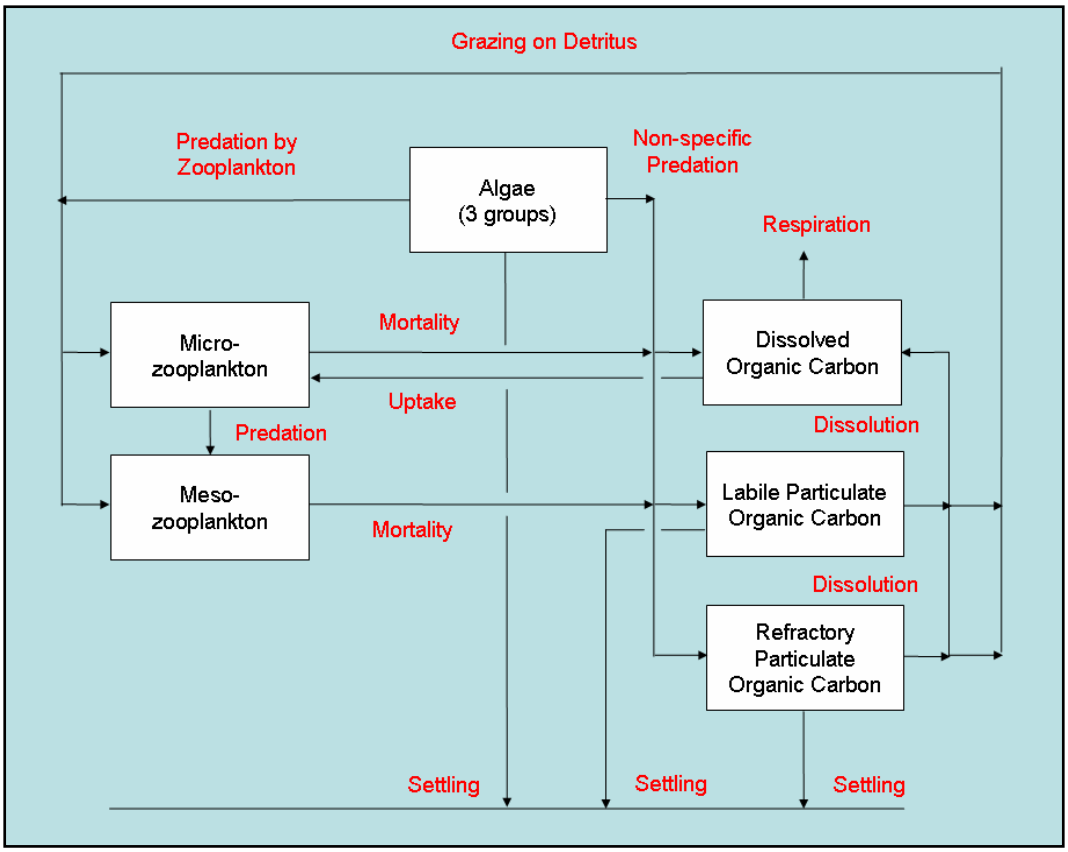

Figure 2. Water-column carbon cycle.

Algal production is the primary carbon source, although carbon also enters the system through external loading and SAV mortality. Predation on algae by zooplankton and other organisms releases particulate and dissolved organic carbon to the water column. A fraction of the particulate organic carbon undergoes first-order dissolution to dissolved organic carbon. Dissolved organic carbon produced by excretion, by predation, and by dissolution is respired at a first-order rate to inorganic carbon. Particulate organic carbon that does not undergo dissolution settles to the bottom sediments.

Algae

Algal sources and sinks in the conservation equation include production, metabolism, predation, and settling. These are expressed by:

$$\frac{\delta}{\delta t} B = \left(G - BM - Wa \times \frac{\delta}{\delta z} \right) B - PR \qquad (2)$$

in which:

B = algal biomass, expressed as carbon (g C m^{-3})
G = growth (d^{-1})
BM = basal metabolism (d^{-1})
Wa = algal settling velocity (m d^{-1})
PR = predation (g C m^{-3} d^{-1})
z = vertical coordinate.

The growth and metabolism functions are described in Cerco and Noel (2004b). The predation term is made up of four components:

- Microzooplankton
- Mesozooplankton
- Filter-feeding benthos
- Other planktivores.

Zooplankton grazing terms are detailed below. Predation by benthos is represented as a loss term in model cells that intersect the bottom. Predation by other planktivores is modeled by assuming that predators clear a specific volume of water per unit biomass:

$$PR = F \times B \times M \tag{3}$$

in which:

F = filtration rate (m^3 g^{-1} predator C d^{-1})
M = planktivore biomass (g C m^{-3}).

Detailed specification of the spatial and temporal distribution of the predator population is impossible. One approach is to assume that predator biomass is proportional to algal biomass, $M = \gamma B$, in which case Equation 3 can be rewritten:

$$PR = \gamma \times F \times B^2 . \tag{4}$$

Since neither γ nor F is known precisely, their product is combined into a single unknown, *Phtl*, determined during the model calibration procedure.

Zooplankton

Each zooplankton group is represented by an identical production equation:

$$\frac{\delta}{\delta t} Z = \left(Gz - BMz - Mz\right) \times Z - PRz \tag{5}$$

in which:

Z = zooplankton biomass (g C m^{-3})
Gz = growth rate of zooplankton group z (d^{-1})
BMz = basal metabolic rate of zooplankton group z (d^{-1})
Mz = mortality (d^{-1})
PRz = predation on zooplankton group z (g C m^{-3} d^{-1}).

The two groups are distinguished by parameter values and by prey composition. Details of individual terms in the production equation may be found in Cerco and Noel (2004b). Prey composition and selection are relevant to the Ecopath linkage and are detailed below.

Prey Composition and Selection

Grazing is represented by a maximum ration formulation equivalent to the familiar Monod formulation used to represent algal nutrient uptake:

$$Gz = \frac{PAz}{KHCz + PAz} \times RMAXz \tag{6}$$

Gz = carbon grazed by zooplankton group z (g prey C g^{-1} zooplankton C d^{-1})
PAz = prey available to zooplankton group z (g C m^{-3})
$KHCz$ = prey density at which grazing is halved (g C m^{-3})
$RMAXz$ = maximum ration of zooplankton group z (g prey C g^{-1} zooplankton C d^{-1}).

The computation of available prey incorporates two principles:

- A constant, between zero and unity, determines the utilization of a prey group by a predator.
- A threshold density exists below which prey is not utilized.

The available portion of an algal group, for example, is determined:

$$BAxz = Max(Bx - CTz) \tag{7}$$

in which:

$BAxz$ = portion of algal group x available to zooplankton group z (g C m^{-3})
CTz = threshold concentration below which prey will not be utilized by zooplankton group z (g C m^{-3}).

Heterotrophic bacteria form a major food source for microzooplankton. Since bacteria are not incorporated in ICM, microzooplankton are considered to graze on dissolved organic carbon, which is the primary food source for the bacteria. Three phytoplankton groups and organic detritus are the remaining food sources for modeled microzooplankton. Modeled mesozooplankton graze on three algal groups, microzooplankton, and organic detritus. The total prey available to each group is determined by "utilization" parameters, which are weighting terms that range between zero and unity. The prey available to microzooplankton, for example, is:

$$\begin{aligned} PAsz = {} & UDsz \times DOCAsz \\ & + \sum UBxsz \times BAxsz + ULsz \times LPOCAsz + URsz \times RPOCAsz \end{aligned} \tag{8}$$

in which:

$PAsz$ = prey available to microzooplankton (g C m^{-3})
$UDsz$ = utilization of dissolved organic carbon by microzooplankton
$UBxsz$ = utilization of algal group x by microzooplankton
$ULsz$ = utilization of labile particulate organic carbon by microzooplankton
$URsz$ = utilization of refractory particulate organic carbon by microzooplankton
$DOCAsz$ = dissolved organic carbon available to microzooplankton (g C m^{-3})
$BAxsz$ = algal group x available to microzooplankton (g C m^{-3})
$LPOCAsz$ = labile particulate organic carbon available to microzooplankton (g C m^{-3})
$RPOCAsz$ = refractory particulate organic carbon available to microzooplankton (g C m^{-3}).

The fraction of the total ration removed from each prey group is determined by the fraction of each utilizable prey group relative to the total utilizable prey.

Predation on Zooplankton

Micro and mesozooplankton are the highest trophic levels represented in the water column. Predation on both zooplankton groups by organisms not included in the model is represented by a quadratic term analogous to Equation 4.

Organic Carbon

Organic carbon dissolution and respiration are represented as first-order processes in which the reaction rate is proportional to the concentration of the reactant. An exponential function relates dissolution and respiration to temperature. A complete representation of dissolved organic carbon sources and sinks in the model ecosystem is:

$$\begin{aligned}\frac{\delta}{\delta t}\,DOC = {} & FCDa \times BMa \times B + FCDPa \times PRa \\ & + FCDz \times \left(BMz + Mz\right) \times Z + FCDPz \times Z \\ & + Klpoc \times LPOC + Krpoc \times RPOC - Kdoc \times DOC + S\end{aligned} \tag{9}$$

in which:

DOC = dissolved organic carbon (g m^{-3})
$LPOC$ = labile particulate organic carbon (g m^{-3})
$RPOC$ = refractory particulate organic carbon (g m^{-3})
$FCDa$ = fraction of algal respiration released as DOC ($0 < FCDa < 1$)
$FCDPa$ = fraction of predation on algae released as DOC ($0 < FCDPa < 1$)
$FCDz$ = fraction of zooplankton respiration released as DOC ($0 < FCDz < 1$)
$FCDPz$ = fraction of predation on zooplankton released as DOC ($0 < FCDPz < 1$)
$Klpoc$ = dissolution rate of $LPOC$ (d^{-1})
$Krpoc$ = dissolution rate of $RPOC$ (d^{-1})
$Kdoc$ = respiration rate of DOC (d^{-1})
S = loading from external sources (g $m^{-3}d^{-1}$).

The complete representation of labile particulate organic carbon sources and sinks in the model ecosystem is:

$$\frac{\delta}{\delta t} LPOC = FCLa \times BMa \times B + FCLPa \times PRa + FCLz \times \left(BMz + Mz\right) \times Z + FCLPz \times PRz - Klpoc \times LPOC - Wl \times \frac{\delta}{\delta z} LPOC + S \quad (10)$$

in which:

$FCLa$ = fraction of algal respiration released as $LPOC$ ($0 < FCLa < 1$)
$FCLPa$ = fraction of predation on algae released as $LPOC$ ($0 < FCLPa < 1$)
$FCLz$ = fraction of zooplankton respiration released as $LPOC$ ($0 < FCLz < 1$)
$FCLPz$ = fraction of predation on zooplankton released as $LPOC$ ($0 < FCLPz < 1$)
Wl = settling velocity of labile particles (m d^{-1}).

An analogous equation describes refractory particulate organic carbon.

Coupling with the Sediment Diagenesis Model

Benthic sediments are represented as two layers with a total depth of 10 cm (Figure 3). The upper layer, in contact with the water column, may be oxic or anoxic depending on the dissolved oxygen concentration in the water. The lower layer is permanently anoxic. The thickness of the upper layer is determined by the penetration of oxygen into the sediments. At its maximum thickness, the oxic layer depth is only a small fraction of the total.

The sediment model consists of three processes. The first is deposition of particulate organic matter from the water column to the sediments. Due to the negligible thickness of the upper layer, deposition proceeds from the water column directly to the lower, anoxic layer. Within the sediments, organic matter is subject to the second process, diagenesis (or decay). The third process is flux of substances produced by diagenesis to the upper sediment layer, to the water column, and to deep, inactive sediments.

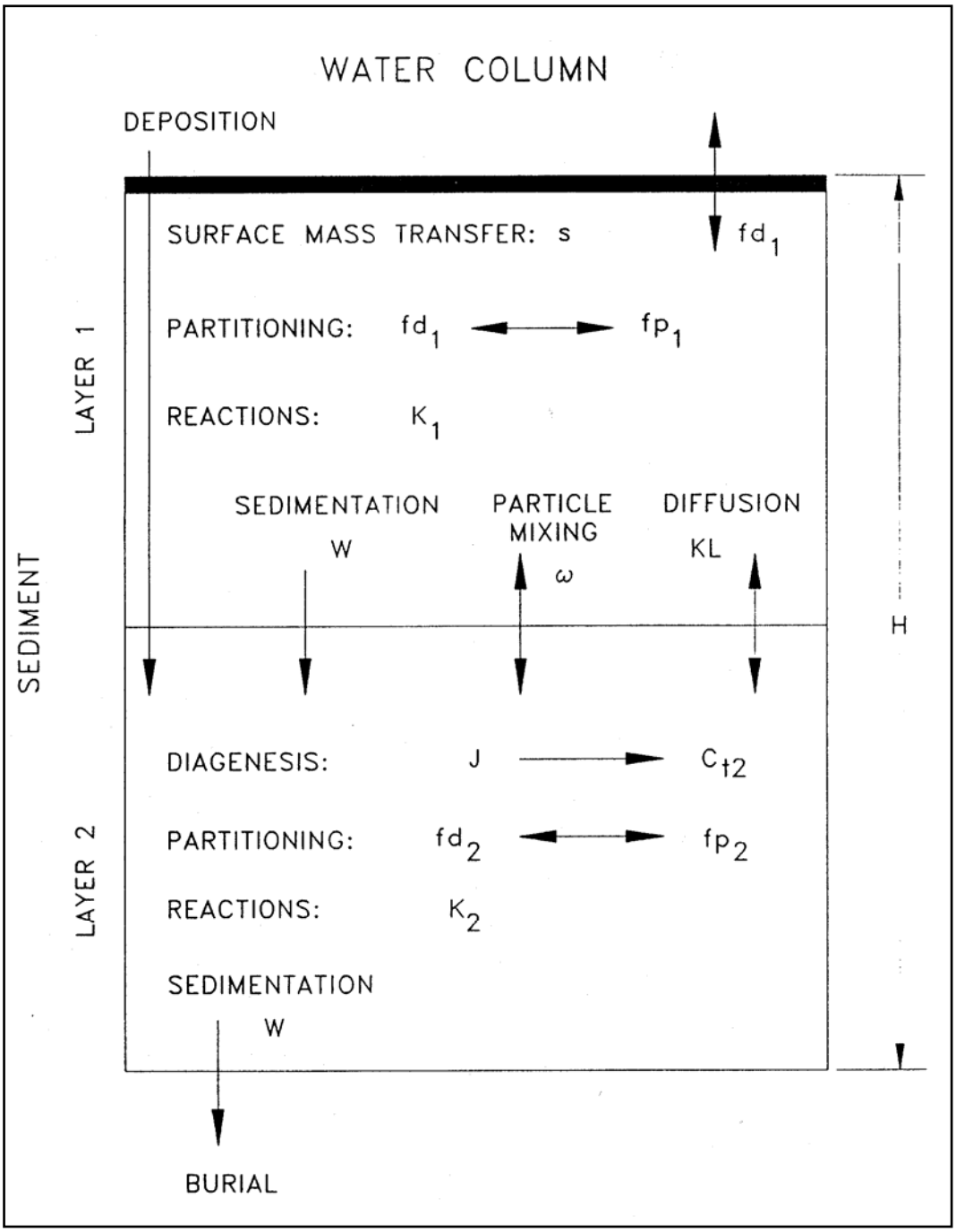

Figure 3. Schematic of the sediment diagenesis model.

Organic matter in the sediments is divided into three G classes or fractions, in accordance with principles established by Westrich and Berner (1984). Division into G classes accounts for differential decay rates of organic matter fractions. The G1, labile, fraction has a half-life of 20 days. The G2, refractory, fraction has a half-life of one year. The G3,

inert, fraction undergoes no significant decay before burial into deep, inactive sediments. Each G class has its own mass-conservation equation:

$$H \times \frac{\delta Gi}{\delta t} = W_{net} \times f_i \times C + S \times fi - W \times Gi - H \times K_i \times Gi \times \theta_i^{(T-20)} \quad (11)$$

in which:

H = total thickness of sediment layer (m)
Gi = concentration organic matter in G class i (g m^{-3})
$Wnet$ = net settling to sediments (m d^{-1})
C = organic matter concentration in water column (g m^{-3})
f_i = fraction of deposited organic matter assigned to G class i
S = local source from *SAV*, benthic algae, and benthos (g m^{-2} d^{-1})
W = burial rate (m d^{-1})
K_i = decay rate of G class i (d^{-1})
θ_i = constant that expresses effect of temperature on decay of G class i.

The sediment model simulates diagenesis of carbon, nitrogen, phosphorus, and silica. Only carbon diagenesis is relevant to the linkage with Ecopath. Details of remaining substances and processes are found in DiToro and Fitzpatrick (1993).

The Benthic Algae Model

Benthic algae are considered to occupy a thin layer between the water column and benthic sediments (Figure 4). Biomass within the layer is determined by the balance of production, respiration, and losses to predation:

$$\frac{\delta BA}{\delta t} = (G - BM) \times BA - PR \quad (12)$$

in which:

BA = algal biomass, as carbon (g C m^{-2})
G = growth (d^{-1})
BM = basal metabolism (d^{-1})
PR = predation (g C m^{-2} d^{-1}).

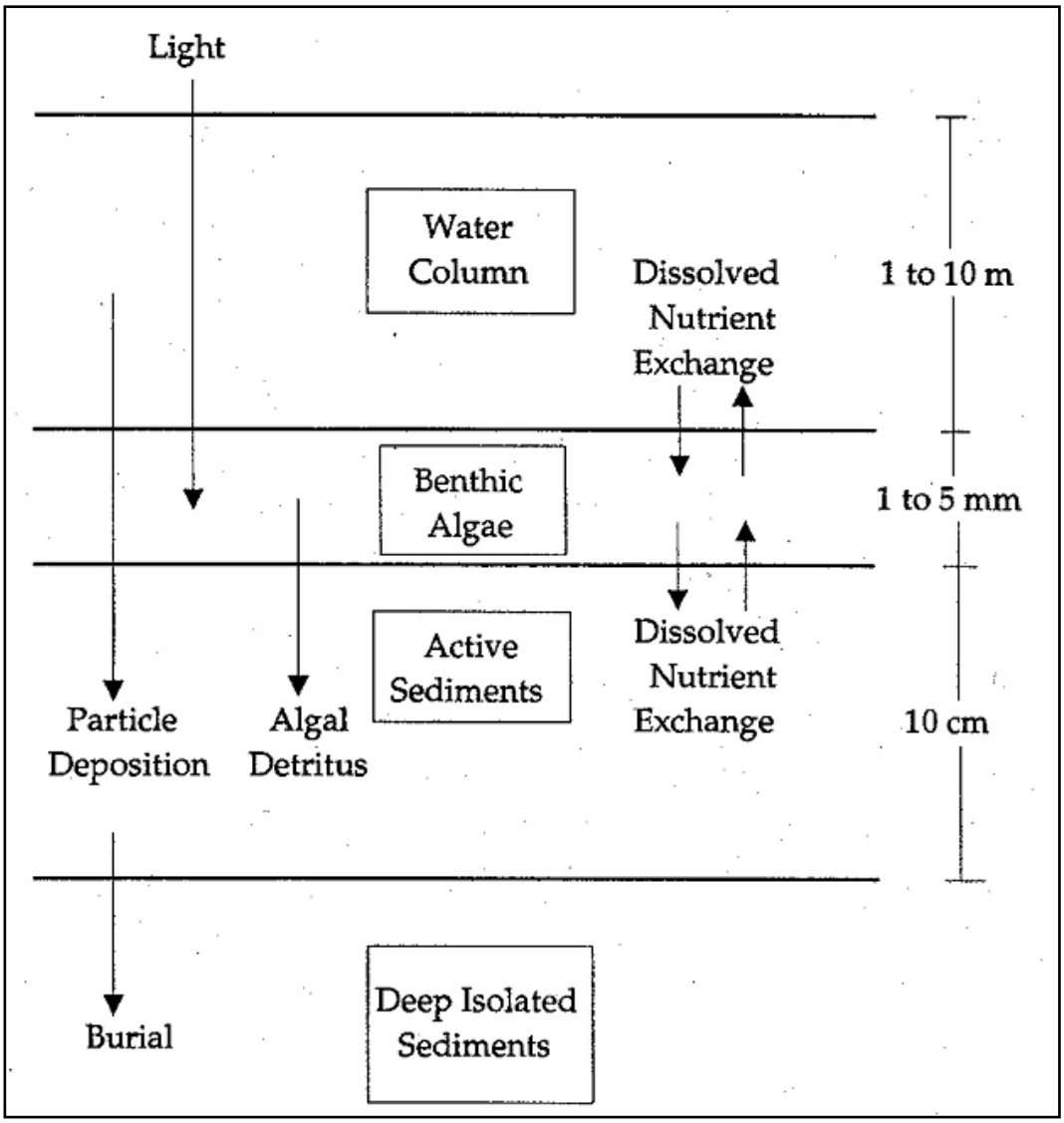

Figure 4. Schematic of benthic algae model.

Formulations for production, respiration, and predation largely follow the formulations for phytoplankton (Cerco and Noel 2004b). Carbonaceous byproducts from algal metabolism and predation are routed to the ICM sediment module.

Submerged Aquatic Vegetation

Three components are required to make up a system-wide SAV model. The first is a unit-level model of a plant. The second is an environmental model that provides light, temperature, nutrient concentrations, and other forcing functions to the plant component. The third is a coupling

algorithm that links the system-wide environmental model to the local-scale plant model.

The SAV unit model (Figure 5) incorporates three state variables: shoots (above-ground biomass), roots (below-ground biomass), and epiphytes (attached growth). Epiphytes and shoots exchange material with the water-column component of the eutrophication model, while roots exchange material with the diagenetic sediment component. Light available to the shoots and epiphytes is computed via a series of sequential attenuations by color, fixed and organic solids in the water column, and self-shading of shoots and epiphytes. Details of the model may be found in Cerco and Noel (2004b).

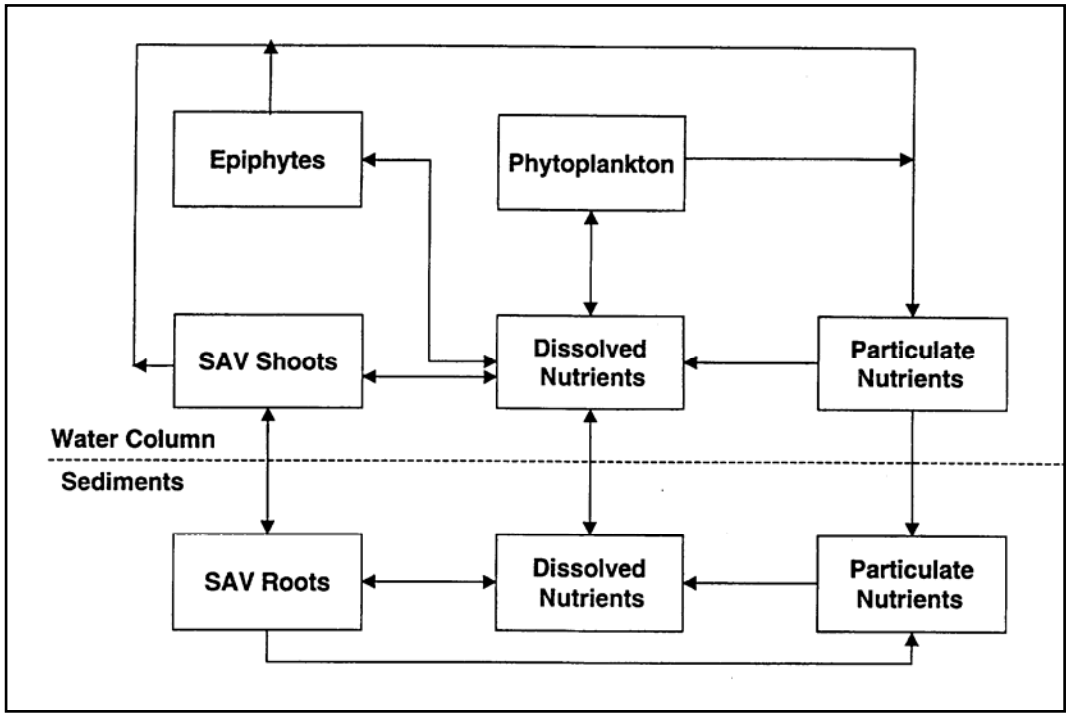

Figure 5. SAV model state variables (boxes) and mass flows (arrows).

Shoots

The governing equation for shoots establishes a balance between sources and sinks of above-ground biomass:

$$\frac{\mathrm{d}SH}{\mathrm{d}t} = \left[P \times (1 - Fpsr) - Rsh - SL\right] \times SH + Trs \times RT \qquad (13)$$

in which:

SH = shoot biomass (g C m^{-2})
P = production (d^{-1})
$Fpsr$ = fraction of production routed from shoot to root
Rsh = shoot respiration (d^{-1})
SL = sloughing (d^{-1})
Trs = rate at which carbon is transported from root to shoot (d^{-1})
RT = root biomass (g C m^{-2}).

Carbonaceous material lost through sloughing is routed to water column state variables via empirical distribution coefficients analogous to those employed to distribute planktonic material.

Roots

The governing equation for roots establishes a balance between sources and sinks of below-ground biomass:

$$\frac{\mathrm{d}RT}{\mathrm{d}t} = Fpsr \times P \times Sh - Rrt \times RT - Trs \times RT \tag{14}$$

in which:

Rrt = root respiration (d^{-1}).

Carbonaceous material lost through root respiration is routed to the model sediment component via empirical distribution coefficients. Epiphytes have a negligible role in the carbon cycle and are omitted from further consideration.

From the Unit to the System

The Chesapeake Bay Environmental Model Package (CBEMP) operates by dividing the continuum of the bay into a grid of discrete cells. For the SAV model, a ribbon of littoral cells was created along the land-water margin of the system. SAV was modeled in these littoral cells and in a few additional cells in regions that historically supported SAV. Littoral cells were represented as having a mean depth of 1 m.

The major problem in coupling the system-wide model with the unit model is the difference in scales represented by the two models. The minimum scale represented by the CBEMP is on the order of kilometers, while the scale on which SAV is distributed is orders of magnitude smaller. Three scaling factors were employed to relate biomass on the unit level to abundance on the grid scale. These were: truncation error, coverage, and patchiness (Figure 6). Truncation error relates the area of model cells to actual littoral zone area and is used in a model postprocessor to relate observed and computed abundance. Coverage is the fraction of a cell occupied by SAV beds, and patchiness represents the fraction of bottom area covered by plants within an SAV bed. Abundance within each cell is then:

$$M = SH \times A \times TE \times C \times P \tag{15}$$

in which:

M = above-ground abundance (g C)
A = cell surface area (m^2)
TE = truncation error
C = coverage
P = patchiness.

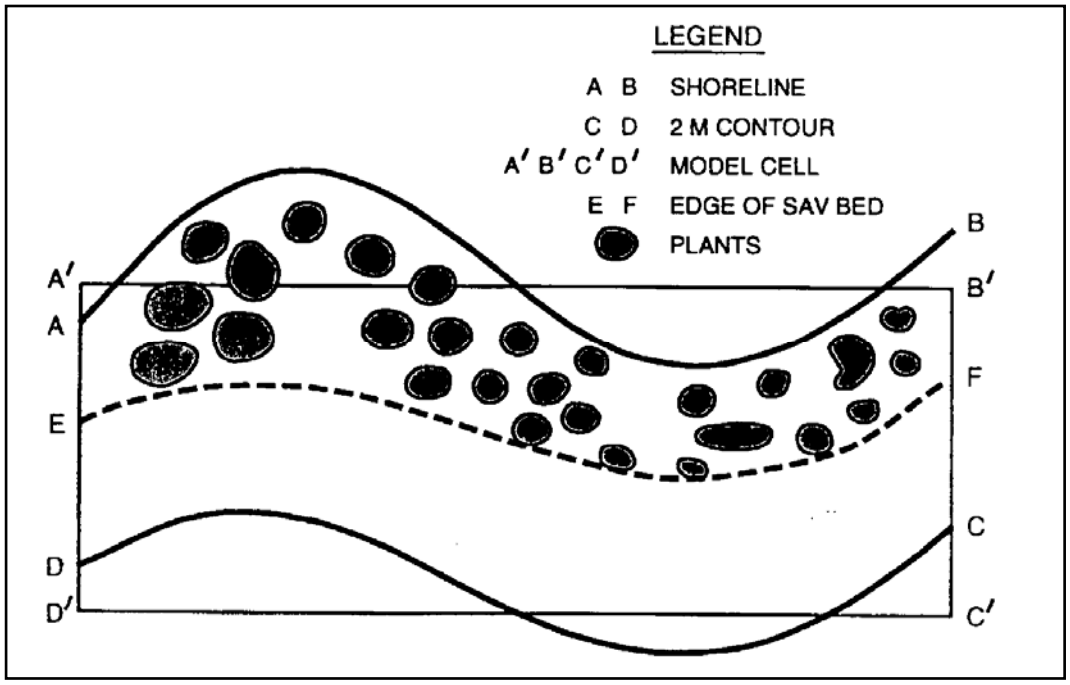

Figure 6. Truncation error, coverage, and patchiness. Truncation error = Area(ABCD)/Area(A′B′C′D′). Coverage = Area(ABEF)/Area(ABCD). Patchiness = Area(plants)/Area(ABEF).

Benthos

Benthos is included in the model because it is an important food source for crabs, finfish, and other economically and ecologically significant biota. In addition, benthos can exert a substantial influence on water quality through filtering of overlying water. The modeled benthos is divided into two groups: deposit feeders and filter feeders (Figure 7). The deposit-feeding group represents benthos organisms that live within bottom sediments and feed on deposited material. The filter-feeding group represents benthos organisms that live at the sediment surface and feed by filtering overlying water.

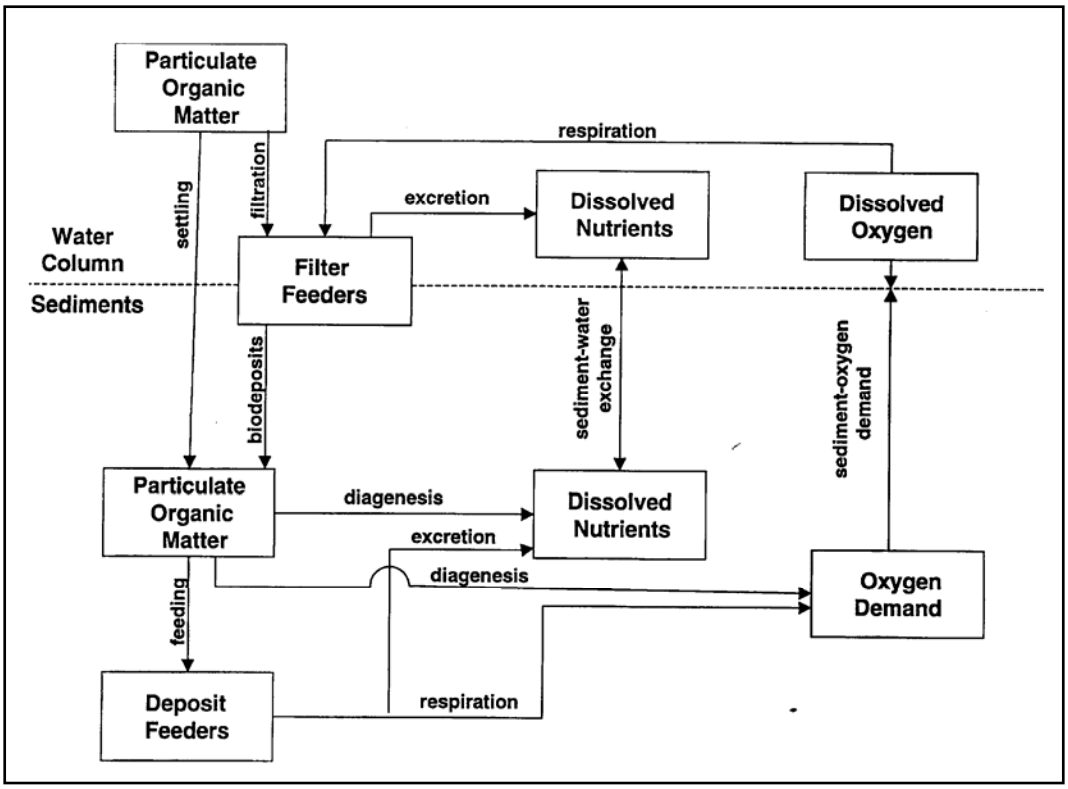

Figure 7. Schematic of benthos model.

The primary reference for the benthos model is HydroQual (2000). The formulations below describe model state variables and fundamental processes within the modeled carbon cycle.

Deposit Feeders

The mass-balance equation for deposit feeders is:

$$\frac{\mathrm{d}DF}{\mathrm{d}t} = \alpha \times \frac{I}{m} \times \frac{POC \times Khdf}{POC + Khdf} \times DF - r \times DF - \beta \times DF^2 - hmr \times DF \quad (16)$$

in which:

DF = deposit feeder biomass (mg C m^{-2})
α = assimilation efficiency ($0 < \alpha < 1$)
m = sediment solids concentration (mg m^{-3})
I = ingestion rate (mg sediment mg^{-1} deposit feeder C d^{-1})
POC = sediment particulate organic carbon (mg m^{-3})
$Khdf$ = half-saturation concentration for carbon uptake (mg m^{-3})
r = specific respiration rate (d^{-1})
β = predation rate (m^2 mg^{-1} deposit feeder C d^{-1})
hmr = mortality rate due to hypoxia (d^{-1})
t = time (d).

The assimilation efficiency and half-saturation concentration are specified individually for G1 (labile) and G2 (refractory) carbon. G3 (inert) carbon is not utilized. An inverse "Michaelis-Menton" function governs ingestion. At low carbon concentrations ($POC << Khdf$), ingestion is proportional to available carbon ($\approx I \times POC$). At high concentrations ($POC >> Khdf$), ingestion approaches a constant value ($\approx I \times Khdf$). All material ingested comes from bottom sediments, and all carbonaceous byproducts, from mortality and predation, are returned to the sediments.

Filter Feeders

The model allows for the specification of multiple filter-feeding groups. Each is governed by the same mass-balance equation:

$$\frac{\mathrm{d}FF}{\mathrm{d}t} = \alpha \times Fr \times POC \times FF - r \times FF - \beta \times FF^2 - hmr \times FF \quad (17)$$

in which:

FF = filter feeder biomass (mg C m^{-2})
α = assimilation efficiency ($0 < \alpha < 1$)

Fr = filtration rate ($m^3\ mg^{-1}$ filter feeder C d^{-1})
POC = particulate organic carbon in overlying water ($mg\ m^{-3}$)
r = specific respiration rate (d^{-1})
β = predation rate ($m^2\ mg^{-1}$ filter feeder C d^{-1})
hmr = mortality rate due to hypoxia (d^{-1})
t = time (d).

The assimilation efficiency is specified individually for each form of particulate organic matter in the water column, including phytoplankton. Carbonaceous byproducts from mortality and respiration are routed to the model sediment component.

Computational Grid and Simulation Period

ICM formulation and parameterization are derived from the Chesapeake Bay model used to guide the development of the 2002 re-evaluation of nutrient control strategies for Chesapeake Bay (Cerco and Noel 2004b). The application operates on a computational grid of 12,000 cells and simulates the period 1985–1994. The computational burden of operating the model hampered the development of new algorithms for coupling ICM with Ecopath. For the present effort, the 2002 kinetics were executed on a grid of 4,000 elements created for the original Chesapeake Bay study (Cerco and Cole 1994). The grid (Figure 8) contains 729 elements (roughly 5 km × 10 km) in the surface plane and from two to fifteen cells in the vertical, depending on local depth. Surface cells are 2.14 m thick. All other cells are 1.53 m thick.

Hydrodynamics, nutrient loads, and boundary conditions were available for three years, 1984–1986. The mean 1984 runoff in the Susquehanna River, the primary freshwater source to the bay, exceeded 90% of the annual mean flows in the period of record ending 1988. The year 1984 was a “wet” year. By contrast, flow in 1985 was unusually low. Roughly 80% of the years on record, up to 1988, had mean flows that exceeded 1985. The year 1985 was a “dry” year. The mean flow in 1986 was near the mean long-term flow. Susquehanna hydrology in 1986 was “average.”

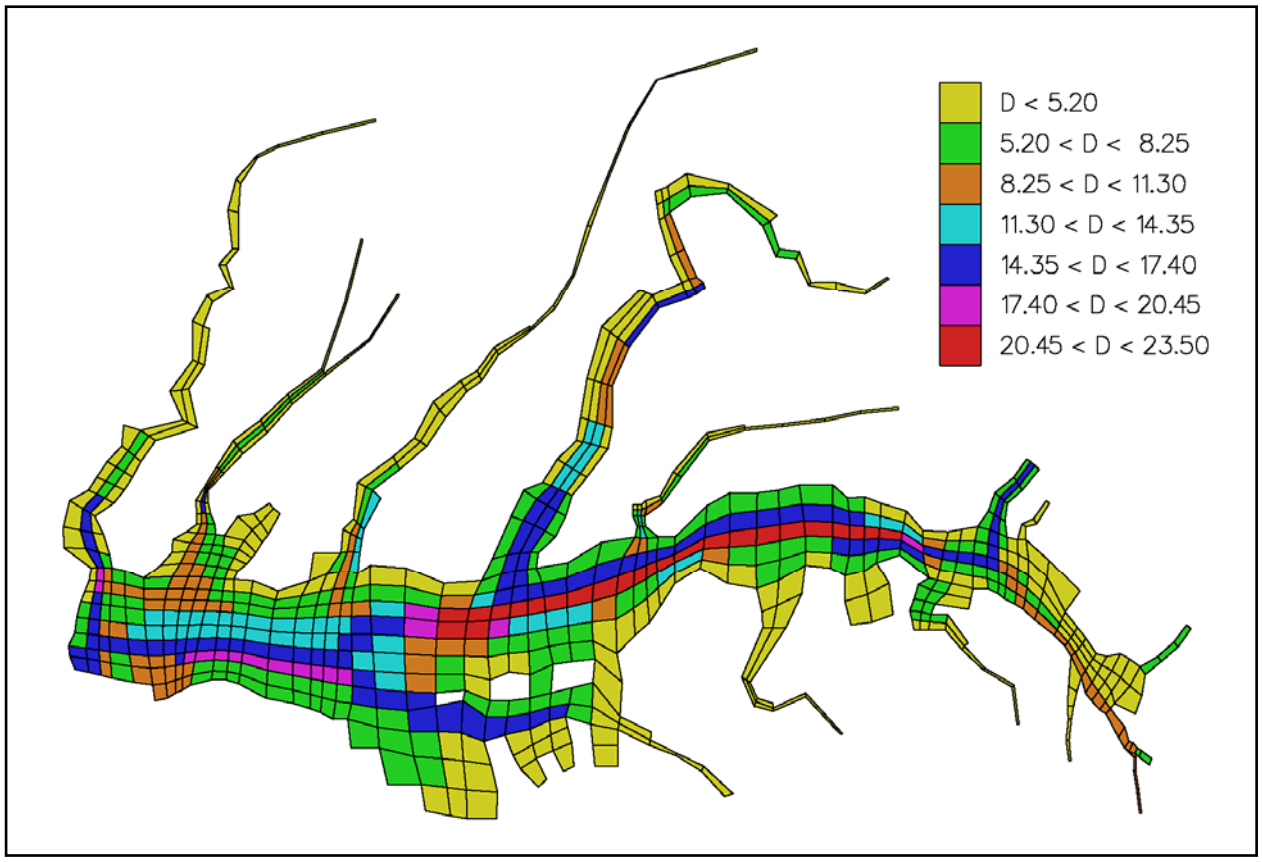

Figure 8. Plan view of the 4000-cell model grid. Depth (D) is in meters.

3 Ecopath Fundamentals

Introduction

Ecopath with Ecosim (EwE) is a suite of ecological models developed at the University of British Columbia Fishery Centre (Christiansen et al. 2000). The software has found extensive worldwide usage, primarily in fisheries management. EwE has three main components: Ecopath, which creates a static mass-balanced representation of a system; Ecosim, which provides time-variable simulations; and Ecospace, which provides space- and time-variable simulations. The formulation of a steady-state Ecopath model usually precedes the application of Ecosim or Ecospace.

Ecopath provides a steady-state view of the biomasses in multiple pools or groups and of the flows between the groups. The biomasses and flows can be expressed in a variety of "currencies," including energy, weight, or nutrients. The model usually describes average or typical conditions over a year or a season rather than conditions in a specific, unique interval. Two or more Ecopath applications are necessary to describe a system in different seasons or subject to major changes.

Basic Equations

The Ecopath model is based on two master equations for each modeled group, one that describes production and one that describes energy balance.

Production

The production equation is:

$$Pi = Yi + Bi \times M2i + Ei + BAi + M0i \tag{18}$$

in which:

Pi = total production rate of group i (mass time^{-1})
Yi = total fishery catch rate of group i (mass time^{-1})
$M2i$ = total predation rate on group i (mass time^{-1})
Ei = net migration rate (positive out) of group i (mass time^{-1})
BAi = biomass accumulation rate of group i (mass time^{-1})
$M0i$ = other mortality of group i (mass time^{-1}).

Other mortality includes all mortality sources other than predation and is represented as:

$$M0i = Pi \times (1 - EEi) \tag{19}$$

in which:

EEi = ecotrophic efficiency of group i.

Ecotrophic efficiency is the fraction of production that is utilized in the system.

The predation term is expressed as:

$$M2i = \sum_{j=1}^{n} Qj \times DCji \tag{20}$$

in which:

Qj = total consumption rate for predator group j (M T^{-1})
$DCji$ = fraction of predator group j's diet contributed by prey group i.

Production and consumption are represented as products of biomass and rate constants. Incorporating these products and the expanded mortality and predation terms into (18) yields:

$$\begin{aligned} Bi \times \left(P/B\right)i - \sum_{j=1}^{n} Bj \times \left(Q/B\right)j \times DCji - \left(P/B\right)i \\ \times Bi \times (1 - EEi) - Yi - Ei - BAi = 0 \end{aligned} \tag{21}$$

in which:

$(P/B)i$ = production to biomass ratio for group i (T^{-1})
$(Q/B)j$ = consumption to biomass ratio for group j (T^{-1}).

Simplifying:

$$Bi \times \left(P/B\right)i \times EEi - \sum_{j=1}^{n} Bj \times \left(Q/B\right)j \times DCji - Yi - Ei - BAi = 0\,. \tag{22}$$

A general system of equations for n groups can be written:

$$\begin{aligned}
&B1\times\left(P/B\right)1\times EE1 - B1\times\left(Q/B\right)1\times DC11 - B2\times\left(Q/B\right)2\times DC21 \\
&\qquad\qquad \ldots\ldots Bn\times\left(Q/B\right)n\times DCn1 - Y1 - E1 - BA1 = 0 \\
&B2\times\left(P/B\right)2\times EE2 - B1\times\left(Q/B\right)1\times DC12 - B2\times\left(Q/B\right)2\times DC22 \\
&\qquad\qquad \ldots\ldots Bn\times\left(Q/B\right)n\times DCn2 - Y2 - E2 - BA2 = 0 \\
&\qquad\qquad .\quad .\quad .\quad .\quad . \\
&\qquad\qquad .\quad .\quad .\quad .\quad . \\
&\qquad\qquad .\quad .\quad .\quad .\quad . \\
&Bn\times\left(P/B\right)n\times EEn - B1\times\left(Q/B\right)1\times DC1n - B2\times\left(Q/B\right)2\times DC2n \\
&\qquad\qquad \ldots\ldots Bn\times\left(Q/B\right)n\times DCnn - Yn - En - BAn = 0
\end{aligned} \tag{23}$$

or

$$\begin{aligned}
&a11\times X1 + a12\times X2 + \ldots. a1m\times Xm = Q1 \\
&a21\times X1 + a22\times X2 + \ldots. a2m\times Xm = Q2 \\
&\qquad .\quad .\quad .\quad .\quad . \\
&\qquad .\quad .\quad .\quad .\quad . \\
&\qquad .\quad .\quad .\quad .\quad . \\
&an1\times X1 + an2\times X2 + \ldots. anm\times Xm = Qn\,.
\end{aligned} \tag{24}$$

The basic operation of the Ecopath model is to solve the system of equations represented by (24). Ecopath includes numerous sophisticated components to deal with singular matrices and under- and over-specified systems. For practical purposes there should be as many equations as

there are groups in the system. Each equation can contain one unknown from the following:

- Biomass
- Production/biomass ratio
- Consumption/biomass ratio
- Ecotrophic efficiency.

Ecotrophic efficiency is the most frequent unknown and is constrained to the range $0 \leq EE \leq 1$. "Calibration" of the Ecopath model amounts to the development of a parameter set that yields EEs in the acceptable range.

Energy Balance

The production equation ensures mass balance. An energy balance must also be satisfied. The energy balance is

Consumption = production + respiration + unassimilated food.

Most often, consumption, production, and unassimilated food are model inputs, and respiration is calculated. The "Energy Balance" constraint on the model is that respiration cannot be negative.

Chesapeake Bay Application

The Ecopath application to Chesapeake Bay is documented in Hagy (2002). Summer (June–August) conditions were modeled for three regions of the Bay (Figure 9) using carbon as currency. The application represented conditions in the bay typical of the years 1985–1999. An application was also created that pictured the bay following nutrient load reductions sufficient to restore phytoplankton production to levels typical of the 1950s to early 1960s. Ecopath input files, as well as documentation, were provided to us by the originator (J.D. Hagy).

The Ecopath application considered 34 groups (Table 2), including 3 detrital pools, 4 primary producers, 9 planktonic consumers, 5 benthic consumers, and 13 nektonic consumers. Application and validation of Ecopath require extensive searches of databases and documentation of information sources. More than 150 sources, ranging from raw data to peer-reviewed literature, provided input to the Ecopath simulation.

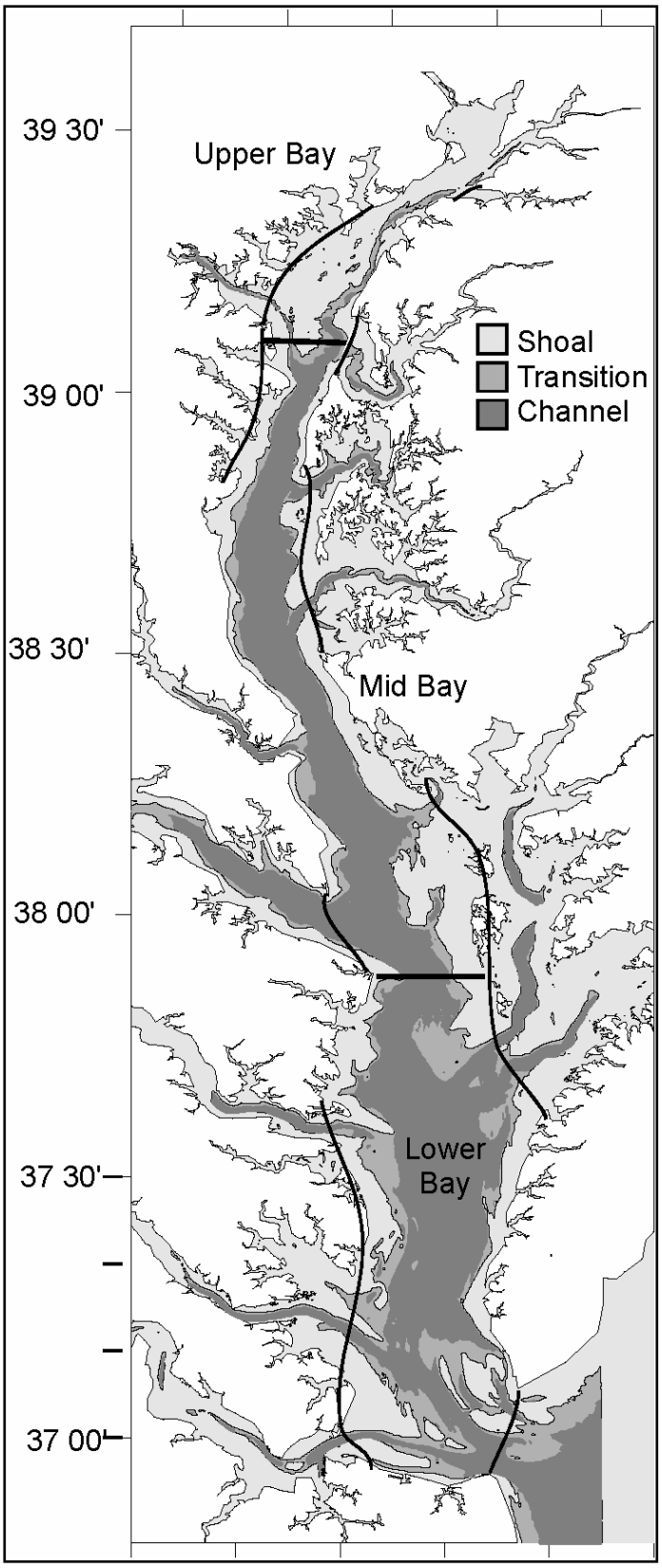

Figure 9. Regions for Chesapeake Bay Ecopath application (after Hagy 2002). Depth contours show shoal (< 7 m), transition (7–10 m), and deep-water (> 10 m) habitats.

Table 2. **Chesapeake Bay ecopath groups.**

Group Number	Description	Trophic Class
1	Net Phytoplankton	Primary Producer
2	Picoplankton	Primary Producer
3	Free Bacteria	Planktonic Consumer
4	Attached Bacteria	Planktonic Consumer
5	Heteroflagellates	Planktonic Consumer
6	Ciliates	Planktonic Consumer
7	Rotifers	Planktonic Consumer
8	Meroplankton	Planktonic Consumer
9	Mesozooplankton	Planktonic Consumer
10	Ctenophores	Planktonic Consumer
11	Chrysora	Planktonic Consumer
12	Microphytobenthos	Primary Producer
13	Submerged Aquatic Vegetation	Primary Producer
14	Benthic Bacteria	Benthic Consumer
15	Meiobenthos	Benthic Consumer
16	Deposit-Feeding Benthos	Benthic Consumer
17	Suspension-Feeding Benthos	Benthic Consumer
18	Oysters	Benthic Consumer
19	Blue Crab	Nektonic Consumer
20	Menhaden	Nektonic Consumer
21	Bay Anchovy	Nektonic Consumer
22	Herring/Shad	Nektonic Consumer
23	White Perch	Nektonic Consumer
24	Spot	Nektonic Consumer
25	Croaker	Nektonic Consumer
26	Hogchoker	Nektonic Consumer
27	American Eel	Nektonic Consumer
28	Catfish	Nektonic Consumer
29	Striped Bass	Nektonic Consumer
30	Bluefish	Nektonic Consumer
31	Weakfish	Nektonic Consumer
32	Dissolved Organic Carbon	Detritus
33	Sediment Carbon	Detritus
34	Particulate Organic Carbon	Detritus

4 Correspondence Between ICM and Ecopath

A major challenge in coupling ICM and Ecopath lies in finding correspondence, or "hooks," between the two models. The models differ in formulation, currency, and terminology. Once correspondences are identified, they must be expressed as computer code. For the initial coupling, all coding was performed on the ICM model or in a separate post-processor, since Ecopath was available only in executable form. Ecopath-specific quantities were defined and computed in ICM and written to a unique file. A post-processor performed spatial summation and averaging on the ICM output and produced results in an "Ecopath-friendly" form.

Correspondence between ICM and Ecopath can be viewed from two perspectives: correspondence between the model formulations and correspondence between the applications to Chesapeake Bay. Correspondences exist between modeled groups (application), quantities computed by ICM and input to Ecopath (formulation), and results generated by both ICM and Ecopath (formulation). The present chapter lists the various correspondences in tabular form followed by a list of symbols employed. A final section is presented that explains areal and temporal aggregation.

Model Groups

Correspondence between ICM and Ecopath groups, as applied to Chesapeake Bay (Hagy 2002, Cerco and Noel 2004b), is presented in Table 3.

Table 3. Groups modeled in ICM and Ecopath application to Chesapeake Bay.

ICM Variable	Ecopath Variable	ICM Formula
Phytoplankton (spring diatoms, green algae)	Picoplankton, Net Phytoplankton	*B*2 + *B*3
Submerged Aquatic Vegetation	Submerged Aquatic Vegetation	*PATCH* × *SH*
Benthic Algae	Microphytobenthos	*BBM*
Microzooplankton	Heteroflagellates, Ciliates, Rotifers, Meroplankton	*SZ*
Mesozooplankton	Mesozooplankton	*LZ*
Deposit Feeders	Deposit-Feeding Benthos	*DF*
Filter Feeders	Filter-Feeding Benthos	*SF*(1) + *SF*(2) + *SF*(3)
Particulate Organic Carbon	Particulate Organic Carbon	*LPOC* + *RPOC*
Dissolved Organic Carbon	Dissolved Organic Carbon	*DOC*
Sediment Organic Carbon	Sediment Carbon	*G*1 + *G*2 + *G*3

Ecopath Inputs

Ecopath inputs are required on three screens entitled “Basic Inputs,” “Diet Composition,” and “Detritus Fate.” Basic inputs (Tables 4–6) include production-to-biomass ratio (primary producers and consumers), consumption-to-biomass ratio (consumers only), and unassimilated consumption (consumers only). A question arises whether production-to-biomass ratio should be based on gross production or net production. For primary producers, gross production is equivalent to the total carbon fixed; net production is gross minus respiration. For consumers, gross production is equivalent to the total amount of food assimilated; net production is gross minus respiration. The issue is resolved through operation of the Ecopath model. Ecopath computes respiration for consumers but not for primary producers. Consequently, gross production from ICM is used for consumer production since Ecopath explicitly accounts for respiration. Net production from ICM is used for primary producers since Ecopath takes no account of their respiration. The production-to-biomass ratio for these organisms represents the amount of carbon fixed that is available for use in the ecosystem. Diet Composition (Table 7) is the fraction of each diet source represented in a consumer’s diet. Production that is not respired or consumed becomes detritus. Detritus Fate (Table 8) is the fraction of detritus routed to each detritus group. Table 9 gives the symbols used in this analysis.

Table 4. Production-to-biomass ratio derived from ICM variables.

Group	Formula	Units
Phytoplankton	$Palg \times (1 - PRSPalg) - BMalg$	D^{-1}
SAV	$Psav - BMsav - SL$	D^{-1}
Benthic Algae	$Pba - BMba$	D^{-1}
Microzooplankton	$Esz \times (1 - RFsz) \times Rsz - BMsz$	D^{-1}
Mesozooplankton	$Elz \times (1 - RFlz) \times Rlz - BMlz$	D^{-1}
Deposit Feeders	$Gdf - Rdf$	D^{-1}
Filter Feeders	$(TCONff - UCONff - RESPff) / SF$	D^{-1}

Table 5. Consumption-to-biomass ratio derived from ICM variables.

Group	Formula	Units
Microzooplankton	Rsz	d^{-1}
Mesozooplankton	Rlz	d^{-1}
Deposit Feeders	$xki0 \times (POC1 + POC2 + POC3) / M2$	d^{-1}
Filter Feeders	$FILTCT \times (B2 + B3 + LPOC + RPOC)$	d^{-1}

Table 6. Unassimilated consumption derived from ICM variables.

Group	Formula	Units
Microzooplankton	$1 - Esz$	< 1
Mesozooplankton	$1 - Elz$	< 1
Deposit Feeders	$\frac{(1 - \alpha 1 \times xpoc1\lim) \times POC1 + (1 - \alpha 2 \times xpoc2\lim) \times POC2 + POC3}{POC1 + POC2 + POC3}$	< 1
Filter Feeders	$\frac{CFECES + RCFECES + CPSFEC + RCPSFEC}{SF \times FILTCT \times (B2 + B3 + LPOC + RPOC)}$	< 1

Table 7. Diet Composition derived from ICM variables.

Consumer	Source	Fraction	Units
Microzooplankton	Dissolved Organic Carbon	$\frac{UDOCsz \times DOC}{PRAsz}$	< 1
	Phytoplankton	$\frac{UB2sz \times B2 + UB3sz \times B3}{PRAsz}$	< 1
	Particulate Organic Carbon	$\frac{ULsz \times LPOC + URsz \times RPOC}{PRAsz}$	< 1
Mesozooplankton	Microzooplankton	$\frac{USZlz \times SZ}{PRAlz}$	< 1
	Phytoplankton	$\frac{UB2lz \times B2 + UB3lz \times B3}{PRAlz}$	< 1
	Particulate Organic Carbon	$\frac{ULlz \times LPOC + URlz \times RPOC}{PRAlz}$	< 1
Deposit Feeders	Bed Sediments	100%	
Filter Feeders	Phytoplankton	$\frac{B2 + B3}{B2 + B3 + LPOC + RPOC}$	< 1
	Particulate Organic Carbon	$\frac{LPOC + RPOC}{B2 + B3 + LPOC + RPOC}$	< 1

Table 8. Detritus Fate derived from ICM variables.

Source	Fate	Formula	Units
Phytoplankton	Detritus Production, CP	$(P2+PRSP\times BMR2)\times B2+(P3+PRSP\times BMR3)\times B3$	G C m^{-3} d^{-1}
	DOC Production, DOCalg	$FCD\times CP+FCDP\times(PR2+PR3)$	g C m^{-3} d^{-1}
	POC Production, POCalg	$(1-FCD)\times CP+(1-FCDP)\times(PR2+PR3)$	g C m^{-3} d^{-1}
	Sedimentation, SEDalg	$WS2NET\times B2+WS3NET\times B3$	g C m^{-2} d^{-1}
	Fraction to DOC	$\frac{H\times DOCalg}{H\times DOCalg+H\times POCalg+SEDalg}$	< 1
	Fraction to POC	$\frac{H\times POCalg}{H\times DOCalg+H\times POCalg+SEDalg}$	< 1
	Fraction to Sediments	$\frac{Sedalg}{H\times DOCalg+H\times POCalg+SEDalg}$	< 1
SAV	Fraction to DOC	$\frac{(BMSH\cdot FCDSH+SL\cdot FCDSL)\cdot SH}{(BMSH\cdot FCDSH+SL)\cdot SH+BMRT\cdot RT}$	< 1
	Fraction to POC	$\frac{(1-FCDSL)\times SL\times SH}{(BMSH\times FCDSH+SL)\times SH+BMRT\times RT}$	< 1
	Fraction to Sediments	$\frac{BMRT\cdot RT}{(BMSH\cdot FCDSH+SL)\cdot SH+BMRT\cdot RT}$	< 1
Benthic Algae	Fraction to Sediments	100%	
Microzooplankton	Fraction to DOC	$FDOCsz$	< 1
	Fraction to POC	$1-FDOCsz$	< 1
Mesozooplankton	Fraction to DOC	$FDOClz$	< 1
	Fraction to POC	$1-FDOClz$	< 1
Deposit Feeders	Fraction to Sediments	100%	
Filter Feeders	Fraction to Sediments	100%	
Dissolved Organic Carbon	Export	100% (This is an Ecopath default value, ICM creates no DOC detritus)	
Particulate Organic Carbon	Amount to Sediments, POC2SED	$WSLNET\times LPOC+WSRNET\times RPOC$	g C m^{-2} d^{-1}
	Amount to DOC, POC2DOC	$H\times(KLPOC\times LPOC+KRPOC\times RPOC)$	g C m^{-2} d^{-1}
	Fraction to Sediments	$\frac{POC2SED}{POC2DOC+POC2SED}$	< 1
	Fraction to DOC	$\frac{POC2DOC}{POC2DOC+POC2SED}$	< 1
Sediment Organic Carbon	Export	100% (This is an Ecopath default value, ICM creates no detritus from sediment organic carbon)	

Table 9. Symbols employed in ICM.

Symbol	Units	Definition
BBM	g C m^{-2}	Benthic algae
BMalg	d^{-1}	Algal basal metabolism
BMba	d^{-1}	Benthic algae basal metabolism
BMlz	d^{-1}	Mesozooplankton basal metabolism
BMRT	d^{-1}	SAV root metabolism
BMsav	d^{-1}	SAV basal metabolism
BMSH	d^{-1}	SAV shoot metabolism
BMsz	d^{-1}	Microzooplankton basal metabolism
B2	g C m^{-3}	Spring diatoms
B3	g C m^{-3}	Green algae
CFECES	mg C m^{-2} d^{-1}	Labile carbon feces produced by filter feeders
CP	g C m^{-3} d^{-1}	Detritus production by phytoplankton metabolism
CPSFEC	mg C m^{-2} d^{-1}	Labile carbon pseudo-feces produced by filter feeders
DF	mg C m^{-2}	Deposit feeders
DOC	g C m^{-3}	Dissolved organic carbon
DOCalg	g C m^{-3} d^{-1}	Phytoplankton dissolved organic carbon production rate
Elz	0 < Elz < 1	Mesozooplankton efficiency
Esz	0 < Esz < 1	Microzooplankton efficiency
FCD	0 < FCD < 1	Fraction of phytoplankton metabolism excreted as dissolved organic carbon
FCDP	0 < FCDP < 1	Fraction of non-specific predation on phytoplankton released as dissolved organic carbon
FCDSH	0 < FCDSH < 1	Fraction of SAV metabolism excreted as DOC
FCDSL	0 < FCDSL < 1	Fraction of SAV leaf sloughing released as DOC
FILTCT	m^3 g^{-1} filter feeder carbon d^{-1}	Filtration rate as determined by temperature, dissolved oxygen, and other factors
Gdf	d^{-1}	Deposit feeder specific growth rate as determined by local temperature, dissolved oxygen concentration, and food availability
G1	mg C m^{-3}	Labile sediment particulate organic carbon
G2	mg C m^{-3}	Refractory sediment particulate organic carbon
G3	mg C m^{-3}	Inert sediment particulate organic carbon
H	m	Depth of water column
KLPOC	d^{-1}	Labile particulate organic carbon dissolution rate
KRPOC	d^{-1}	Refractory particulate organic carbon dissolution rate
LPOC	g C m^{-3}	Labile particulate organic carbon
LZ	g C m^{-3}	Mesozooplankton
M2	mg m^{--3}	Bed sediment solids concentration
Palg	d^{-1}	Algal specific production rate as determined by local irradiance, temperature, and nutrient availability

Symbol	Units	Definition
Pba	d^{-1}	Benthic algae specific production rate as determined by local irradiance, temperature, and nutrient availability
POCalg	g C m^{-3} d^{-1}	Phytoplankton particulate organic carbon production rate
Psav	d^{-1}	SAV specific production rate as determined by local irradiance, temperature, and nutrient availability
PATCH	0 < PATCH < 1	Product of coverage and patchiness
POC1	mg C m^{-3}	G1 carbon concentration in bed sediments
POC2	mg C m^{-3}	G2 carbon concentration in bed sediments
POC2DOC	g C m^{-2} d^{-1}	Particulate organic carbon dissolution to dissolved organic carbon
POC2SED	g C m^{-2} d^{-1}	Particulate organic carbon deposition to sediments
POC3	mg C m^{-3}	G3 carbon concentration in bed sediments
PRAsz	g C m^{-3}	Prey available to microzooplankton
PRalg	g C m^{-3} d^{-1}	Non-specific predation on phytoplankton
PRAlz	g C m^{-3}	Prey available to mesozooplankton
PRSPalg	0 < PRSPalg < 1	Algal photorespiratory fraction
RCFECES	mg C m^{-2} d^{-1}	Refractory carbon feces produced by filter feeders
RCPSFEC	mg C m^{-2} d^{-1}	Refractory carbon pseudo-feces produced by filter feeders
Rdf	d^{-1}	Deposit feeder specific respiration rate
RESPff	mg C m^{-2} d^{-1}	Filter feeder respiration
RFlz	0 < RFlz < 1	Mesozooplankton active respiration
RFsz	0 < RFsz < 1	Microzooplankton active respiration
RPOC	g C m^{-3}	Refractory particulate organic carbon
Rlz	d^{-1}	Mesozooplankton specific ration as determined by local temperature and prey availability
Rsz	d^{-1}	Microzooplankton specific ration as determined by local temperature and prey availability
RT	g C m^{-2}	SAV roots
SEDalg	g C m^{-2} d^{-1}	Phytoplankton sedimentation rate
SF(I)	mg C m^{-2}	Filter feeder group I
SH	g C m^{-2}	SAV shoots
SL	d^{-1}	SAV leaf sloughing rate
SZ	g C m^{-3}	Microzooplankton
TCONff	mg C m^{-2} d^{-1}	Filter feeder total consumption
UB2lz	0 < UB2lz < 1	Utilization of spring diatoms by mesozooplankton
UB2sz	0 < UB2sz < 1	Utilization of spring diatoms by microzooplankton
UB3lz	0 < UB3lz < 1	Utilization of green algae by mesozooplankton
UB3sz	0 < UB3sz < 1	Utilization of green algae by microzooplankton
UCONff	mg C m^{-2} d^{-1}	Filter feeder unassimilated consumption

Symbol	Units	Definition
UDOCsz	0 < UDOCsz < 1	Utilization of dissolved organic carbon by microzooplankton
ULlz	0 < ULlz < 1	Utilization of labile particulate organic carbon by mesozooplankton
ULsz	0 < ULsz < 1	Utilization of labile particulate organic carbon by microzooplankton
URlz	0 < URlz < 1	Utilization of refractory particulate organic carbon by mesozooplankton
URsz	0 < URsz < 1	Utilization of refractory particulate organic carbon by microzooplankton
USZlz	0 < USZlz < 1	Utilization of microzooplankton by mesozooplankton
WSalgNET	m d^{-1}	Net phytoplankton settling rate into bottom sediments
WSLNET	m d^{-1}	Net labile particulate organic carbon settling rate into bottom sediments
WSRNET	m d^{-1}	Net refractory particulate organic carbon settling rate into bottom sediments
xki0	mg sediment mg^{-1} deposit feeder carbon d^{-1}	Ingestion rate, as influenced by temperature
xpoc1lim	Function that saturates deposit feeder G1 carbon uptake at high concentrations	0 < xpoc1lim < 1
xpoc2lim	Function that saturates deposit feeder G2 carbon uptake at high concentrations	0 < xpoc2lim < 1
α1	G1 carbon assimilation efficiency	0 < α1 < 1
α2	G2 carbon assimilation efficiency	0 < α2 < 1

Ecopath Results

Execution of the Ecopath model generates quantities of information on multiple output screens. Some outputs echo the inputs, while other outputs are the result of Ecopath computations. Not all of the output is relevant or comparable to ICM results. Three quantities that are both meaningful and comparable are:

- Flow to detritus on the “Key Indices” screen
- Consumption summed by group on the “Consumption” screen
- Respiration on the “Respiration” screen.

These results all involve mass as opposed to the dimensionless fractions or rates, involving time only, input to Ecopath.

Temporal and Spatial Aggregation

ICM computes quantities at discrete time intervals on a three-dimensional spatial grid. The time intervals are in minutes, and the grid elements are on the order of kilometers in spatial extent and meters in vertical thickness. Ecopath represents quantities averaged over temporal scales of seasons or years and considers systems in their entirely or else divided into a few major segments. Consequently ICM results must be aggregated for comparison with Ecopath. Temporal averaging occurs first and takes advantage of an existing algorithm incorporated in ICM. Model results in each grid element are averaged according to:

$$Cavg = \frac{1}{T} \times \sum_{1}^{n} C_i \times \Delta t \tag{25}$$

in which:

C_i = quantity computed by ICM at discrete time interval i
$Cavg$ = temporal average of C_i
Δt = model time step
T = duration of averaging interval
n = number of time steps in averaging interval.

Ecopath quantifies biomass and similar quantities in areal units, while ICM employs volumetric units. Where necessary, summations over the water column are conducted according to:

$$Careal = \sum_{1}^{n} Cavg \times \Delta z \tag{26}$$

in which:

$Careal$ = quantity expressed in areal units
Δz = thickness of model cell
n = number of cells in water column.

The remaining step is the averaging of quantities computed in ICM cell columns up to the Ecopath region:

$$Creg = \frac{1}{Areg} \times \sum_{1}^{n} Careal_i \times A_i \quad (27)$$

in which:

$Creg$ = regionally and temporally averaged quantity for comparison with Ecopath
$Areg$ = regional area
A_i = surface area of ICM cell column i
n = number of cell columns in region.

5 ICM and Ecopath Applications to Chesapeake Bay

Introduction

Distinction must be made between comparison of the ICM and Ecopath models and comparison of the ICM and Ecopath applications. Correspondences between the two models were described in the preceding chapter. Here, applications are considered, in particular two applications to Chesapeake Bay. The Ecopath application (Hagy 2002) describes three regions of the Bay (Figure 9) and represents summer (June–August) conditions typical of the years 1985–1999. The ICM application describes the same three regions for June–August 1986, considered a year of "average" hydrology.

To facilitate the comparisons, an Ecopath model was constructed of ICM. The initial purpose of the "model of the model" was quality control. Since both Ecopath and ICM are based on mass-balance principles, an Ecopath model of ICM should also conserve mass. Problems in this regard indicated errors in formulations or post-processing. Following quality assurance, the model of the model provided a convenient means for comparison of corresponding quantities.

The intention of this comparison is to examine representations of one ecosystem rendered by two different models. Questions arise as to what degree of correspondence is expected and what constitutes agreement or disagreement between the two models. Ecopath describes multiple years and provides a steady-state approximation. ICM provides a dynamic representation of a specific year. Ecopath is based on multiple data sources that differ from the data used for ICM calibration. The two applications may each provide good representations of their periods and observations and still differ from each other. In our comparisons, we focus on differences in ecosystem function and substantial, order-of-magnitude, quantitative differences. Comparisons are, of course, limited to the biota and processes common to the two applications.

Biomass and Production

Primary producer biomass described by the two models is usually consistent within a factor of two (Tables 10–13). In view of the disparities in application periods and other factors, we consider a factor of two to be good agreement. For two of the primary producers, phytoplankton and SAV, good agreement is not surprising, since observations are widely available and both models are tuned to them.

The production-to-biomass ratio (P/B) can be thought of as an in-situ, realized growth rate. These stray, although not widely, from the factor-of-two agreement deemed "good" for biomass. More significantly, ICM P/B tends to be lower than that of Ecopath for the two major producers, phytoplankton and benthic algae. A problem in judging the comparisons is that observations of P/B are not available. In ICM, P/B results from computations in which the specified maximum growth rate is reduced by various limiting factors. These limiting factors are primarily, but not exclusively, evaluated through calibration exercises conducted to bring about agreement between computed and observed biomass. For Ecopath, we believe P/B results from division of observed primary production ($g\ m^{-2}\ d^{-1}$) by observed biomass ($g\ m^{-2}$) prior to model input. Phytoplankton growth rate in ICM follows a previously detected pattern in which the growth rate declines with distance away from the Susquehanna River nutrient source. Ecopath shows exactly the opposite trend. The growth rate increases with distance away from the nutrient source.

Multiplication of biomass by P/B yields net primary production. Both models agree that phytoplankton production is dominant. In ICM, phytoplankton production follows the pattern of growth rate; net primary production declines with distance away from the Susquehanna River. Ecopath represents the greatest phytoplankton production in the mid bay. ICM phytoplankton production is twice that of Ecopath in the upper bay but only half that of Ecopath elsewhere. Benthic algal production in ICM is only a fraction of that of Ecopath, attributable primarily to the disparity in growth rates. The growth rate computed in ICM is always less than the rate specified in Ecopath. ICM SAV net production exceeds that of Ecopath, largely due to greater ICM biomass. In either model, SAV production is a minor fraction of the total.

Table 10. Biomass, production/biomass, and production as represented by Ecopath and ICM in the upper bay.

	Biomass			P/B			Production		
	Ecopath (g C m^{-2})	ICM (g C m^{-2})	ICM: Ecopath	Ecopath (d^{-1})	ICM (d^{-1})	ICM: Ecopath	Ecopath (g C m^{-2} d^{-1})	ICM (g C m^{-2} d^{-1})	ICM: Ecopath
Phytoplankton	1.60	3.13	1.96	0.567	0.603	1.06	0.904	1.885	2.08
Benthic Algae	0.29	0.25	0.84	0.600	0.222	0.37	0.176	0.055	0.31
SAV	2.09	3.89	1.86	0.008	0.032	4.00	0.017	0.124	7.46
Microzooplankton	0.08	0.12	1.39	2.060	0.017	0.01	0.171	0.002	0.01
Mesozoplankton	0.28	0.21	0.76	0.380	0.117	0.31	0.107	0.025	0.23
Deposit Feeders	3.07	0.42	0.14	0.027	0.084	3.11	0.083	0.036	0.43
Filter Feeders	27.23	2.98	0.11	0.008	0.001	0.13	0.218	0.003	0.01
DOC	12.50	18.95	1.52						
POC	5.25	11.60	2.21						

Table 11. Biomass, production/biomass, and production as represented by Ecopath and ICM in the mid bay.

	Biomass			P/B			Production		
	Ecopath (g C m^{-2})	ICM (g C m^{-2})	ICM: Ecopath	Ecopath (d^{-1})	ICM (d^{-1})	ICM: Ecopath	Ecopath (g C m^{-2} d^{-1})	ICM (g C m^{-2} d^{-1})	ICM: Ecopath
Phytoplankton	3.91	2.93	0.75	0.630	0.480	0.76	2.463	1.405	0.57
Benthic Algae	0.27	0.21	0.81	0.600	0.193	0.32	0.159	0.041	0.26
SAV	0.53	1.94	3.64	0.009	0.010	1.11	0.005	0.019	4.04
Microzooplankton	0.19	0.35	1.86	2.030	0.003	0.00	0.382	0.001	0.00
Mesozoplankton	0.53	0.28	0.53	0.500	0.072	0.14	0.263	0.020	0.08
Deposit Feeders	1.52	0.31	0.20	0.032	0.065	2.03	0.049	0.020	0.41
Filter Feeders	0.42	0.75	1.79	0.014	0.001	0.07	0.006	0.001	0.13
DOC	28.20	14.47	0.51						
POC	10.30	15.04	1.46						

Table 12. Biomass, production/biomass, and production as represented by Ecopath and ICM in the lower bay.

	Biomass			P/B			Production		
	Ecopath (g C m^{-2})	ICM (g C m^{-2})	ICM: Ecopath	Ecopath (d^{-1})	ICM (d^{-1})	ICM: Ecopath	Ecopath (g C m^{-2} d^{-1})	ICM (g C m^{-2} d^{-1})	ICM: Ecopath
Phytoplankton	2.49	2.41	0.97	0.856	0.295	0.34	2.131	0.712	0.33
Benthic Algae	0.29	0.19	0.66	0.799	0.145	0.18	0.234	0.028	0.12
SAV	1.99	3.16	1.59	0.009	0.006	0.67	0.018	0.019	1.06
Microzooplankton	0.13	0.27	2.18	1.890	0.001	0.00	0.236	0.000	0.00
Mesozoplankton	1.07	0.11	0.10	0.250	0.001	0.00	0.268	0.000	0.00
Deposit Feeders	4.79	0.34	0.07	0.022	0.046	2.09	0.105	0.016	0.15
Filter Feeders	6.96	0.00	0.00	0.014	0.000	0.00	0.097	0.000	0.00
DOC	26.92	10.55	0.39						
POC	8.31	7.94	0.96						

Table 13. Total biomass by trophic level for all EWE runs.

Trophic Level / Major 3 Groups within Level	EWE Base total biomass (mgC m^{-2} day^{-1})	EWE 1950s restored bay total biomass (mgC m^{-2} day^{-1})	EWE-M20% total biomass (mgC m^{-2} day^{-1})	EWE-ICM base total biomass (mgC m^{-2} day^{-1})	EWE-ICM 20%P total biomass (mgC m^{-2} day^{-1})	EWE-ICM 90%R total biomass (mgC m^{-2} day^{-1})
IX / Chrysara, Bay Anchovy	0.019	0.001	–	–	–	0.000
VIII / Mesozooplankton, Ctenphores, and Chrysaora	0.393	0.174	0.043	0.043	0.043	0.049
VII / Ctenophores, Chrysaora, Bay Anchovy, and	7.200	9.249	5.416	5.412	5.412	4.173
VI / Mesozooplankton, Ctenophores, and Bay Anchovy	45.117	57.82	42.181	43.651	43.396	37.504
V / Meroplankton, Mesozooplankton, and Bay Anchovy	150.997	100.158	138.226	163.595	170.459	100.559
IV / Ciliates, Mesozooplankton, and Bay Anchovy	593.799	420.228	563.86	587.701	596.945	438.322
III / Hetroflagellates, Mesozooplankton, and Ciliates	1928.96	2584.011	1974.55	1772.672	1769.841	1553.734
II / Free Bacteria, Benthic Bacteria, and Mesozooplankton	6794.818	12958.45	7088.576	5367.958	5329.808	5225.112
I / Net Phytoplankton, DOC, and Sediment POC	4711.00	9057.00	4711.000	4952.00	4778.00	3650.00

Agreement in zooplankton biomass represented by the two models falls within the factor-of-two range except for mesozooplankton in the lower bay (Tables 10–13). There Ecopath represents an anomalously high biomass that exceeds ICM by an order of magnitude. The most significant difference in the two models is in zooplankton P/B ratios. ICM ratios are always less than those of Ecopath, occasionally by orders of magnitude. A significant portion of the disparity is attributed to the ICM temperature functions that govern zooplankton grazing rates. The functions (Figures 10, 11) force a decline in grazing rates at temperatures in excess of 25°C. Simultaneously, increasing temperature produces an exponential

(Q10 = 2) increase in respiration. The combined effects of increasing metabolism and declining filtration result in declining biomasses over the summer (Figures 12, 13) and little or no zooplankton production. The observations on which the ICM temperature functions are based allow wide latitude in fitting the model function. No doubt, the model functions should be revised to provide increased filtration at temperatures in excess of 25°C.

Little correspondence exists between macrobenthic biomass represented by the two models (Tables 10–13). Deposit-feeding biomass in ICM is as much as an order of magnitude less than in Ecopath. Filter-feeding biomass represented in the two models is roughly equivalent in the mid bay, but, as with deposit feeders, ICM biomass is an order or magnitude lower elsewhere. Filter-feeder P/B ratio and production, as represented by ICM, are also much less than in Ecopath.

The most significant disparity, from the view of system function, is the representation of filter feeders in the upper bay. Although the biomass calculated in ICM is higher than elsewhere, it is still only a tenth of the Ecopath biomass. The shortfall in ICM biomass was recognized when the benthos component was developed (HydroQual 2000) but could not be overcome. Algorithms for filter feeders have been substantially revised for application to oyster studies (Cerco and Noel 2005), and improved representation of filter feeders in the upper bay should be possible in future applications. The shortfall in ICM filter-feeding biomass in the lower bay is attributed to different model frameworks. ICM represents bivalve filter feeders. Observations indicated that bivalve biomass was negligible in the lower bay, so these organisms were not represented in the model of that region. Ecopath includes the polychaeate *Chaetopterus* (Thompson and Schaffner 2001) in the filter-feeding biomass of the lower bay. The significance of the ICM omission of *Chaetopterus* is unclear. The large population of bivalve filter feeders in the shallow water of the upper bay may be assumed to effect significant transfers of material from the water column to sediments. The role of benthic filtration is diminished in deep water, however, so the omission of *Chaetopterus* may be insignificant.

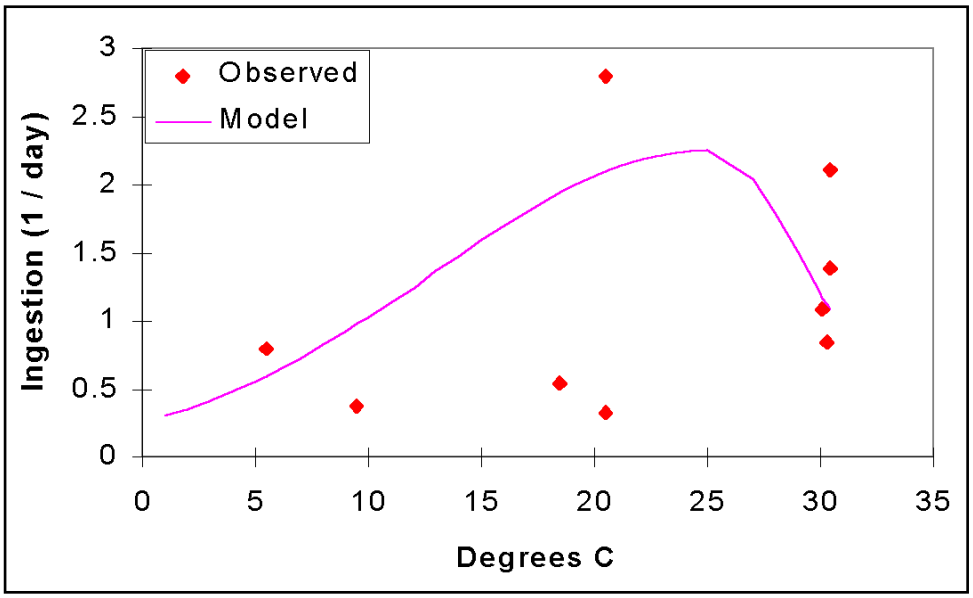

Figure 10. Effect of temperature on microzooplankton grazing rate as observed and computed in ICM.

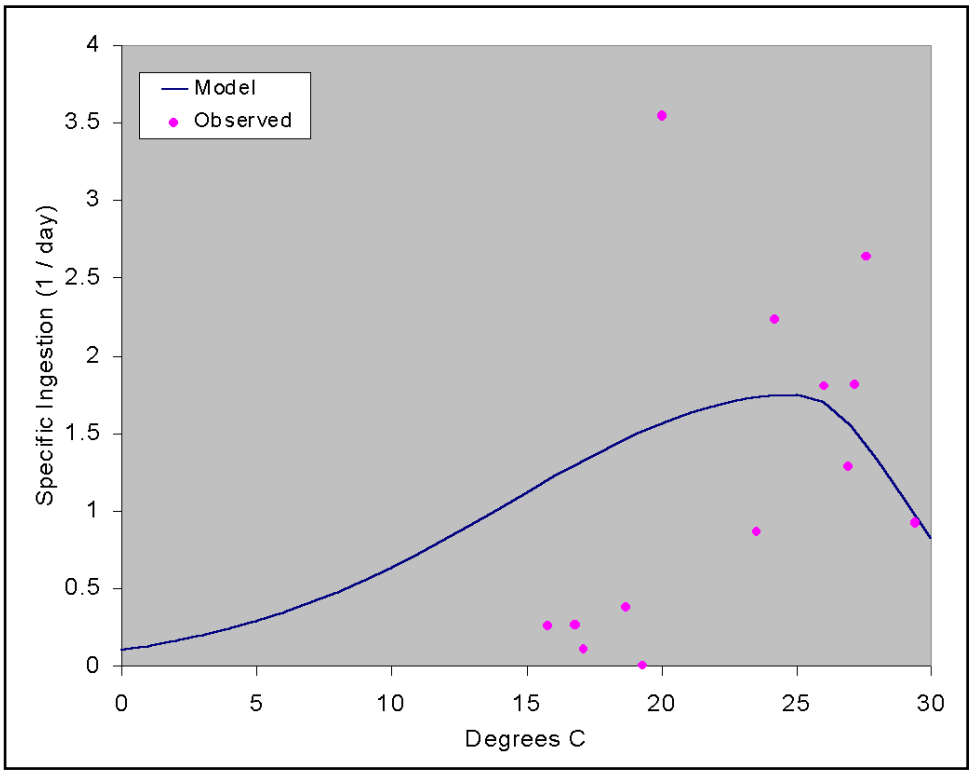

Figure 11. Effect of temperature on mesozooplankton grazing rate as observed and computed in ICM.

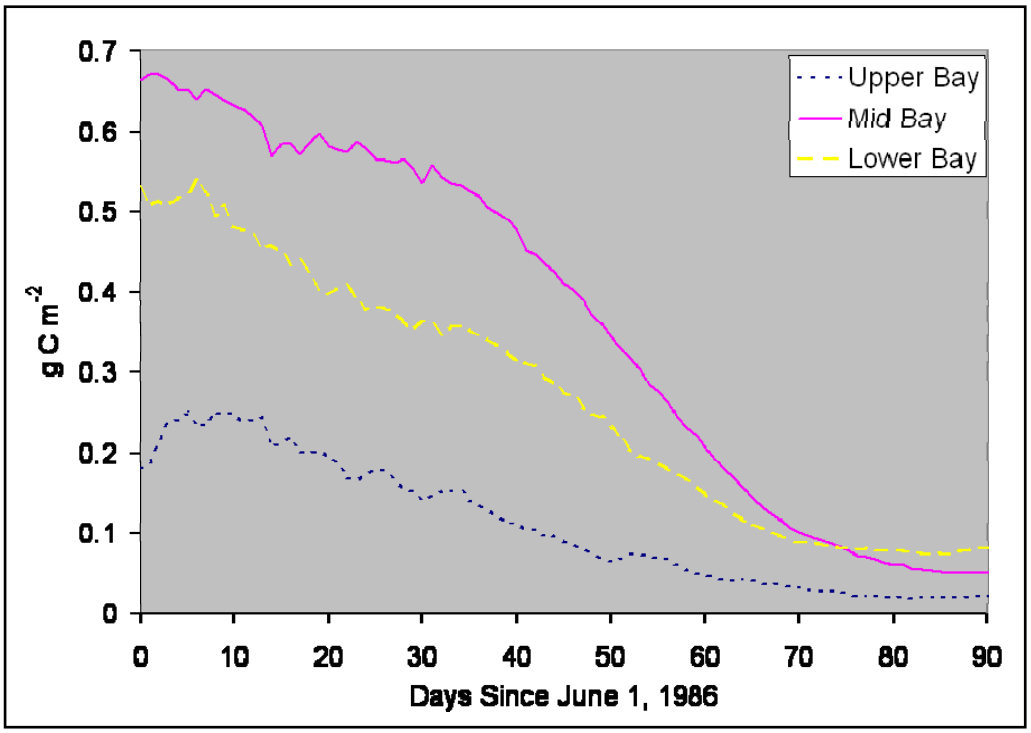

Figure 12. Microzooplankton biomass computed in ICM for three regions of Chesapeake Bay, summer 1986.

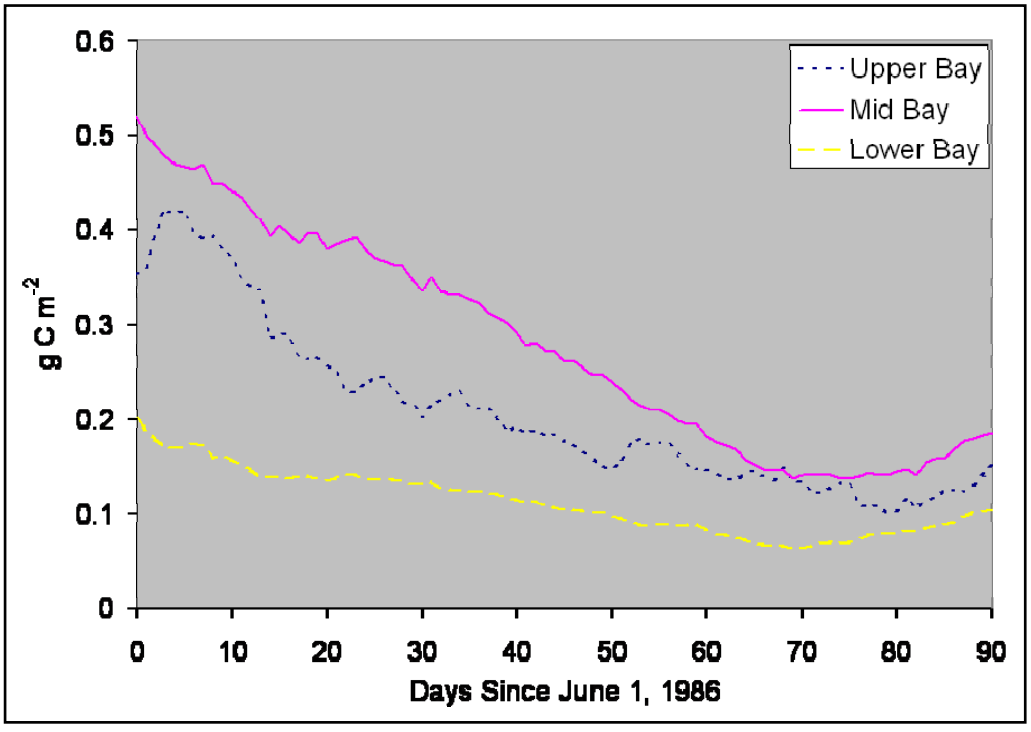

Figure 13. Mesozooplankton biomass computed in ICM for three regions of Chesapeake Bay, summer 1986.

The origin of the differences in deposit-feeder biomass is unclear. Both models are based on the same Chesapeake Bay Program monitoring database. Examination of this database indicates enormous, multiple-order-of-magnitude fluctuations in biomass at single locations. The different representations can likely be attributed to interpretation of the database, among other factors. The differences are not significant, in any event, since ICM deposit feeders have no functional role in the model ecosystem.

Ecosystem Fluxes

Phytoplankton

Simplified charts, based on the ICM carbon cycle, were prepared for comparison of carbon fluxes as represented in the two models (Figure 14). As noted previously, the models differ in the amount of planktonic primary production (Figures 15–17). One difference is that gross primary production was input to the Ecopath model (Hagy 2002), while net primary production was derived from ICM for comparison with Ecopath. We feel strongly that net production is correct, since the Ecopath formulation does not treat respiration by primary producers. Consequently, net production represents the amount of carbon that is truly available for use in the ecosystem. Net planktonic primary production in Chesapeake Bay is roughly 75% of gross production (Cerco and Noel 2004a). Reducing primary production, as represented in the Ecopath application, by 25% improves comparison with ICM in the mid and lower bay, where ICM was lower than Ecopath, and exacerbates the disparity in the upper bay, where ICM exceeded Ecopath.

The excess ICM production in the upper bay is associated with the major disparity in phytoplankton carbon fluxes between the two applications. In the ICM upper bay, three-quarters of algal production is routed to detritus (Figure 18). Less than 10% of algal production goes directly to detritus in the Ecopath upper bay. The major sink is to benthic filter feeders (categorized as “other”) followed by zooplankton. As noted previously, ICM under-represents filter feeders in the upper bay. Improvement in this model component is expected to reduce algal biomass, reduce algal production, and bring ICM into improved agreement with the Ecopath representation of carbon fluxes.

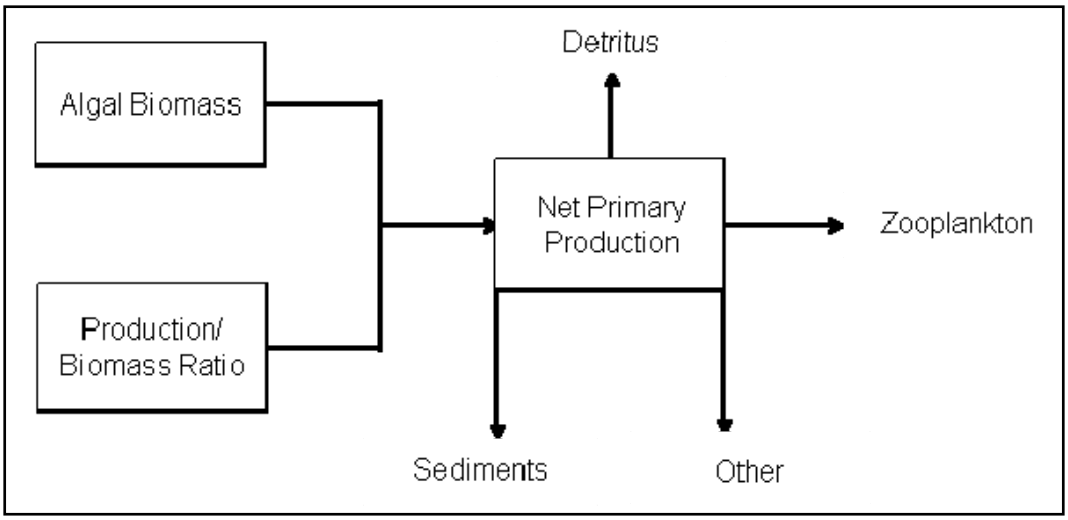

Figure 14. Schematic diagram of phytoplankton carbon fluxes as represented by ICM and Ecopath.

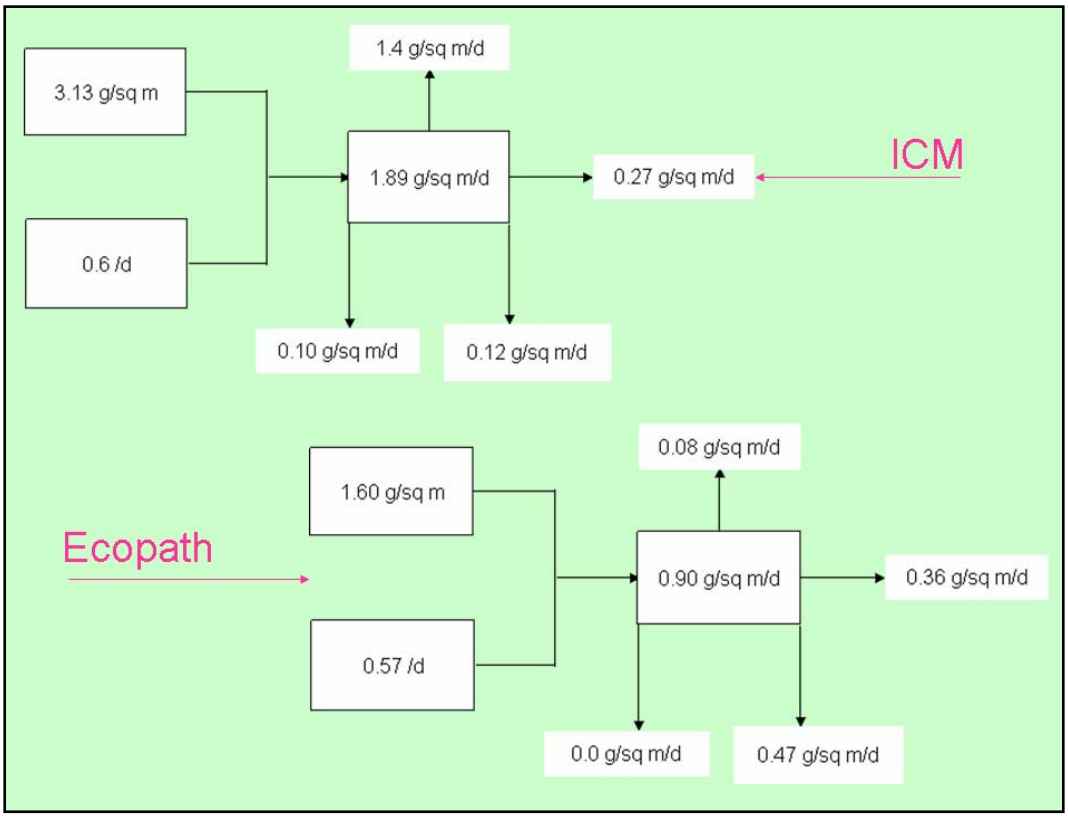

Figure 15. Phytoplankton carbon mass fluxes in upper Chesapeake Bay as represented by ICM and Ecopath.

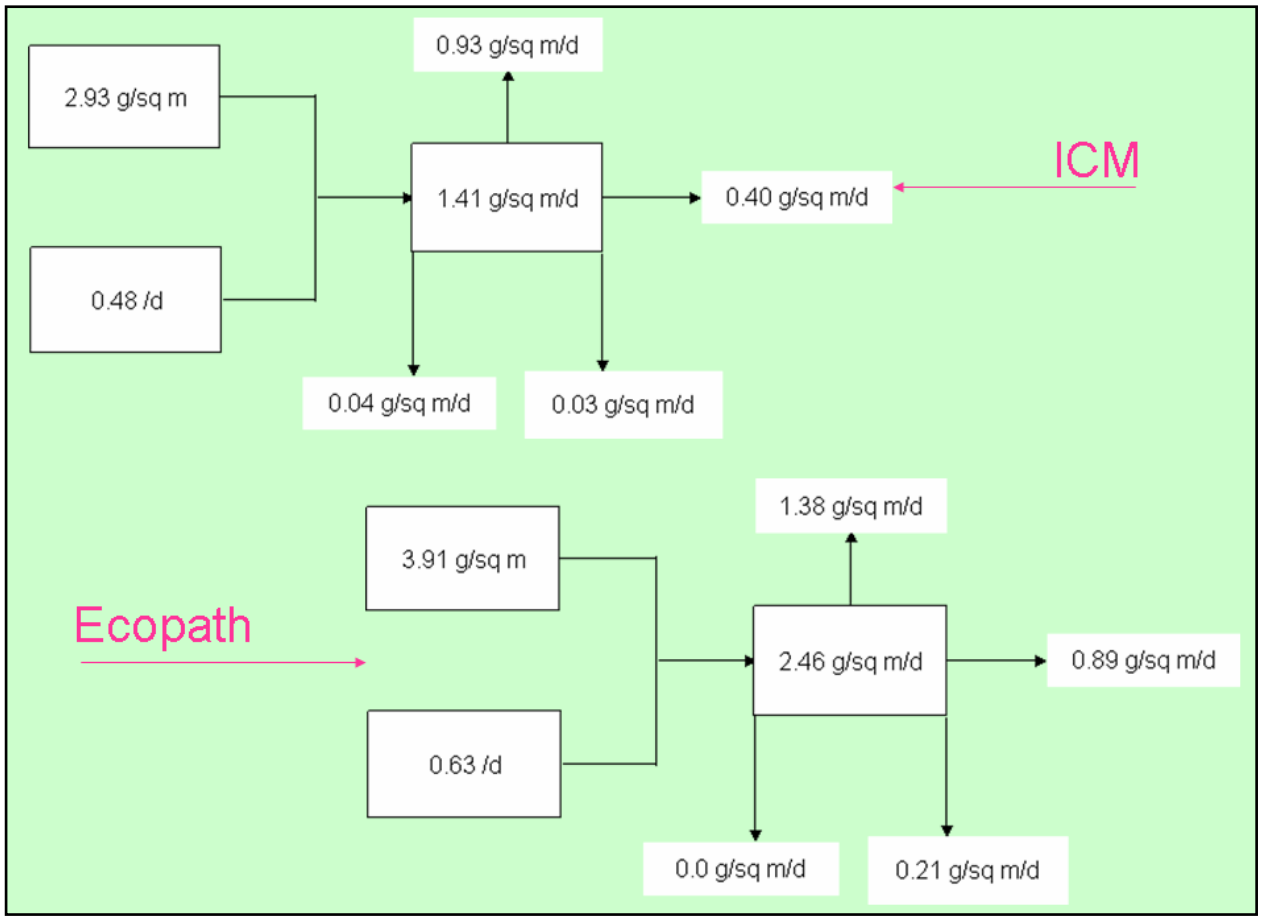

Figure 16. Phytoplankton carbon mass fluxes in mid Chesapeake Bay as represented by ICM and Ecopath.

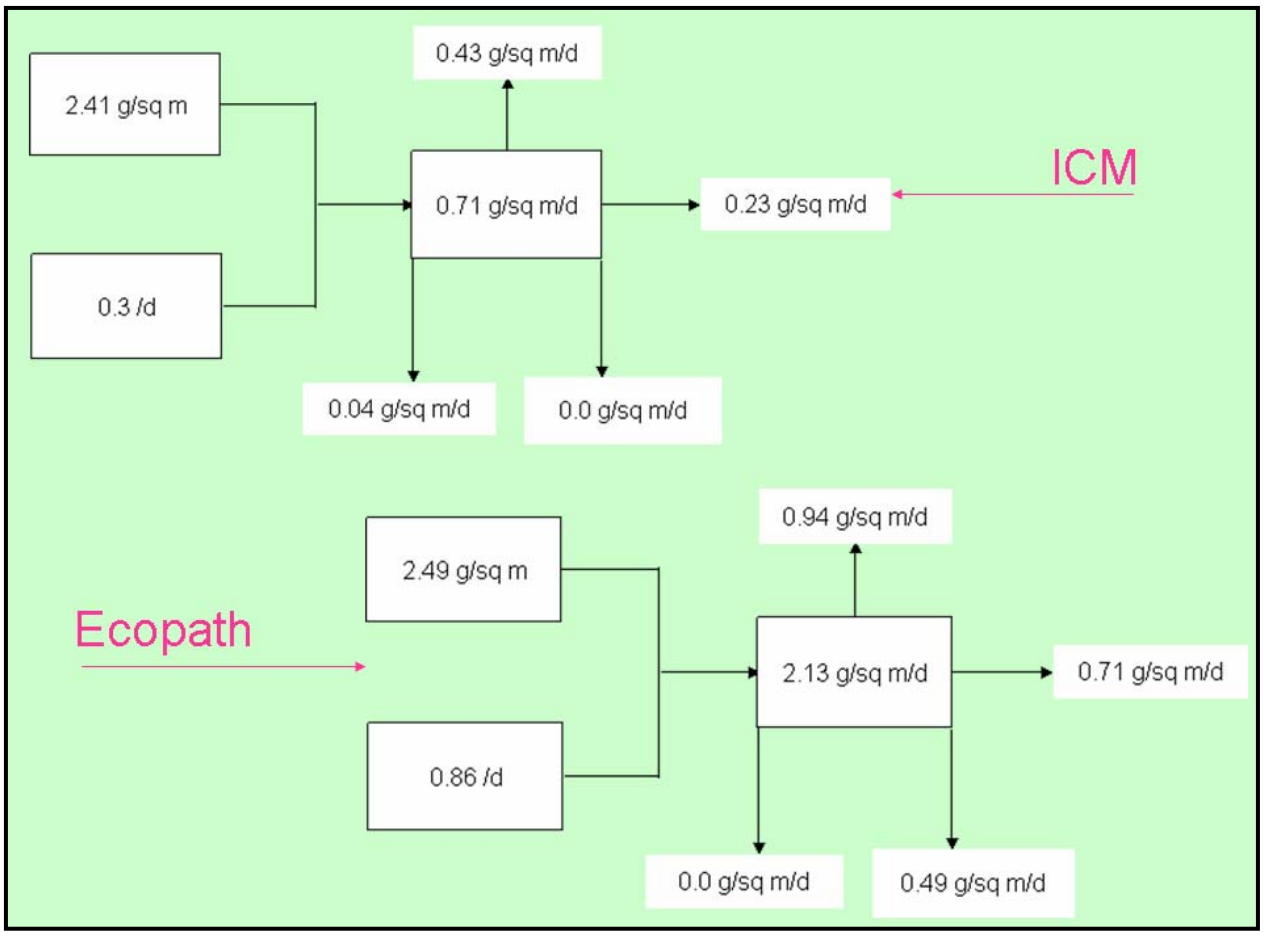

Figure 17. Phytoplankton carbon mass fluxes in lower Chesapeake Bay as represented by ICM and Ecopath.

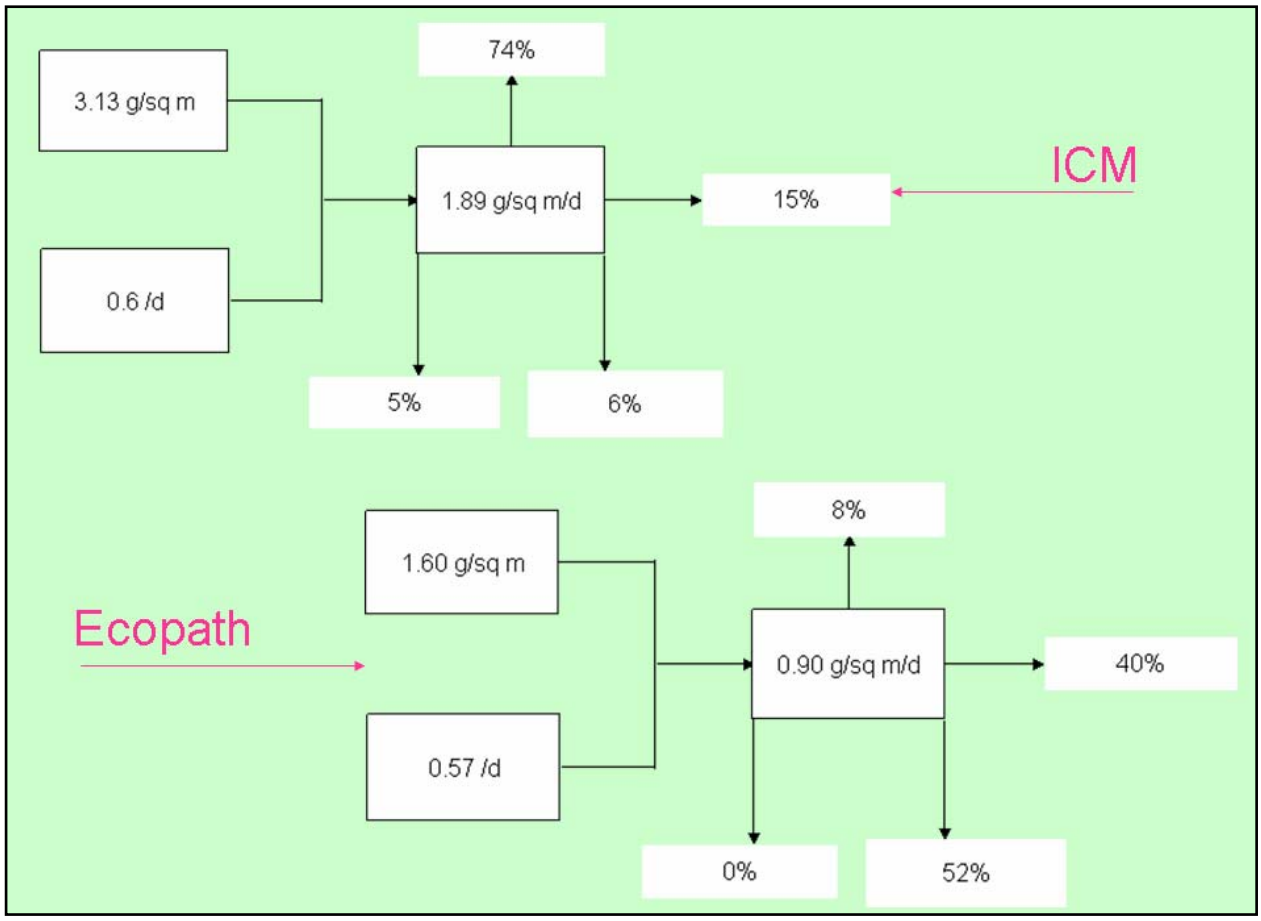

Figure 18. Phytoplankton carbon fluxes, as fractions of primary production, represented by ICM and Ecopath in upper Chesapeake Bay.

Independent comparison of ICM with observations indicates good agreement between computed and observed primary production in the mid bay (Cerco and Noel 2004a). Differences between ICM and Ecopath in the mid bay, aside from the gross versus net issue, must be attributed to interpretations of data and application periods. In the lower bay, ICM has been noted to under-compute production (Cerco and Noel 2004a). Here, an important distinction between Ecopath and ICM is noted. Production is input to Ecopath based on observations. In ICM, production must be computed based on nutrient inputs, nutrient transport, nutrient cycling, temperature, light attenuation, and other factors. We have found no combination of computed factors that will allow high algal production in the lower bay, far removed from upland nutrient sources.

The fractional distributions of algal production in the mid and lower bay are similar between the two models (Figures 19, 20). The largest fraction of algal production goes to detritus, followed by zooplankton. ICM

indicates direct settling of phytoplankton into the sediments, which is not represented in Ecopath, but the fraction is small. Ecopath includes benthic grazing by *Chaetopterus* in the lower bay, which is absent in ICM.

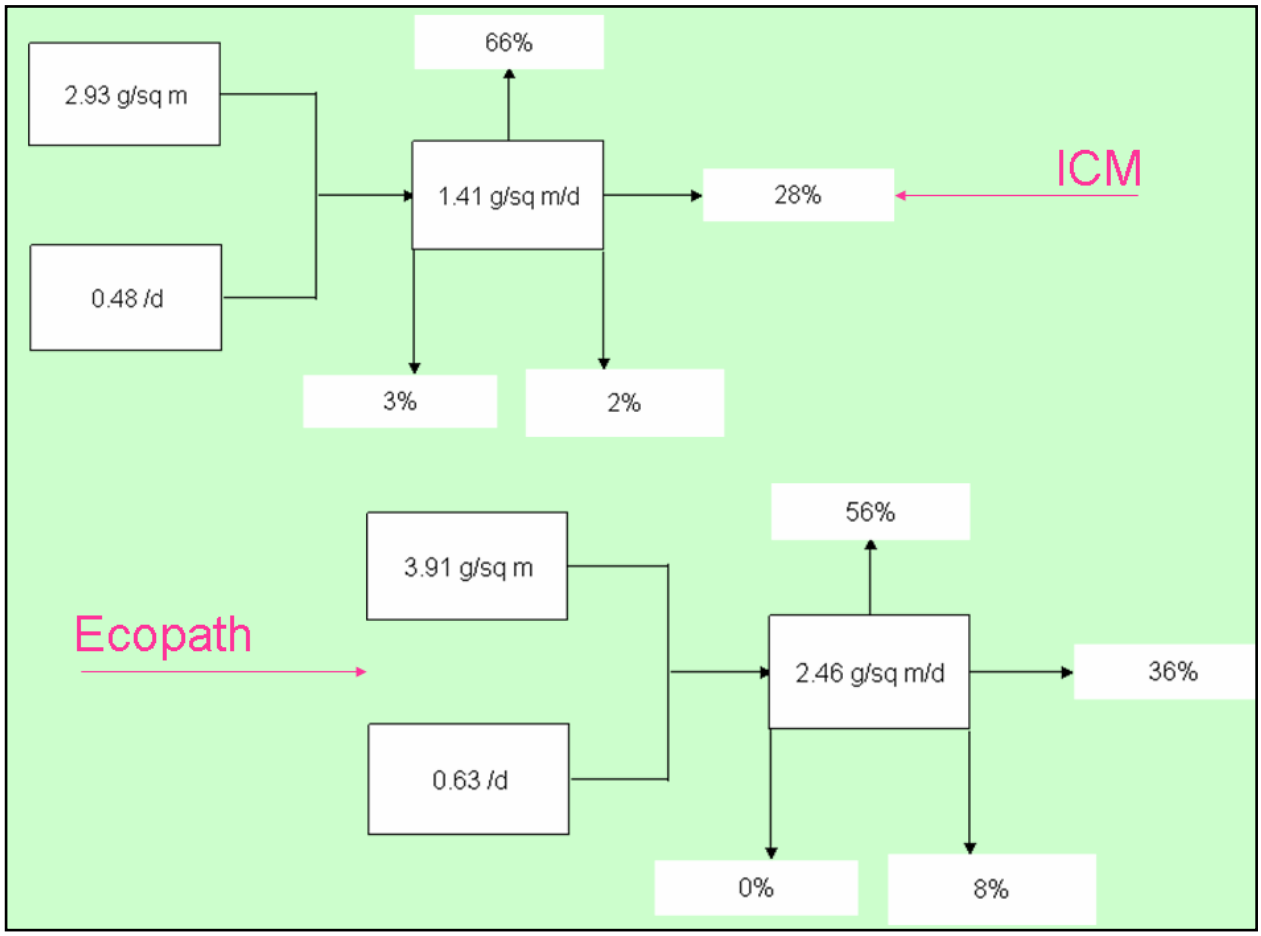

Figure 19. Phytoplankton carbon fluxes, as fractions of primary production, represented by ICM and Ecopath in mid Chesapeake Bay.

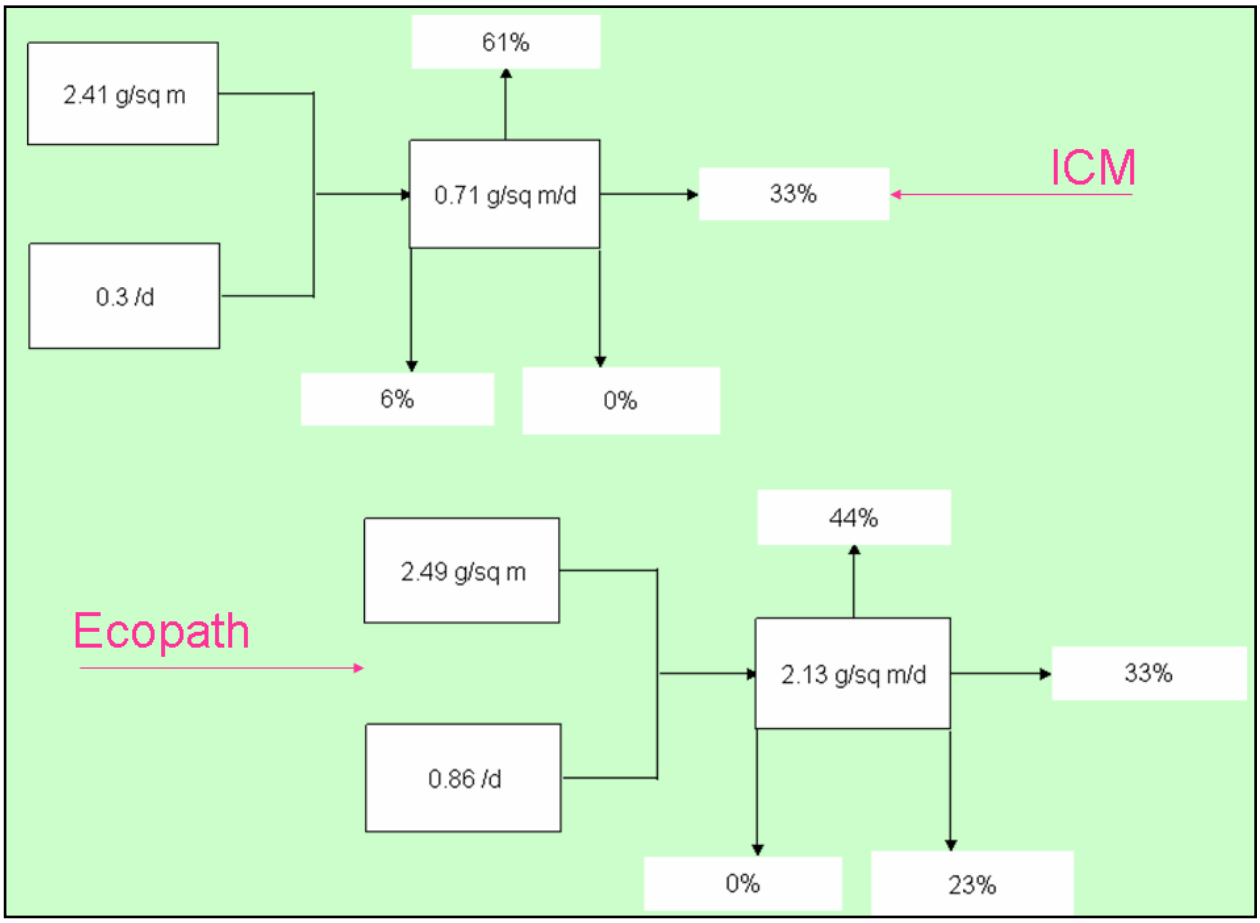

Figure 20. Phytoplankton carbon fluxes, as fractions of primary production, represented by ICM and Ecopath in lower Chesapeake Bay.

Zooplankton

Rates of total carbon grazed by microzooplankton in the two models (Figure 21) are not substantially different (Figures 22–24). The apparent differences are in the carbon sources. ICM microzooplankton primarily graze phytoplankton and detritus; Ecopath microzooplankton primarily graze phytoplankton and bacteria (categorized as “other”). The different sources are forced by model formulations. ICM does not explicitly include bacteria, which are a significant microzooplankton food source. In the absence of bacteria, ICM microzooplankton are allowed to directly graze dissolved organic carbon, which is a primary bacterial food source. The passage from dissolved organic carbon to bacteria to microzooplankton is reduced to passage from dissolved organic carbon to microzooplankton.

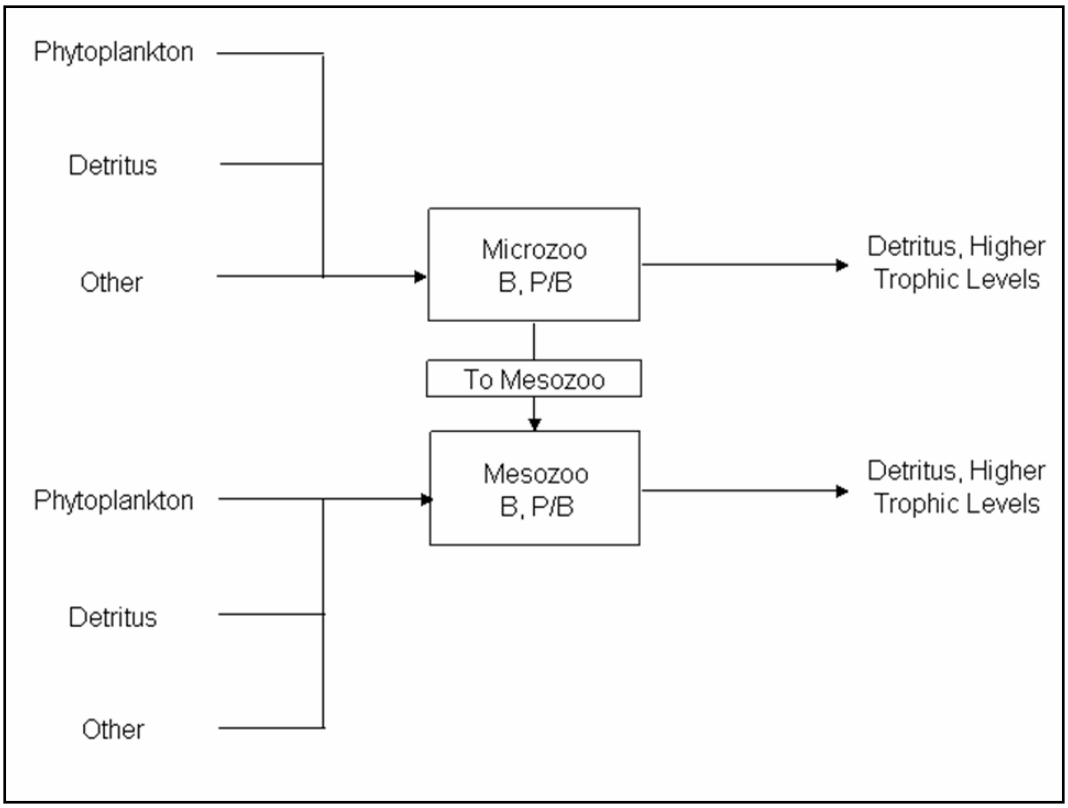

Figure 21. Schematic diagram of zooplankton carbon fluxes as represented by ICM and Ecopath.

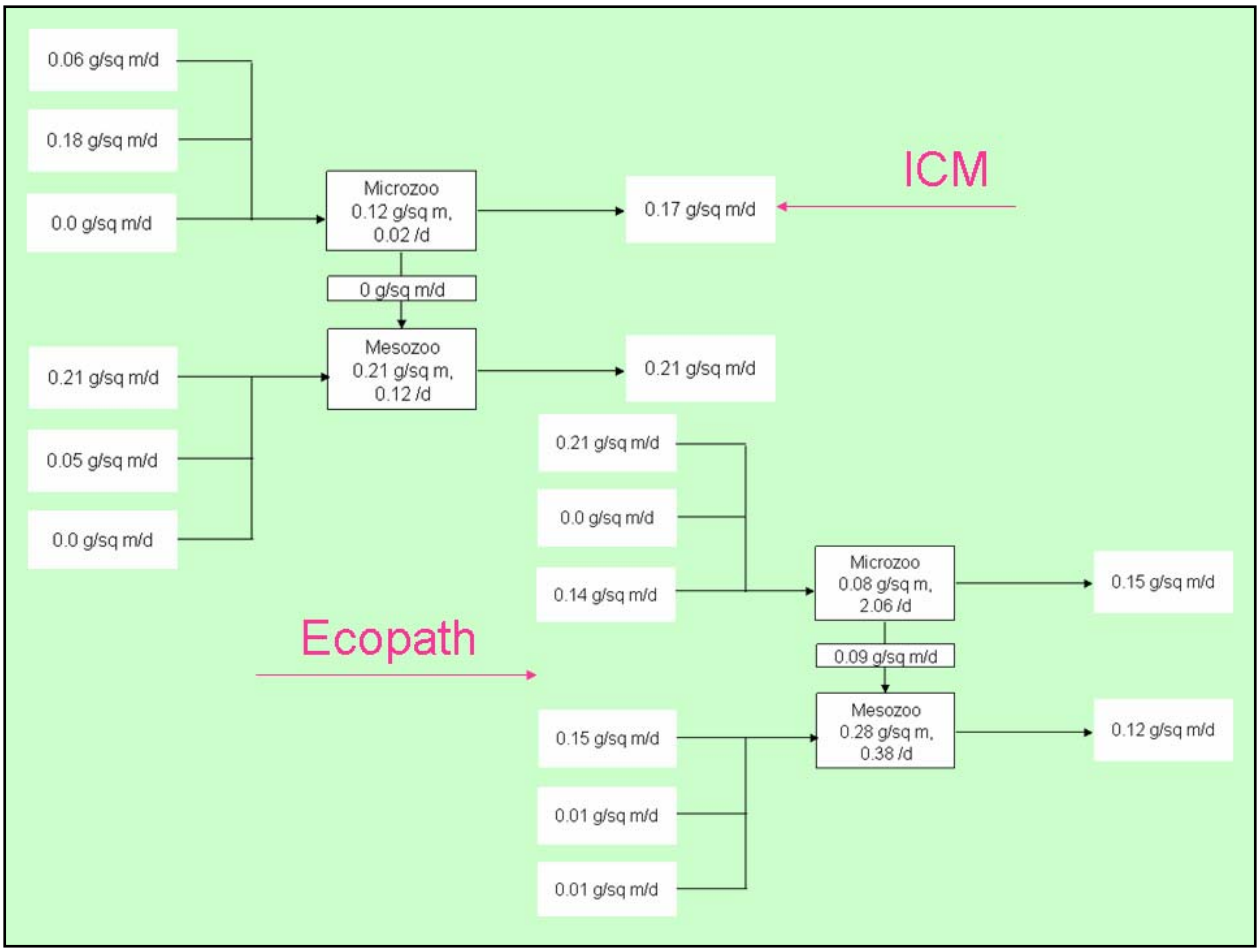

Figure 22. Zooplankton carbon mass fluxes in upper Chesapeake Bay as represented by ICM and Ecopath.

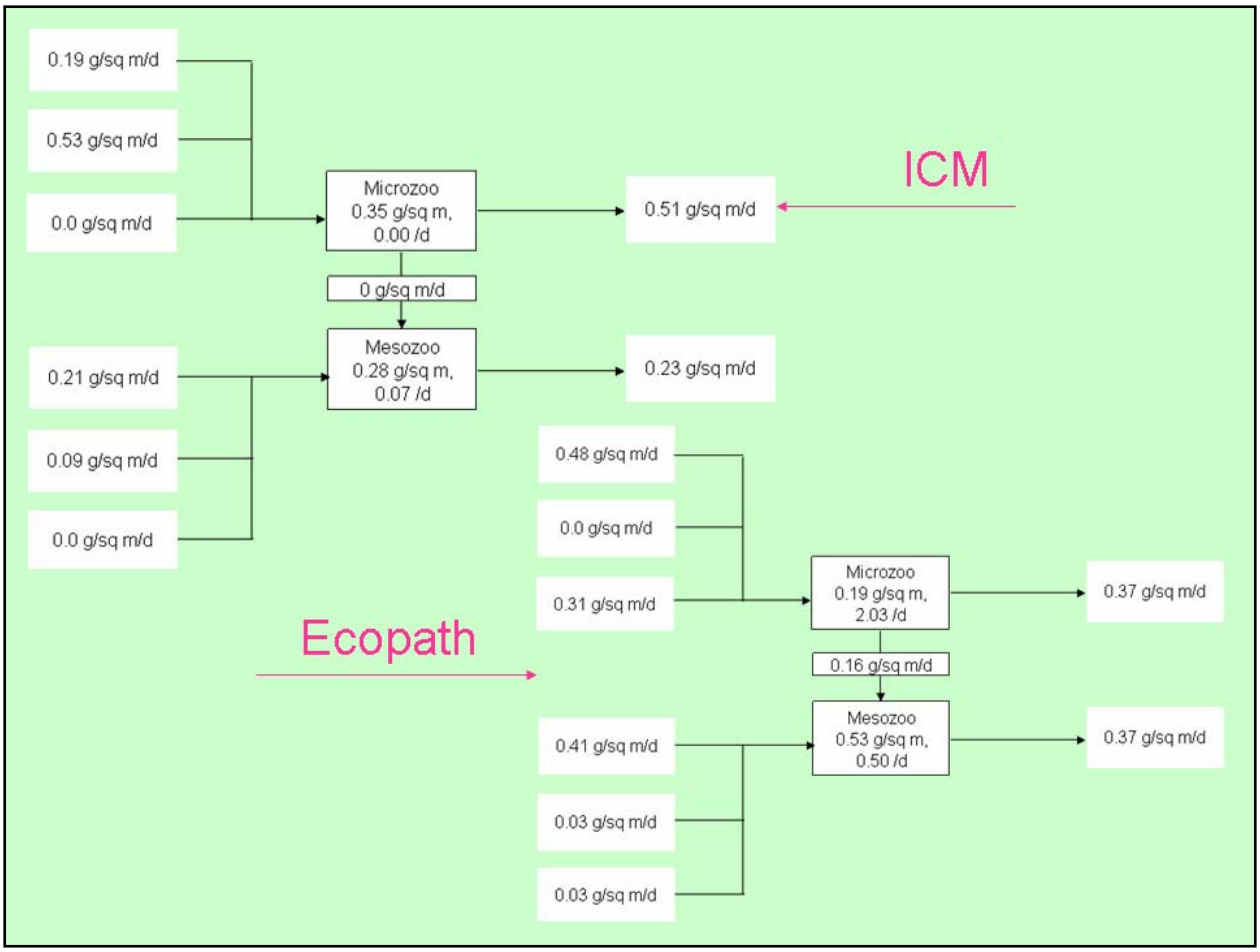

Figure 23. Zooplankton carbon mass fluxes in mid Chesapeake Bay as represented by ICM and Ecopath.

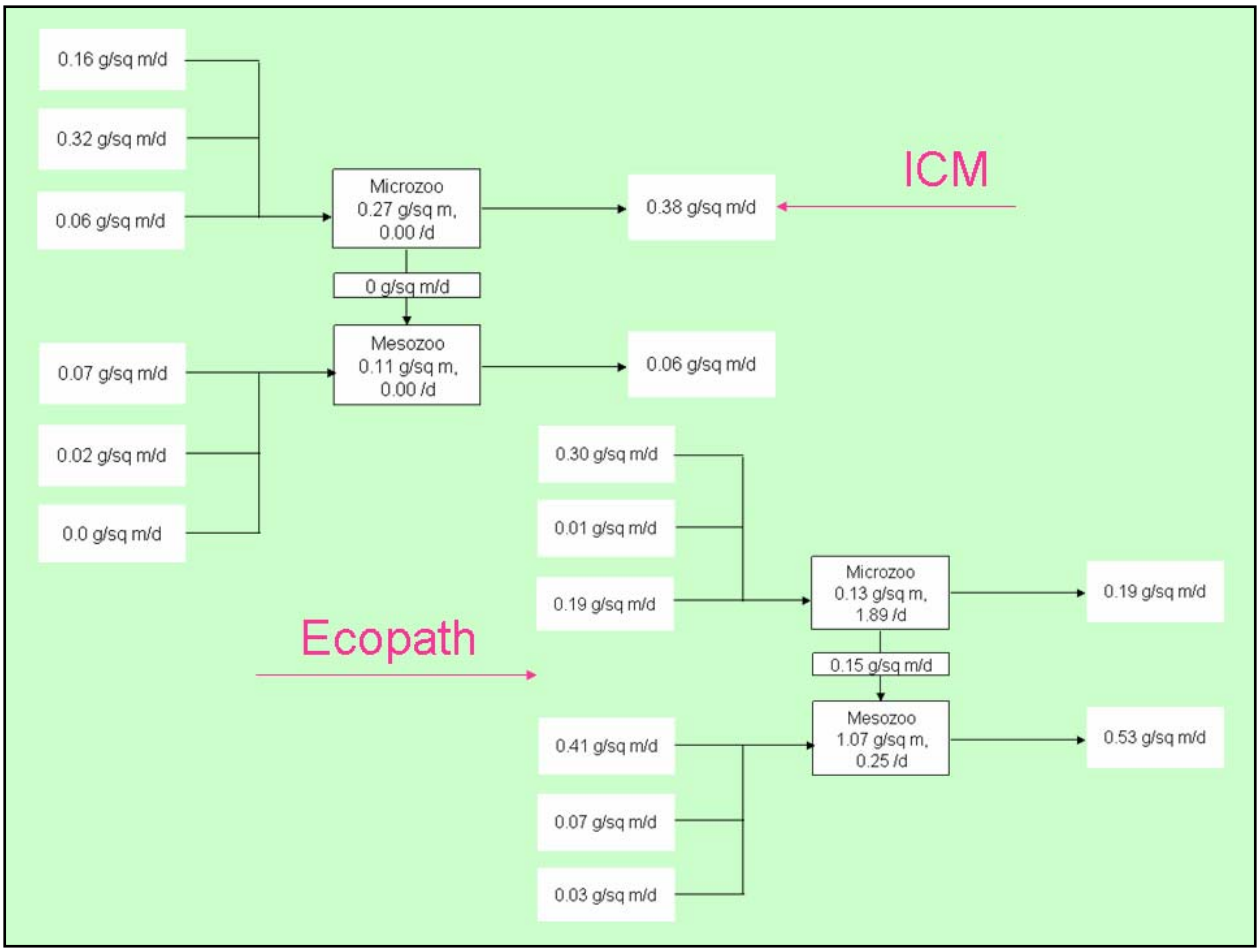

Figure 24. Zooplankton carbon mass fluxes in lower Chesapeake Bay as represented by ICM and Ecopath.

Rates of total carbon grazed by mesozooplankton in the two models are similar in the upper bay (Figure 22). From there, the models depart. Grazing diminishes with distance downstream in ICM and increases in Ecopath (Figures 23, 24). Trends in grazing correspond to patterns in algal biomass and production represented in the two models. The correspondence between phytoplankton and consumers is reasonable and suggests no adjustment in either model. A more significant difference is the grazing of microzooplankton. Virtually no grazing of microzooplankton by mesozooplankton occurs in ICM. Absent microzooplankton in their diet, ICM mesozooplankton take up a larger fraction of detritus than Ecopath mesozooplankton. The absence of grazing on microzooplankton is no doubt a function of the weighting factors used to determine mesozooplankton diet. Equal weighting factors were assigned to phytoplankton and microzooplankton. Consequently, diet composition is effectively proportional to biomass. Since phytoplankton biomass is much

greater than microzooplankton, grazing on phytoplankton is much greater than on microzooplankton.

Sediment-Water Fluxes

The benthic communities in the three Ecopath regions are differentiated largely by the nature and biomass of the suspension feeders (Tables 10-13). In the upper bay, suspension feeders consist largely of bivalves and are orders of magnitude more abundant than in the mid bay. Biomass increases from mid bay to lower bay, and the community changes from bivalve dominance to dominance by the polychaeate *Chaetopterus*. ICM also indicates greater bivalve abundance in the upper bay than in mid bay, but the difference between the two regions is not as great as in Ecopath. ICM does not represent polychaeate suspension feeders at all. The different representations of suspension feeders, combined with other factors, create distinctly different pictures of sediment-water carbon fluxes in the two models (Figure 25).

Gravitational settling is the dominant process by which carbon is transferred from water to sediments in ICM (Figures 26–28). The dominant transfer process varies by region in Ecopath. In the upper and mid bay, the largest net source to the sediments is an import representing carbon remaining from the spring diatom bloom. Import is also significant in the lower bay, although the greatest net source is deposition from suspension feeders. Benthic algal production is always greater in Ecopath than in ICM, but the difference in production is not always reflected in carbon flux to the sediments. A significant difference is that the Ecopath benthic algae release carbon to the water column, while ICM benthic algae do not.

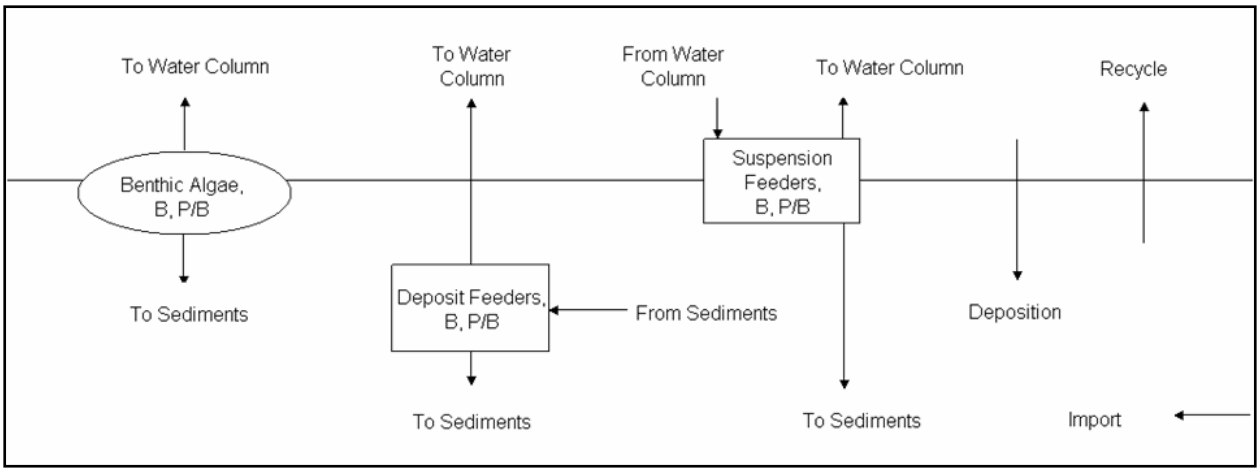

Figure 25. Schematic of detailed sediment-water carbon fluxes as represented by ICM and Ecopath.

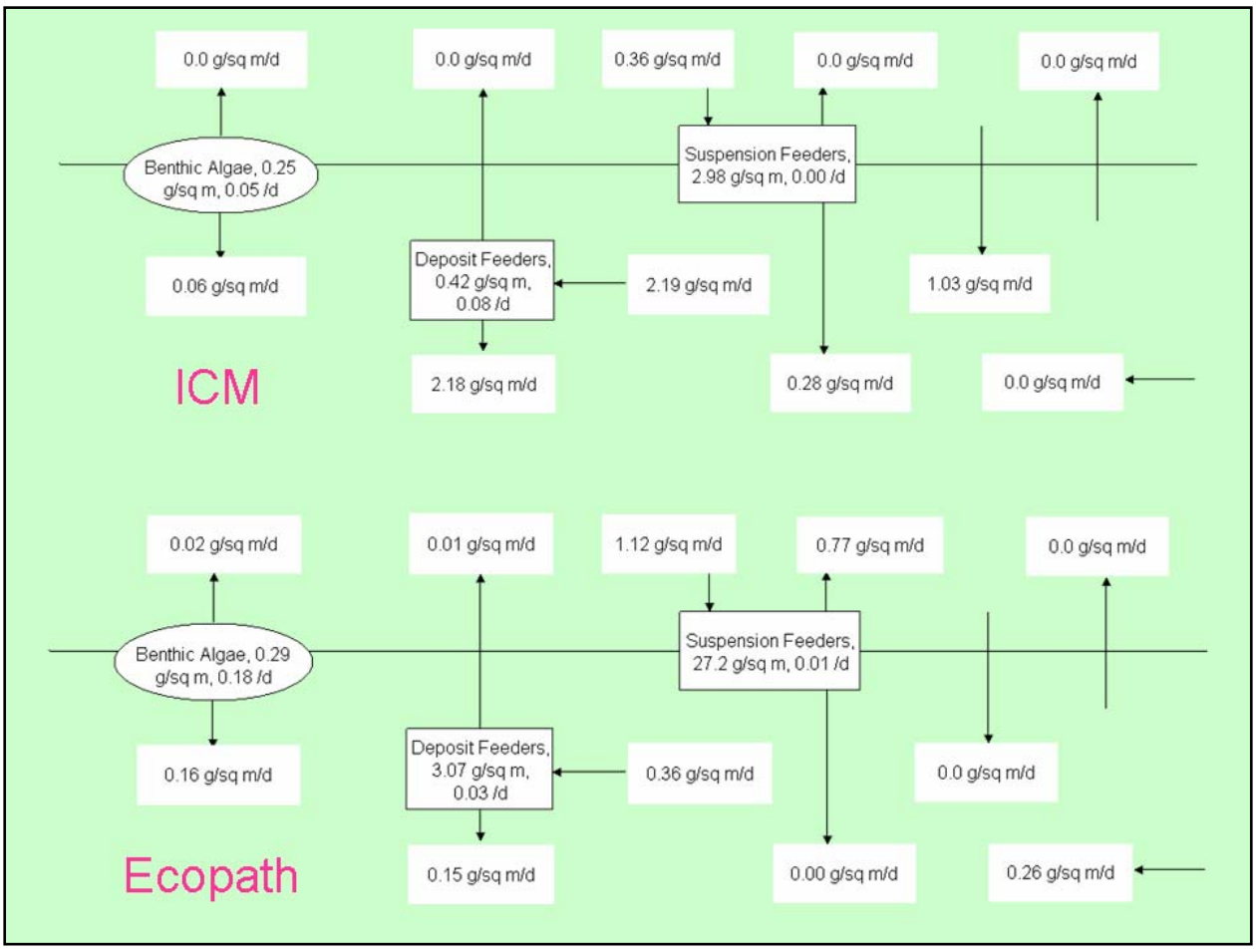

Figure 26. Sediment-water carbon fluxes in upper Chesapeake Bay as represented by ICM and Ecopath.

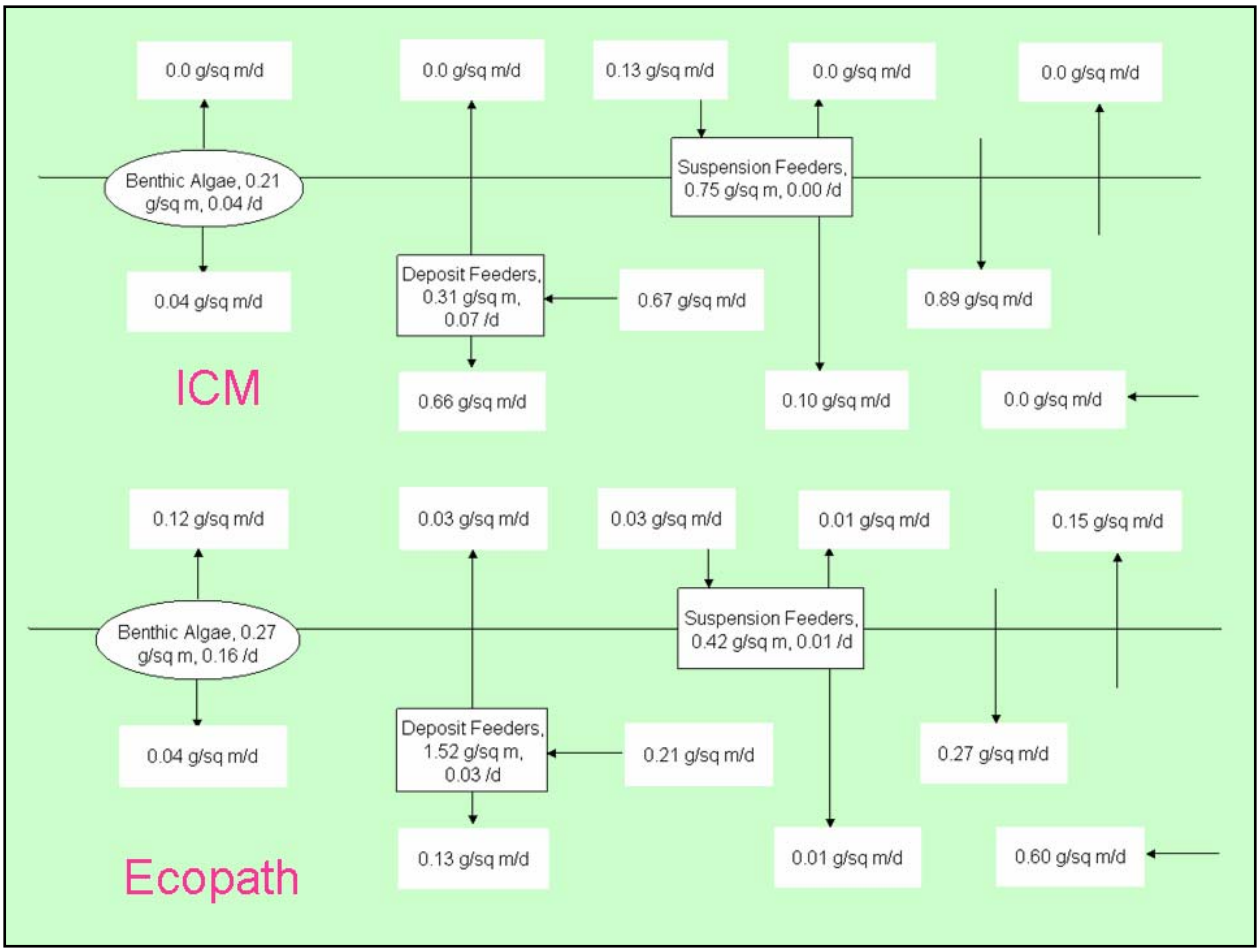

Figure 27. Sediment-water carbon fluxes in mid Chesapeake Bay as represented by ICM and Ecopath.

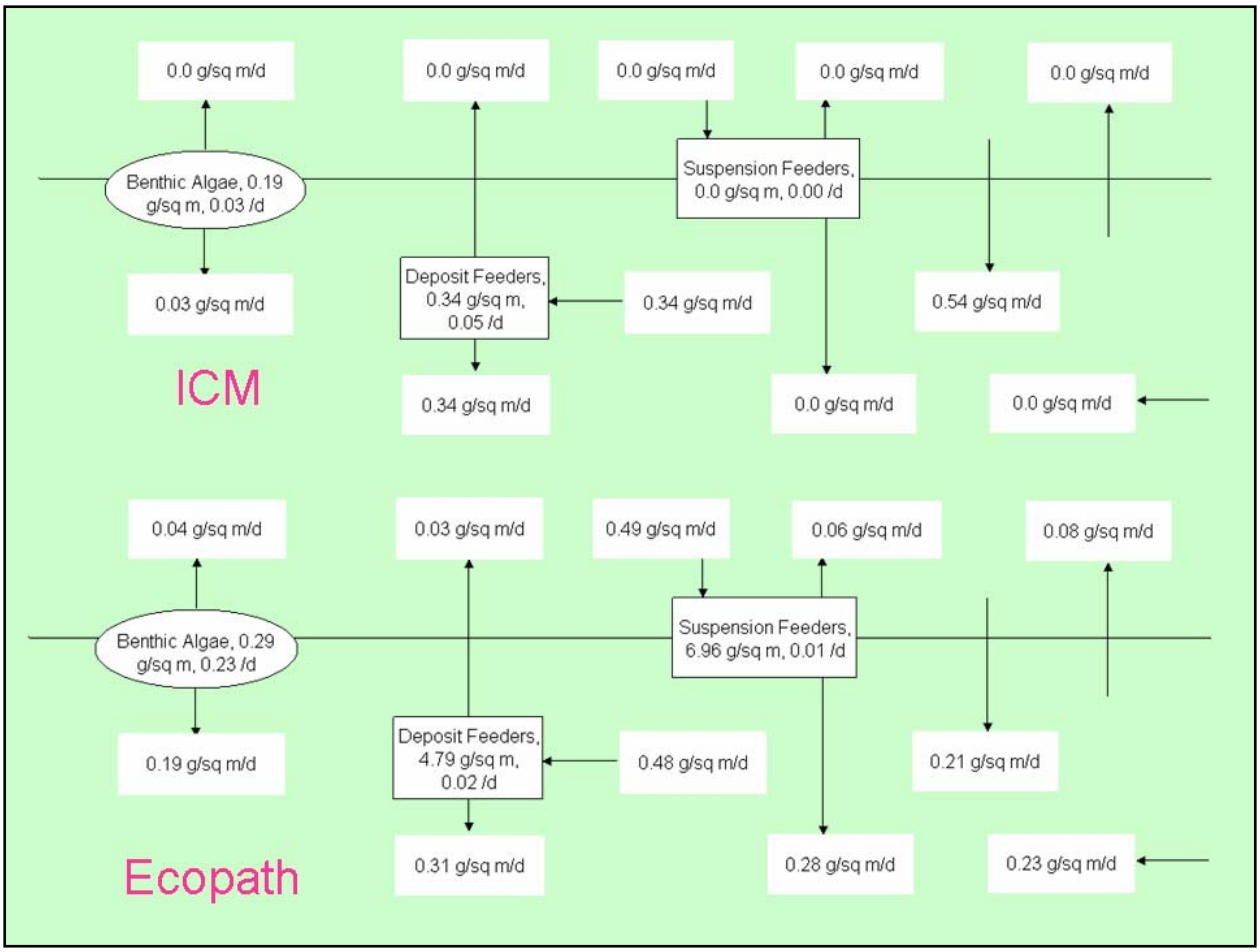

Figure 28. Sediment-water carbon fluxes in lower Chesapeake Bay as represented by ICM and Ecopath.

The requirement to produce mass balance in Ecopath leads to inconsistencies in several areas that are avoided in ICM. The most apparent of these is in the recycling of material consumed by suspension feeders. In the upper bay, 0.4% of suspension feeder consumption is deposited to the sediments, while 69% is recycled to the water column. In the mid bay, these fractions change: 41% of consumption is deposited to the sediments, while 34% is recycled to the water. In the lower bay, the fractions change again: 57% of suspension feeder consumption is deposited in the sediments, while 13% is recycled to the water column. A biological origin for the different fates of material released from suspension feeders in different regions is not apparent. In the absence of physical resuspension, the varying splits of material released by suspension feeders may incorporate resuspension effects such that more material eventually is routed to the water column in the shallow upper bay than in deeper downstream regions.

When the individual processes are aggregated into larger net fluxes (Figure 29), a distinguishing difference between ICM and Ecopath becomes apparent. The ICM sediments are a dead end. Carbon fixed by ICM benthic algae is deposited exclusively in the sediments, as is consumption not assimilated by deposit feeders and suspension feeders (Figures 30–32). Once deposited to the sediments, material remains there or else is lost through respiration. In contrast, material is recycled from the Ecopath sediments back to the water column. In Ecopath, benthic algae, deposit feeders, and suspension feeders all release material to the water column, augmented by carbon released by benthic bacteria. Releases are significant in the upper bay, such that Ecopath sediments are a net source of carbon to the water column in summer. The source is supported by carbon carried over from the spring algal bloom. In mid bay, summer fluxes of carbon from the water to sediments are almost exactly balanced by returns from the sediments to the water. As with the upper bay, the sediment release is supported by carry-over from the spring bloom. Only in the lower bay are Ecopath sediments a net sink of carbon during summer.

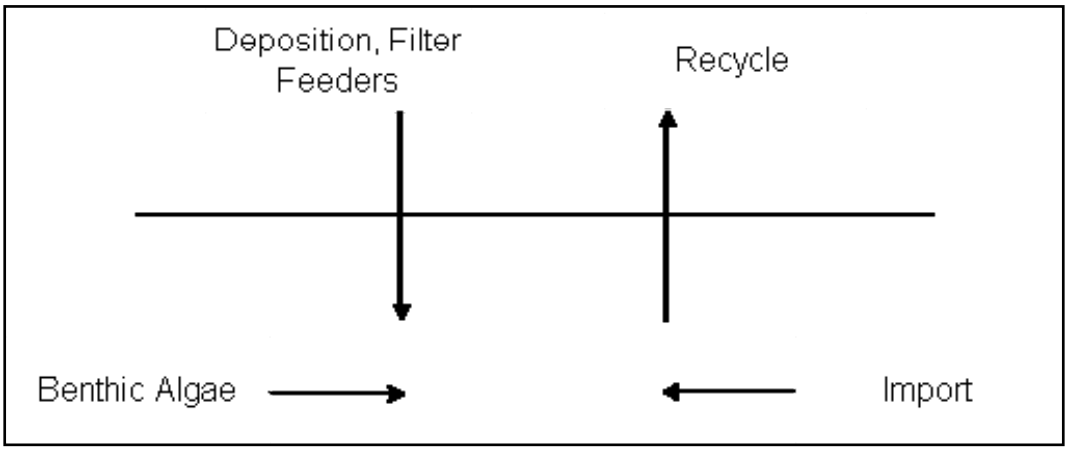

Figure 29. Schematic of aggregated sediment-water carbon fluxes as represented by ICM and Ecopath.

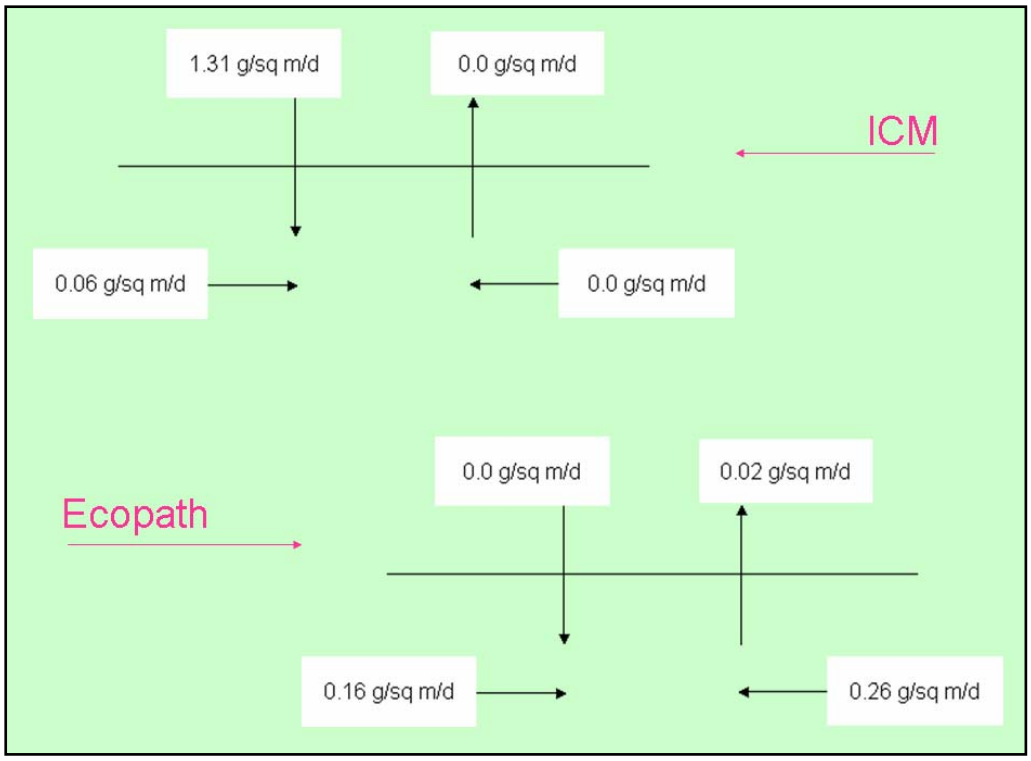

Figure 30. Aggregated sediment-water carbon fluxes in upper Chesapeake Bay as represented by ICM and Ecopath.

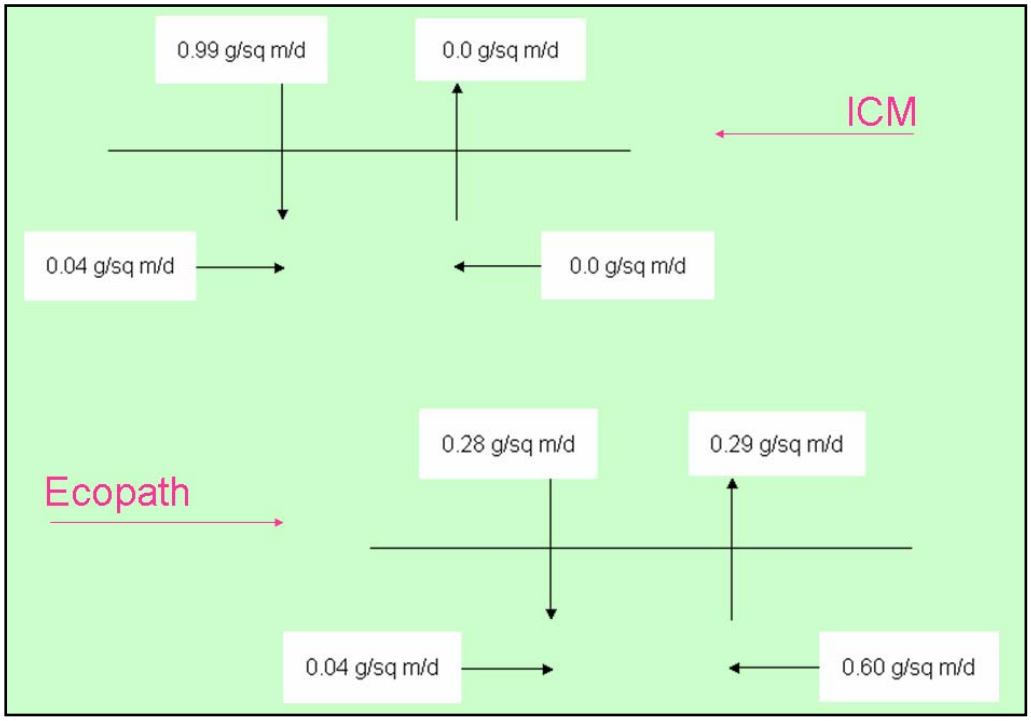

Figure 31. Aggregated sediment-water carbon fluxes in mid Chesapeake Bay as represented by ICM and Ecopath.

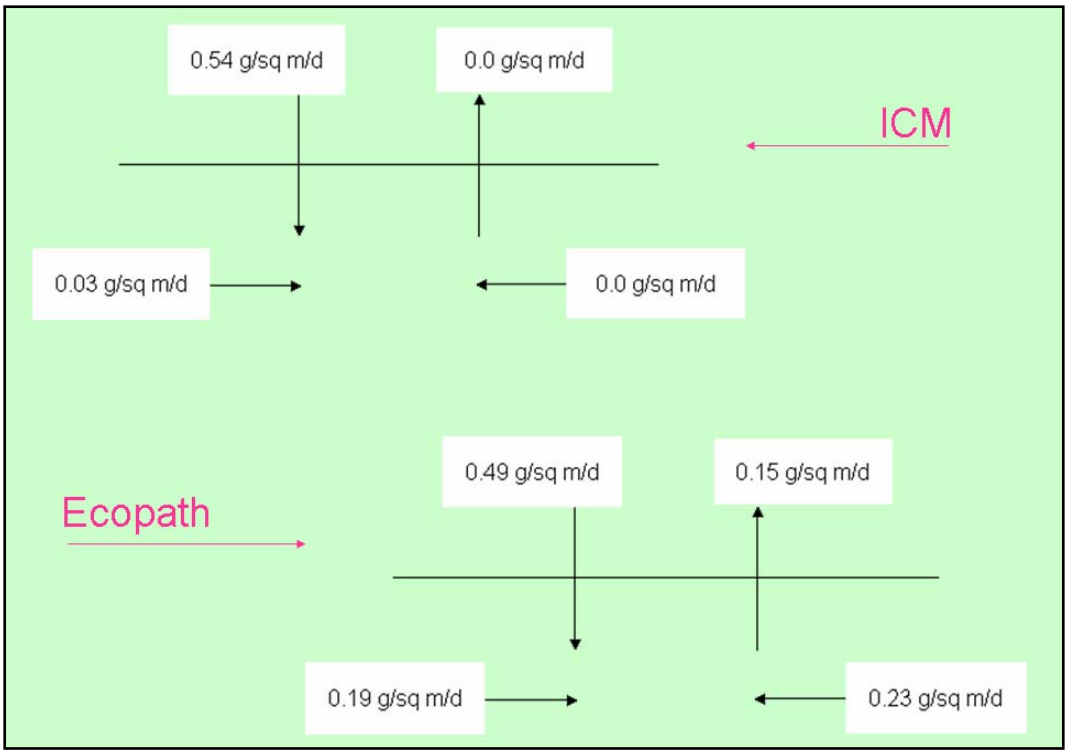

Figure 32. Aggregated sediment-water carbon fluxes in lower Chesapeake Bay as represented by ICM and Ecopath.

Conclusions

The carbon cycles of both ICM and Ecopath are driven by primary production, the largest fraction of which originates with phytoplankton. Primary production in ICM is computed from first principles, based on temperature, light, and nutrient availability. Primary production is input to Ecopath based on observed values. Production computed by ICM is double the Ecopath input in the upper bay, roughly equivalent in the mid bay, and less than Ecopath in the lower bay. The excess ICM production in the upper bay coincides with an under-representation of benthic suspension feeders. Improved representation of these organisms, which feed on phytoplankton, is recommended as a way of reducing ICM algal biomass and production into the observed range. A shortfall in computed production in the lower bay has been noted previously (Cerco and Noel 2004a), and substantial effort has been devoted to remedying the deficiency. The path to increasing production in this region is not clear. Kemp et al. (1997) suggest that production in the channel of the lower bay is supported by nutrient recycling in the shoals. Increased attention to processes that recycle nutrients and direct them from shallows to deep regions may prove worthwhile.

Ecopath mass balances suggest that carbon moves in both directions across the sediment-water interface. In contrast, ICM sediments are exclusively a carbon sink. A persistent feature of ICM is under-representation of anoxia in the lower bay. Kemp et al. (1997) suggest that respiration in the channel of the lower bay is supported by carbon fixed in the shoals and transported to the channel. Refinement of ICM is recommended to recycle sediment material back to the water column. This recycling will move the model representation towards the process suggested by Kemp et al. (1997).

ICM zooplankton production is negligible in summer. This property has been previously noted and is emphasized through comparison with Ecopath. ICM zooplankton temperature relationships should be re-evaluated to provide higher filtration rates in summer.

The ICM/Ecopath comparisons provide excellent guidance for revisions of processes in ICM. Complete consistency between the two models is unlikely to be attained, however. Difficulties reconciling primary production computed by ICM with production input to Ecopath have already been noted. A second problem is that models such as ICM provide comprehensive, system-wide representations. Arbitrary, local variations in formulation or parameterization are avoided to the greatest extent possible. In contrast, the present Ecopath application is three independent model applications. No unity is sought between the regions, so large differences can occur in parameter values and mass fluxes. The regional difference in material recycling by suspension feeders, noted above, is an example. Still, the comparisons between the eutrophication model and the network model are most worthwhile and are recommended whenever an independent network model is available.

6 Ecosystem Projections from ICM

Background

Managing nutrients based on a "top down" approach by increasing algal predators requires the ability to model higher trophic levels such as fish, as well as the eutrophication processes driving production of primary producers in an aquatic ecosystem. ICM and EWE were two models selected for linkage to investigate the "top down" approach of nutrient control. ICM is a time- and spatial-varying eutrophication model that uses nutrient loads to predict primary producers, while EWE is a static mass balance model representing an average time period (e.g., season or year) and uses values of primary producers and other groups to predict fish biomass. Linking the two models will provide the means of going up the food chain by trophic levels from supplying nutrients to primary producers, then primary producers to fish. As a first attempt in understanding the effect of nutrient management on higher trophic levels, ICM production can be inserted into EWE to see if fish biomass can be supported in the mid Chesapeake Bay.

Primary producers are seen as the backbone of a viable ecosystem. In an aquatic system, all groups of phytoplankton are the major primary producers. They provide the necessary energy in the form of carbon production for increased biomass. They are the bottom tier of the food chain and pass energy and nutrients up through a chain of consumers to help sustain life at upper trophic levels (Kiely 1997).

Net primary production is the rate at which new organic matter or energy of a system accumulates minus energy needed for respiration (Campbell 1987). This variable, along with primary producer biomass, is common to ICM and EWE. Since both models have been applied to the Chesapeake Bay mainstem (Hagy 2002, Cerco and Cole 1994), replacing these EWE parameters with ICMs made it possible to examine questions of higher trophic level sustainability. Although the modeling frameworks of the models are vastly different, a mass balanced system results once both models have been calibrated. As demonstrated by Tillman et al. (2006), ICM can reasonably predict the rate of primary production and phytoplankton biomass similar to values used in the EWE calibration run given the appropriate boundary conditions.

With net primary production of carbon by phytoplankton being an essential process to sustain upper trophic levels, an analysis was devised to see the implications of substituting values of net primary production predicted by ICM into the EWE calibration input data set developed by Hagy from literature values for the mid bay (Hagy 2002). Interchanging ICM's values with EWE's will also help further the possibility of linking the two models or if not linking, then perhaps using both models simultaneously to answer management questions for fishery improvement or nutrient control. A number of questions addressed during this analysis were:

1. Are the biomasses of fish and other trophic levels (higher than phytoplankton) computed in Ecopath consistent with primary production computed in ICM? This run was conducted to see if simply replacing ICM primary producers and production/biomass (P/B) ratios could maintain mass balance and give similar results to Hagy's EWE base run. If not, what has to be done to re-establish mass balance?
2. Are the biomasses of fish and other trophic levels (higher than phytoplankton) computed in the EWE base run consistent with primary production computed in ICM from the 90% nutrient reduction run? Reducing ICM nutrients loads by 90% was an attempt to produce primary producer biomasses similar to what Hagy used for his 1950s restored bay run. ICM nutrients loads were initially reduced by 50%. When this did not produce the results needed, ICM loads were further reduced by 90%.
3. What happens when the menhaden biomass is increased 20% in the EWE base input data file? Is this consistent with increasing predation by 20% in the ICM base run and substituting the resulting primary producer biomasses in EWE? Do these EWE runs produce similar results? In one run the predators are increased, while in the other the preys are decreased.
4. How does the EWE 1950s restored bay run compare to the EWE base run where values for primary producer biomass and P/B ratios were replaced with ICM values from the 90% nutrient reduction run? According to Hagy (2002), conditions in the Chesapeake Bay were very different than they are now. For one thing, the bay water was much clearer than what exists today. Will simply changing primary producer biomass produce the same biomass elsewhere?

Analysis Procedure

For this analysis, two calibrated models that had been applied to the same study area (e.g., mid bay) were used: ICM and EWE. The Cerco and Noel

(2004b) kinetics were adapted to the Cerco and Cole (1994) grid to produce the ICM calibration run representing 26 water quality constitutes. Data used in this calibration effort were collected under the Chesapeake Bay Monitoring Program for 1984–1994, and results from the calibration run for 1984 was used for this study. Hagy (2002) had previously calibrated EWE for a total of 34 groups. He also used data in the EWE calibration from the Chesapeake Bay Monitoring Program for the same years as ICM calibration as well as data from literature. These calibration runs were considered base runs and will be referred to as such for this analysis.

Several steps were performed in completing the analysis, including:

- Making three ICM model runs to get values for common variables of primary producer biomasses and P/B ratios to substitute into the EWE runs.
- Substituting ICM common variables of primary producer biomasses and P/B ratios from the three ICM runs into the EWE base run.
- Re-establishing mass balance in the modified EWE model runs containing the ICM primary producer biomasses and P/B ratios when necessary.
- Making a run of the EWE base model with the original menhaden biomass increased and re-establishing mass balance if necessary.

The modeling effort began by conducting ICM runs to get values for common variables/"hooks" used in substitution into the EWE base input data files originally developed by Hagy. There were three runs conducted: (1) the ICM calibration run, considered the base run, (2) the ICM 90% reduced nutrient loading run, and (3) the ICM 20% increase in predation run. ICM output from these runs was then processed for the common "hooks" between the two models into units and regional/seasonal averages compatible to EWE units. All "hooks" had previously been identified by Tillman et al. (2006), but as mentioned above, only the "hooks" of primary producer biomasses and net primary production rates were needed for this analysis.

The EWE runs made were those starting with the EWE base input data file and substituting the ICM common "hooks" of primary producer biomasses and P/B ratios for all three ICM runs. Also a EWE base run was conducted

with the menhaden biomass increased by 20%. No new EWE models were created from scratch. In all, four modified EWE base runs were made.

Model and data preparations to make runs to address the questions posed above were similar for all runs. Beginning with the first question, values for primary producer biomasses and P/B ratios from the ICM base run were substituted into the EWE base run input data file. Groups considered primary producers were net phytoplankton, picoplankton, microphytobenthos, and submerged aquatic vegetation (SAV). Because the ICM net phytoplankton value includes picoplankton, the picoplankton biomass used for substitution had to be estimated. The percentage of picoplankton compared to net phytoplankton in the EWE data set was found by summing the values of net phytoplankton and picoplankton, dividing this number into picoplankton biomass, and multiplying by 100. ICM net phytoplankton biomass was then multiplied by this percentage to get the picoplankton biomass needed for substitution. The ICM original net phytoplankton value was then adjusted to account for the picoplankton value used in the modified EWE input data file. The ICM value for P/B ratio for all groups except picoplankton was calculated by dividing the net primary production of a group by the biomass of that group. Like biomass, the picoplankton P/B value used for substitution was estimated based on the percentage of picoplankton production to the total production (calculated as the sum of net phytoplankton and picoplankton production) in the EWE base input data. Adjustment to the ICM net phytoplankton P/B ratio was made to account for this. The new values of primary producer biomasses and P/B ratios were substituted into the EWE base input data set, with all other groups remaining unchanged. This was saved as a modified EWE base model identified as EWE-ICM base.

Addressing the second question above again involved substituting ICM "hooks" of primary producer biomasses and P/B ratios into the EWE base run, but this time from the ICM run with nutrient loads reduced by 90%. This run was conducted to see if replacing the EWE base values with values from the ICM reduced nutrient run could produce results similar to the EWE 1950s restored bay run conducted by Hagy. The same groups discussed above were considered primary producers. ICM net phytoplankton and picoplankton biomasses were estimated as before, as well as their P/B ratios. Again, only the primary producer biomasses and P/B ratios were substituted for the EWE values, while all other groups

remained unchanged. This was saved as a modified EWE base model identified as EWE-ICM 90%R.

Making two runs using a modified version of the EWE base run addressed the third question. First, modifications were made to the EWE base input data file by simply increasing menhaden biomass by 20% without using any ICM output. Ortiz and Wolff (2002) performed a similar assessment on increased scallops (*A. purpuratus)* in the subtidal area in Tongoy Bay (Chile). All other group variables remained the same for this run. This run was saved as a modified EWE base model identified as EWE-M20%. The second run to address question 3 was made by replacing primary producer biomasses in the EWE base input data file with values from an ICM run with predators increased by 20%. This ICM run was performed to emulate the EWE run with menhaden increased by 20%. This run was saved as another modified EWE base model identified as EWE-ICM 20%P. These model runs were called the menhaden runs.

The final question was addressed without making any new runs with ICM or EWE. By using results from the EWE 1950s restored mid bay run developed by Hagy and the modified EWE-ICM 90%R run, comparisons were made.

Mass Balancing EWE

With all the ICM runs completed and substitutions of common "hooks" made into the EWE base model, mass balance had to be re-established for the modified EWE models. This was done through reparameterization of the model [similar to the procedure described by Ortiz and Wolff (2002) and Kavanagh et al. (2004)].

In EWE, a set of linear equations representing all the groups modeled are set up and solved for one of four parameters [for a discussion of the equations and parameters, see Christensen et al. (2004)]. These parameters are biomass, P/B ratio, consumption/biomass ratio (C/B), and ecotrophic efficiency (EE). In this study, the unknown parameter was EE, which is defined as the portion of production utilized by the system. The value of EE must be between zero and one. Having EE > 1 for a group indicates that the system is overutilizing that group, so other steps have to be taken to reach mass balance. These steps included reducing predator biomasses of groups having EE > 1 and/or adjusting the diet composition of predators when necessary. This was an iterative procedure, since

making these adjustments did not always produce EE < 1 for a group. Sometimes if a predator biomass was reduced too much, EE > 1 resulted for other groups utilizing this predator. When this happened, adjustments had to be made again until the EEs of all groups involved were less than one.

Results and Discussion

ICM was used to predict carbon production for the mid CB for three separate runs to replace common variables of primary producer biomasses and P/B ratios in the original EWE base model developed by Hagy. This was an exercise to see if ICM predictions could maintain the higher trophic level organisms in EWE for the mid CB. In addition to the three EWE models developed from using ICM variables, another EWE model was developed by increasing the original menhaden biomass by 20%. Results from these model runs are presented in Figures 33–43. In the figure legends and axis titles, the EWE runs are identified with the following abbreviations:

- EWE Base is Hagy's original mid CB run.
- EWE-ICM Base is Hagy's original mid CB EWE run with ICM base values of primary producer biomasses and P/B ratios substituted.
- EWE-ICM 90%R is Hagy's original mid CB EWE run with ICM 90% nutrient reduction values of primary producer biomasses and P/B ratios substituted.
- EWE-ICM 20%P is Hagy's original mid CB EWE run with values of primary producer biomasses and P/B ratios from the ICM run with a predation increase of 20% substituted.
- EWE-M20% is Hagy's original mid CB run with menhaden increased by 20%.
- EWE 1950s restored bay is Hagy's original mid CB EWE 1950s restored bay run.

ICM Base Primary Production Replaced in EWE Base Run

Differences in biomass between the EWE (blue) and ICM (red) values of primary producers for the base runs are shown in Figure 33. In terms of biomass, net phytoplankton was the most important of the primary producers. Values for net phytoplankton and estimated picoplankton from the ICM base run were similar to the EWE base values Hagy obtained from literature and monitored data. The greatest differences between the ICM

and EWE primary producers occurred for microphytobenthos and SAVs. ICM's microphytobenthos biomass was slightly less than half of the EWE value, and ICM's SAV biomass was more than double the EWE value. Comparison of P/B ratios in Figure 34 shows that values from the ICM base run (red) are less than the EWE values (blue) except for picoplankton. This suggests that net primary production rates from ICM are lower. The picoplankton P/B ratio is about the same as EWE's value. This was probably because the estimate of this value was based on the percentage of picoplankton production from total production of net phytoplankton and picoplankton in the EWE base run.

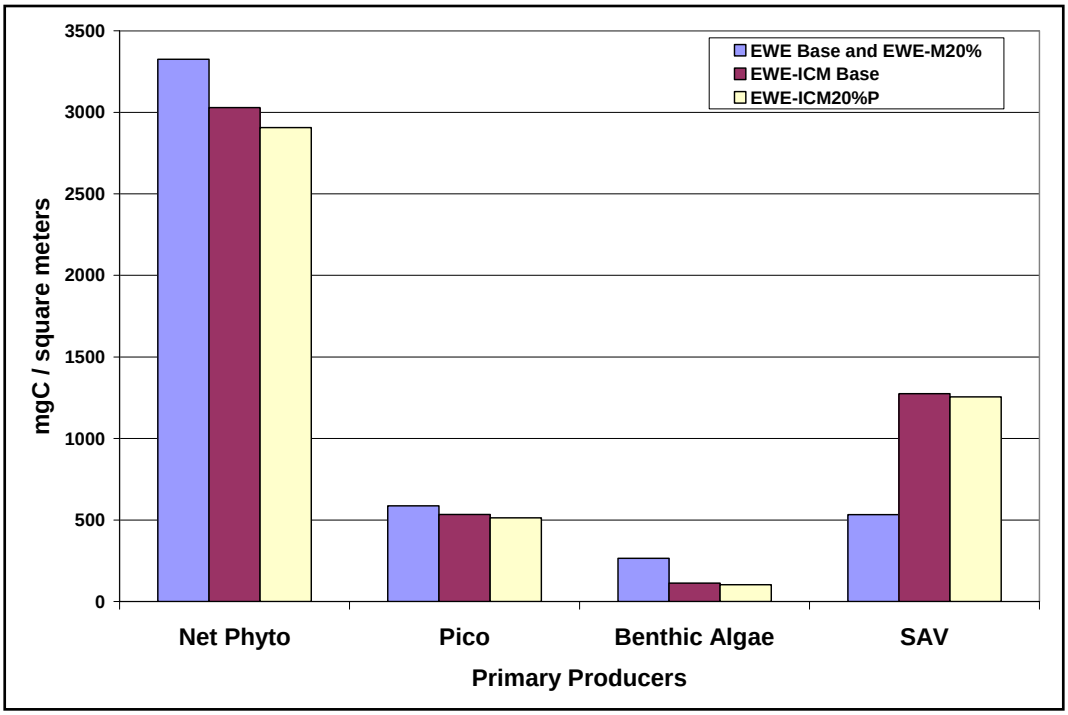

Figure 33. Primary producer biomass from EWE base and EWE-M20% (blue), EWE-ICM base (maroon), and EWE-ICM 20%P (light yellow) runs.

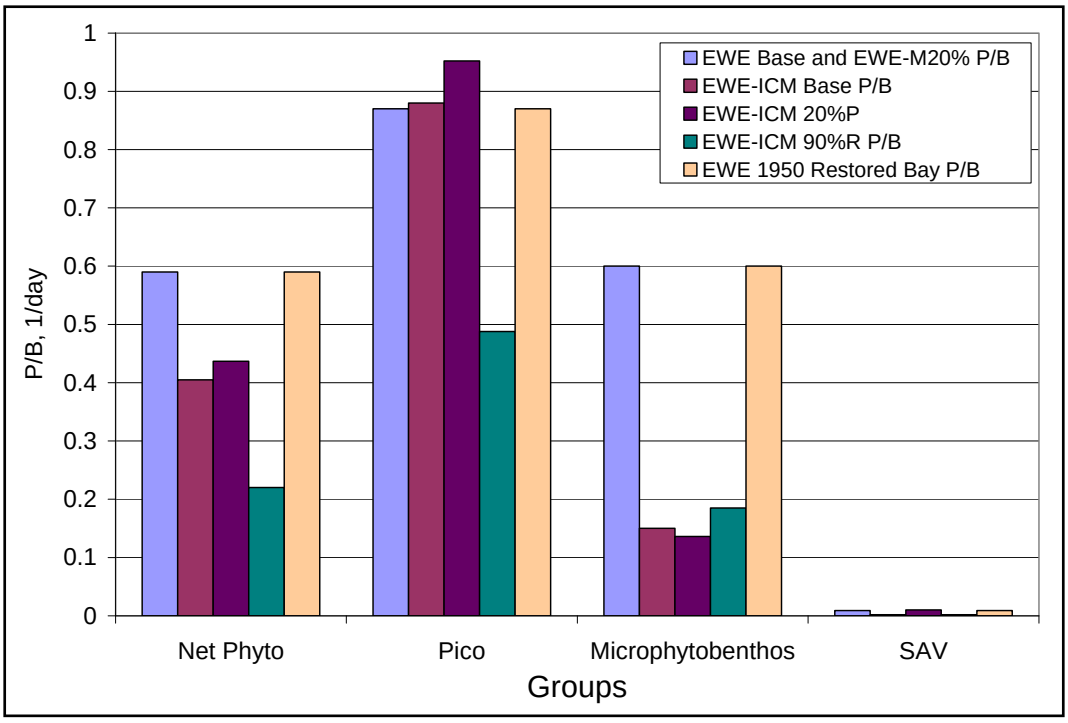

Figure 34. P/B ratios for primary producers all EWE runs.

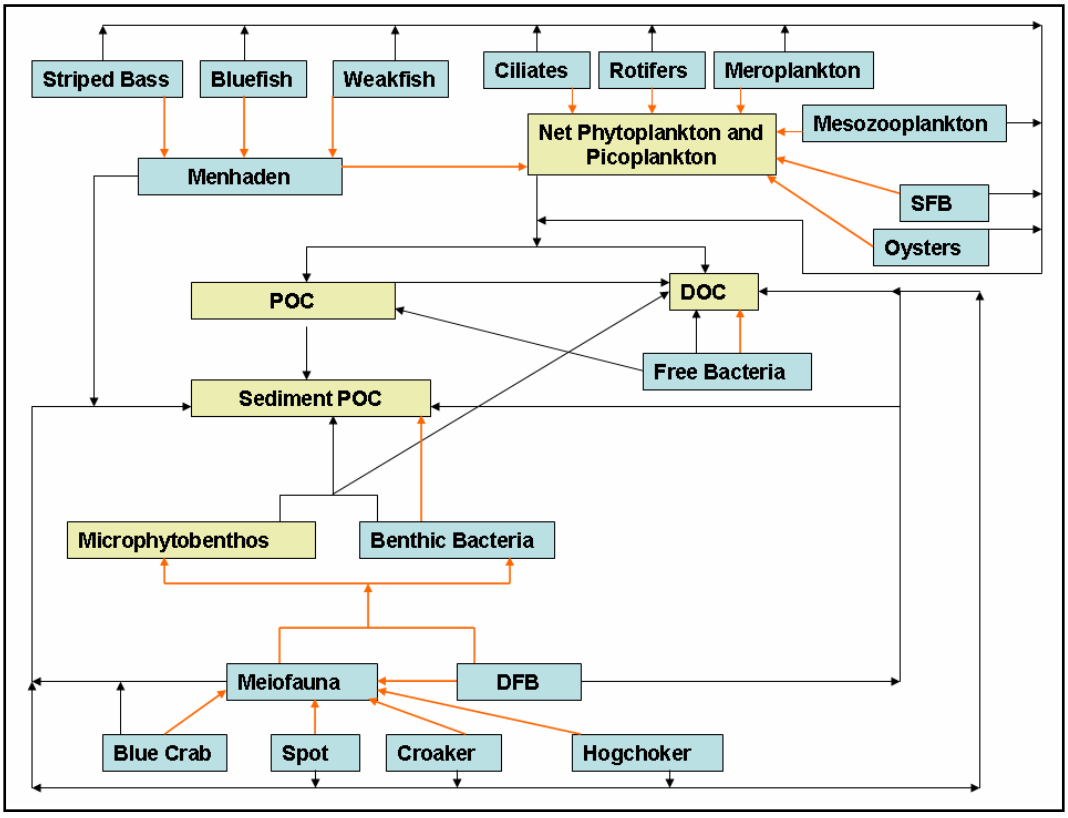

Figure 35. Network interactions through detrital flow (black arrows) and predators (orange arrows) of groups with EE > 1.

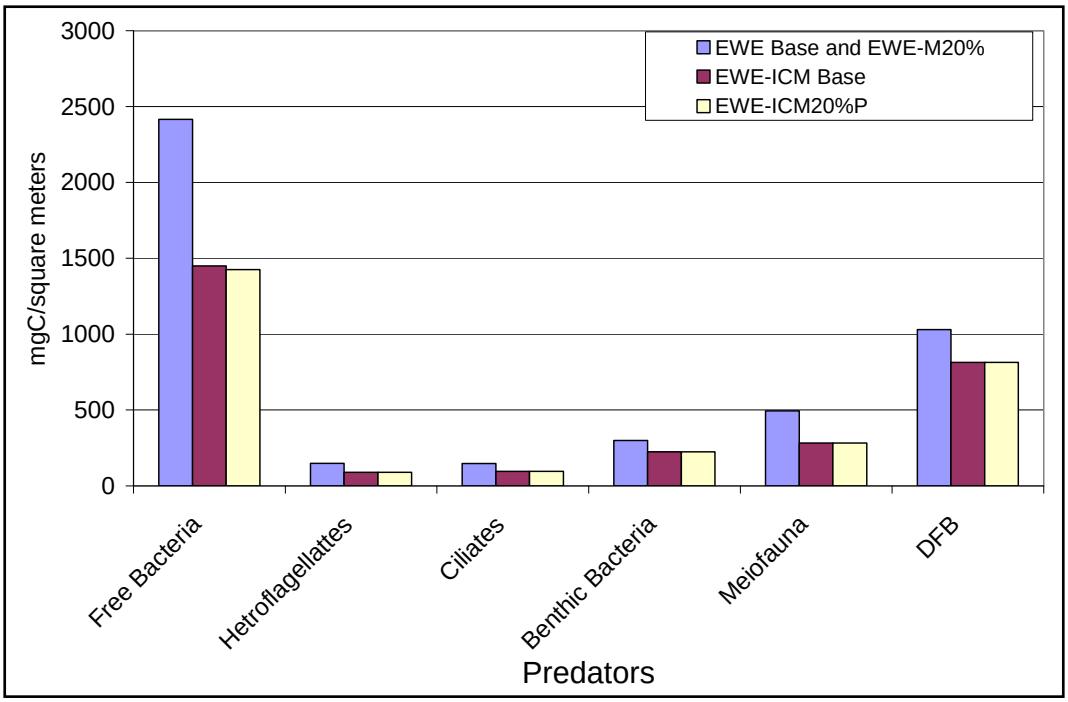

Figure 36. Adjusted predator biomasses of microphytobenthos, DOC, and sediment POC from the EWE base, EWE-ICM base, and EWE-M20% runs.

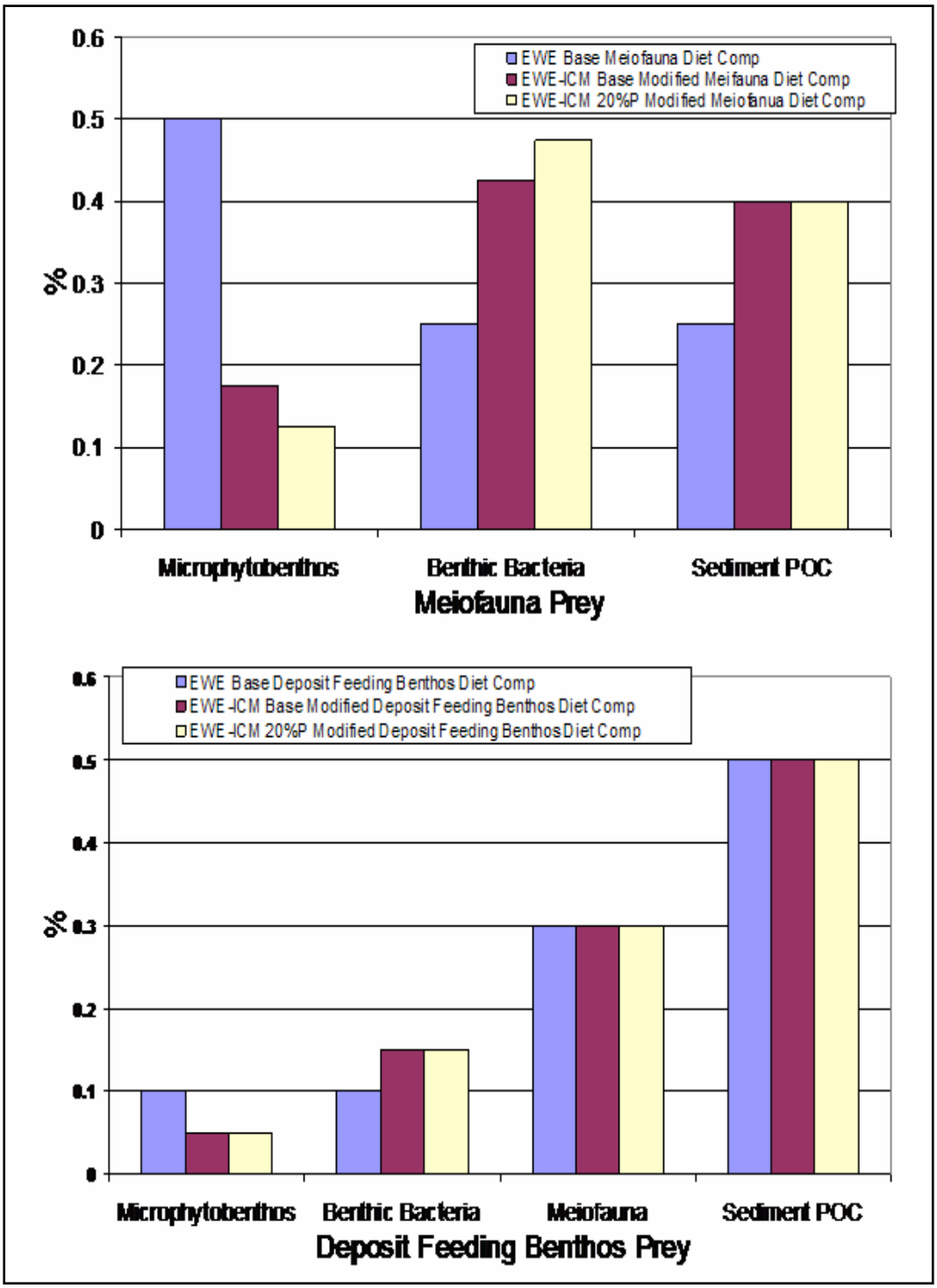

Figure 37. Diet composition adjustments to predators of microphytobenthos

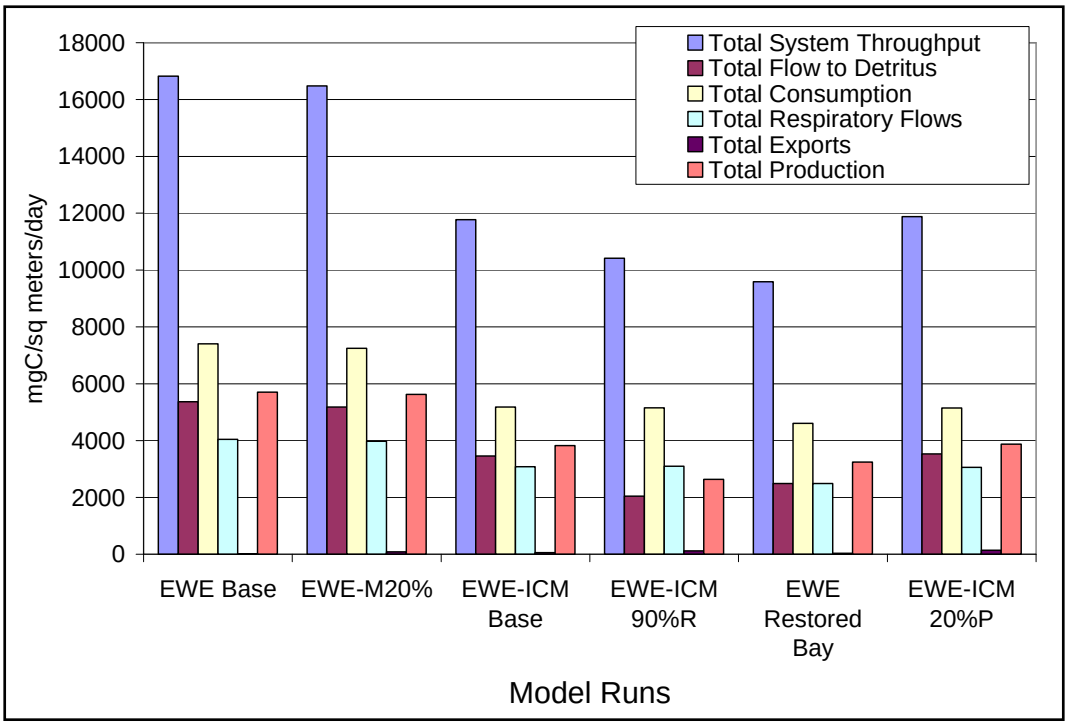

Figure 38. Sum of system production and TST including variables making up TST.

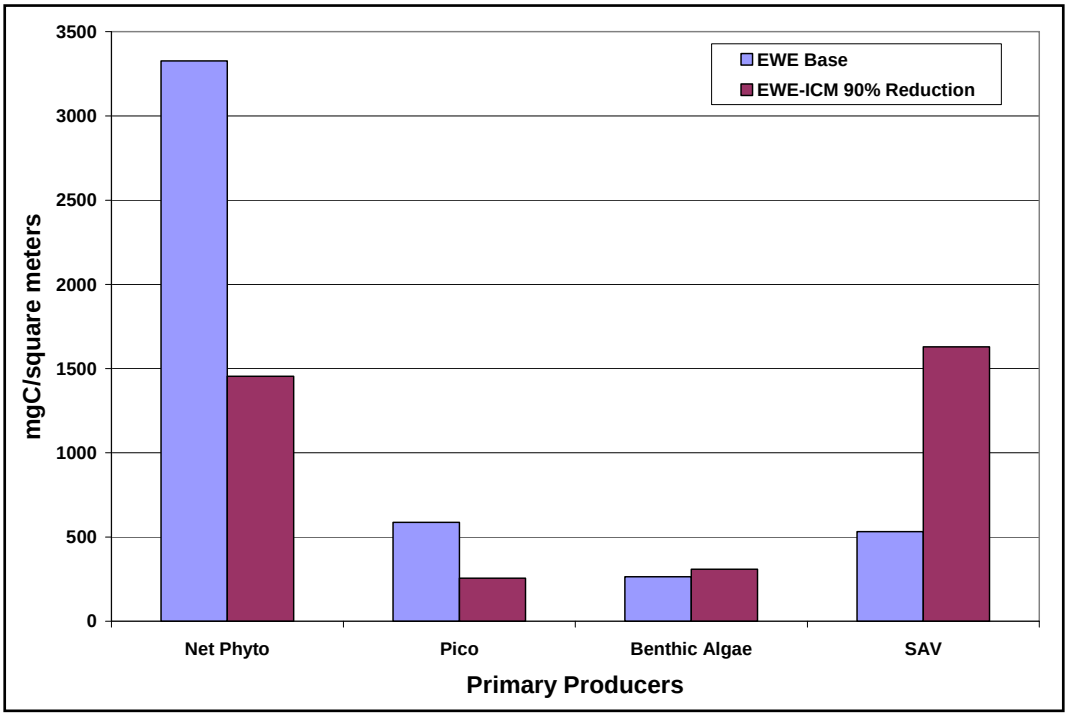

Figure 39. Primary producer biomass from EWE base (blue) and EWE-ICM 90%R (maroon) runs.

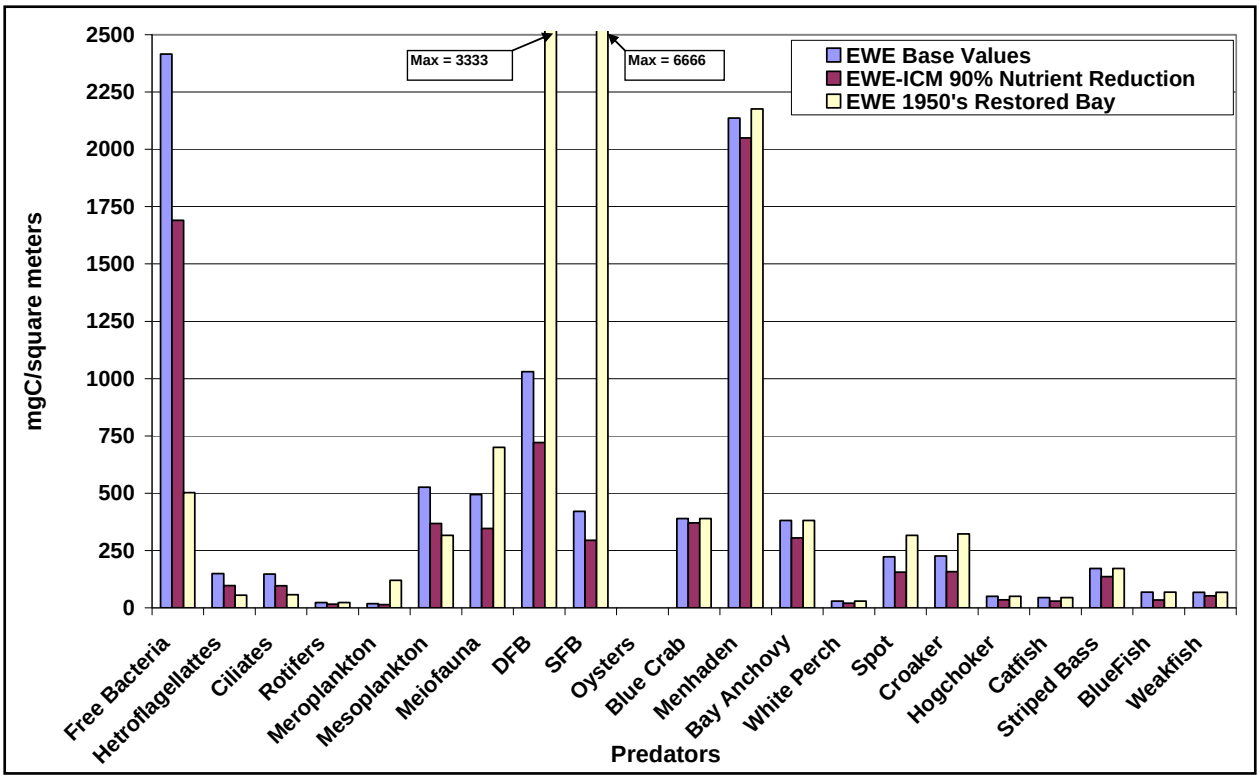

Figure 40. Predators of net phytoplankton in the EWE base (blue), EWE-ICM 90%R (maroon), and EWE 1950s restored bay (light yellow) runs.

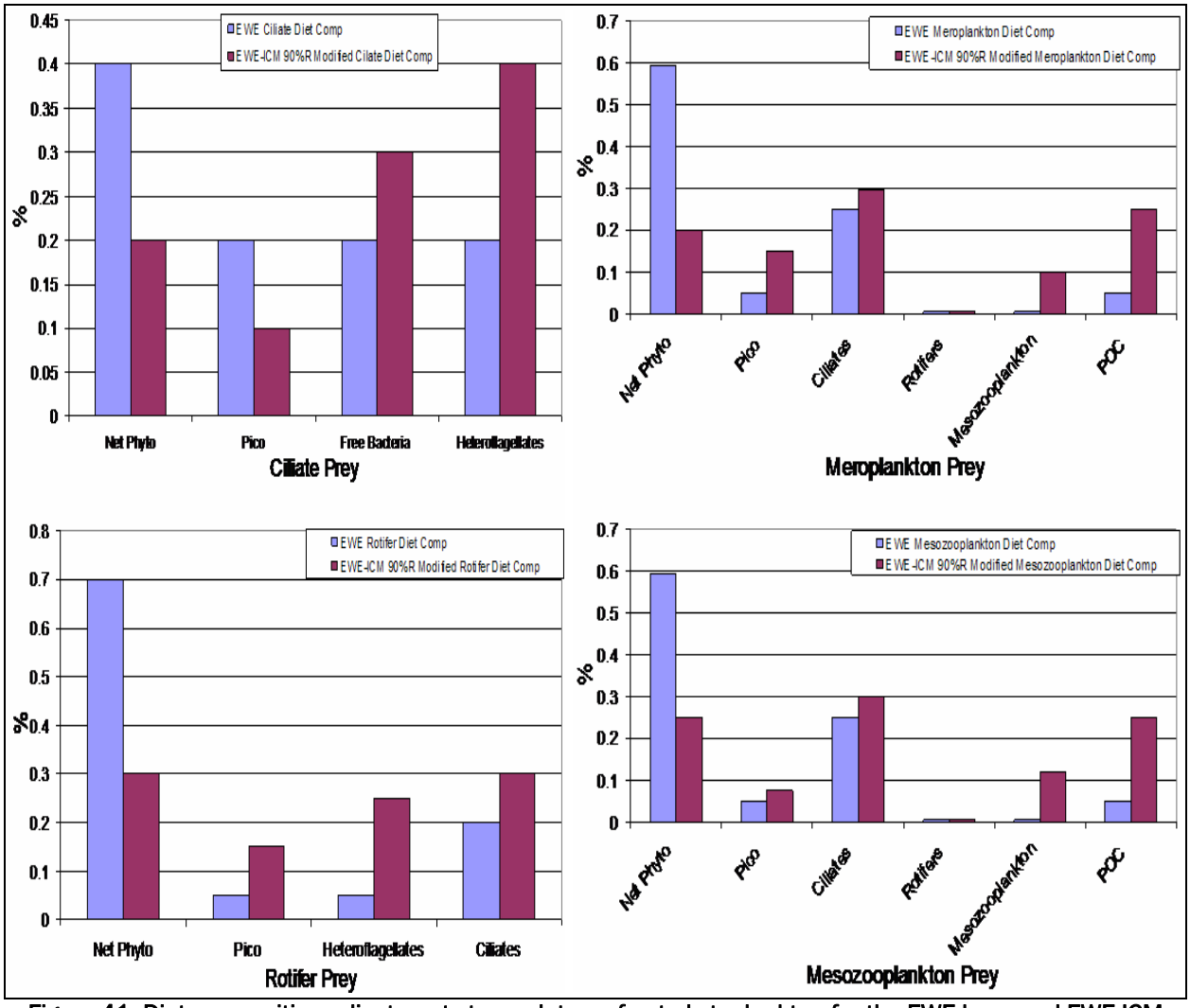

Figure 41. Diet composition adjustments to predators of net phytoplankton for the EWE base and EWE-ICM 90%R runs.

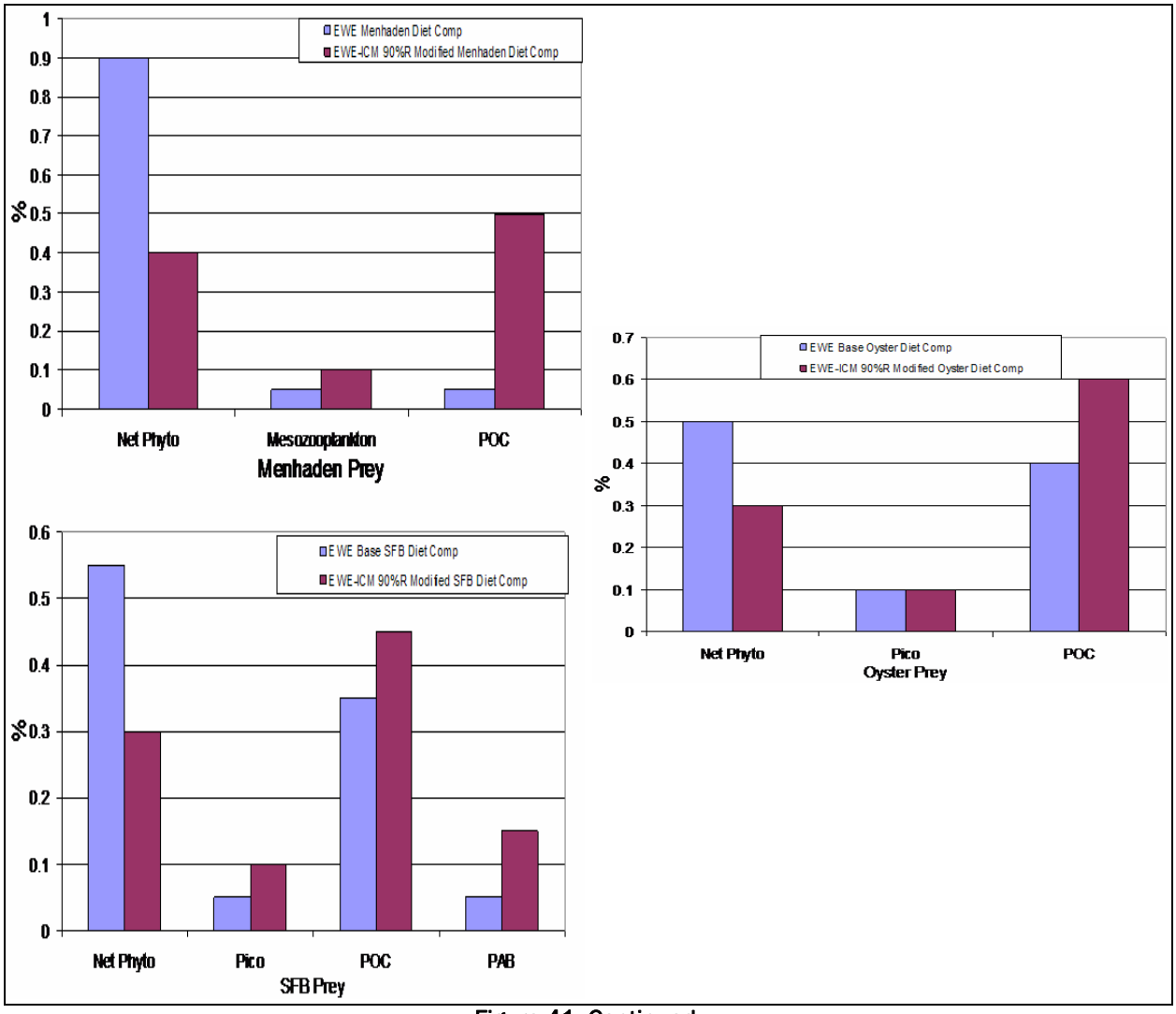

Figure 41. Continued.

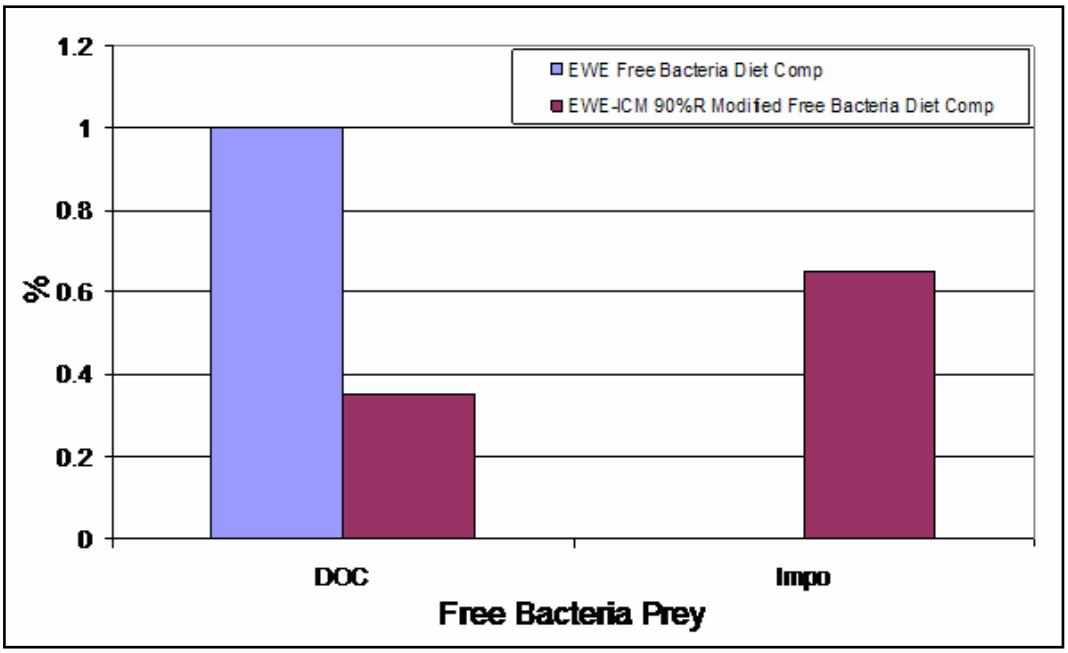

Figure 42. Diet composition modifications to predators of DOC.

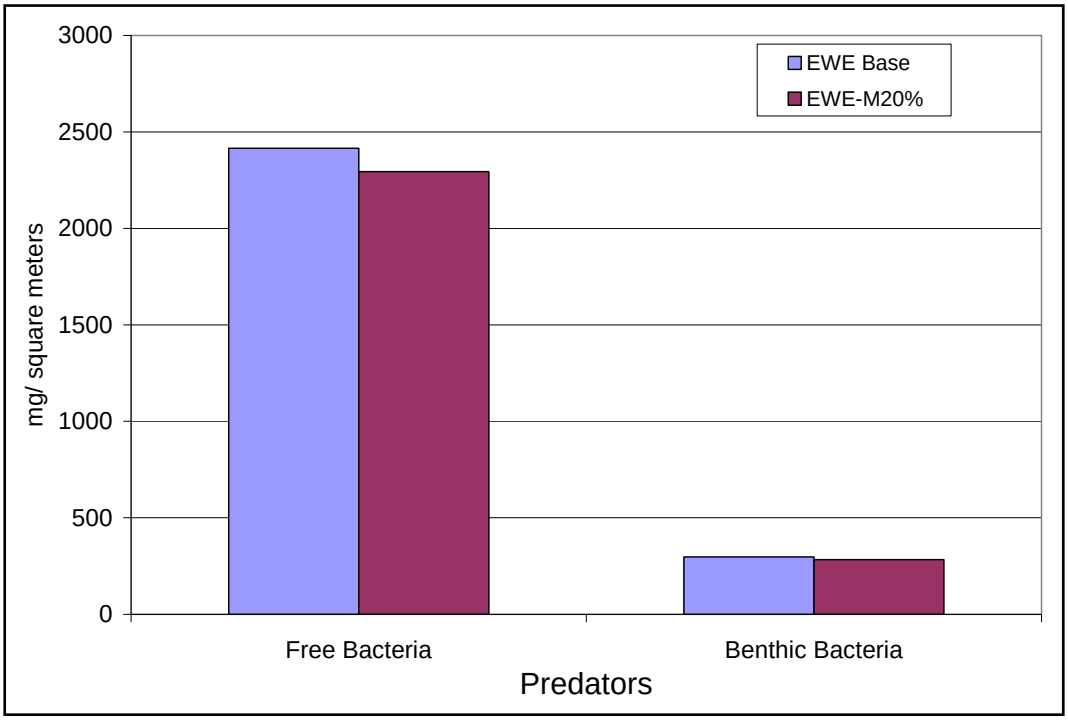

Figure 43. Diet composition modifications to predators of sediment POC.

Substituting ICM's primary producer biomasses and P/B ratios for EWE values and reparameterizing EWE produced some initial EEs > 1 for the following groups: microphytobenthos, dissolved organic carbon (DOC), and sediment particulate organic carbon (POC). Their EE values were 4.5,

1.35, and 1.16, respectively. These values indicate that all of these groups are being overutilized and that the model is not mass balanced. Figure 35 illustrates the interactions between groups with EEs > 1 and is only a small portion of the overall network of the groups modeled. In Figure 35, yellow boxes represent groups providing only detrital flow between groups; blue boxes represent groups providing detrital flow and/or predator/prey interaction with other groups. Additionally, black arrows indicate detrital flow pathways, while orange arrows indicate predator/prey interactions. Efforts to reduce the EEs began by reducing the biomass of their predators. EWE original predator biomass values were compared to the reduced values and are shown in Figure 36. Predator biomasses were reduced approximately 20–40%, depending on the effect to EE values. For DOC, the only predator was free bacteria (Figure 35). This group is in the lower trophic level II as calculated by EWE. Sediment POC had more predators [e.g., benthic bacteria, meiofauna, deposit-feeding benthos (DFB), blue crab, spot, croaker, hogchoker, and catfish] than DOC, but only the predator biomasses in the lower trophic level groups were modified (benthic bacteria, meiofauna, and DFB). Some of the same predators of sediment POC are also predators of microphytobenthos and included meiofauna and DFB. An iterative process of reducing predator values and reparameterizing EWE continued until all EEs of groups were reduced to less than one or until EEs of other groups became adversely affected. For example, meiofauna biomass was reduced so much that there was not enough meiofauna biomass to sustain all of its predators (i.e., DFB, blue crab, spot, croaker, and hogchoker; Figure 35); consequently, meiofauna EE increased to greater than one.

Reducing predator biomass helped reduce EEs for all groups except microphytobenthos. Although the EE for this group had not been reduced to less than one, its initial EE value had been reduced from 4.5 to 2.7. The difference between the original EWE base microphytobenthos biomass and the ICM biomass was so great that simply reducing the predator biomass was not enough to reach mass balance. To further reduce the EE of microphytobenthos, the diet compositions of its predators (again meiofauna and DFB) were modified as shown in Figure 37. By comparison, the diet composition of the meiofauna changed the most of the two predators. Originally 50% of meiofauna's diet came from microphytobenthos but was modified to 17.5%, with more of its diet coming from benthic bacteria and sediment POC. This seemed like a

reasonable change to diet composition since the preferred prey was no longer available or limited.

There were many options available to perform mass balance on the modified EWE-ICM base model, but in this study changes in lower trophic level groups were preferred over changes in upper trophic level groups unless it was necessary. This ensured that the original fish biomasses were maintained. Table 13 shows the total biomass of the system broken down by trophic level for the EWE base run and all modified EWE base runs. From the table, the majority of the total biomass is found in the lower trophic levels (i.e., trophic levels I, II, and III). In Table 13, the top three groups found in each trophic level are listed. Data in Table 13 also show changes in biomass distribution for all runs.

After mass balance was reached for the modified EWE-ICM base run, comparisons were made between system parameters for this run and the EWE base run. These parameters included such variables as total system throughput (TST), all variables making up TST, and the sum of all production. TST is defined as the size of the whole system in terms of flow (Christensen et al. 2004) and is found by summing total consumption, total export, total respiration, and total flows to detritus. Values of TST for the EWE-ICM base run were reduced by approximately 30% from 16,822 mg C m^{-2} day^{-1} (EWE base run) to 11,759 mg C m^{-2} day^{-1}. This reduction is also seen for the parameters making up TST except total export (Figure 37). Total export [defined by Christensen et al. (2004) as the part of production that is exported from or consumed by predators of the system] increased from 9.25 to 59.14 mg C m^{-2} day^{-1}. ICM net primary production rates for all primary producers were less than the values in the EWE base; this means that less carbon is produced. This is reflected in the sum of all production being 33% less for the EWE-ICM base run (Figure 38) than for the EWE base run. With less carbon production, there is less material to sustain the system as originally modeled.

ICM 90% Nutrient Reduction Primary Production Replaced in EWE Base Run

Replacing values of primary producers and P/B ratios in the EWE base run with ICM values from the 90% nutrient reduction run was an attempt to emulate the EWE 1950s restored bay run developed by Hagy. Differences between the EWE base values of primary producers and the EWE-ICM 90%R values are shown in Figure 39. Biomass values for net

phytoplankton and estimated picoplankton were less than about half the values set in the EWE base run. ICM's microphytobenthos biomass was slightly greater than the EWE base values, and again ICM's SAV biomass was more than double the EWE base values. Although net phytoplankton biomass was less than half the value set in the EWE base run, this group and SAVs were the most important of the primary producers based on biomass. Differences in P/B ratios (Figure 34) were also evident between the two runs. Values of net primary production rate from ICM were again less for all primary producers than values used by Hagy to calculate P/B for EWE.

Substituting ICM values of primary producer biomass and P/B ratios from the 90% nutrient reduction run in for the EWE base values and reparameterizing EWE produced EEs > 1 for a number of groups. These groups included net phytoplankton, picoplankton, microphytobenthos, DOC, and sediment POC. Their initial EE values were 2.86, 1.46, 1.34, 2.84, and 1.3, respectively. These were the same groups, with the inclusion of net phytoplankton and picoplankton, having EEs > 1 from the EWE-ICM base run. With biomass of net phytoplankton and picoplankton being half of the original values and all other groups remaining the same, producing EE values for these groups of greater than one is no surprise. Efforts to reduce the EE of these groups to re-establish mass balance began as before by reducing the biomass of their predators. Figure 40 shows the EWE base predator biomass values (blue) and the reduced values (maroon) from the EWE-ICM 90%R run. As before, changing lower trophic level groups was preferred over changing the upper trophic level groups so that the original fish biomasses could be maintained. Unfortunately, for this EWE run, upper trophic level groups had to be modified to re-establish mass balance. Net phytoplankton biomass from ICM was reduced so much from the original EWE value that reducing fish biomass could not be avoided. Its major predator biomass, menhaden, could be reduced only so much until its EE was affected. Consequently, there were not enough menhaden to sustain their predators (Figure 35). As discussed previously, all predator biomasses were reduced until EEs < 1 were re-established or the EE of other groups became adversely affected. After many iterations, all groups' EEs except net phytoplankton and DOC had been reduced to less than one. The EEs for these groups were still 2.115 and 2.579, respectively.

To further reduce the EE of net phytoplankton and DOC, diet compositions for a number of predators (Figures 41 and 42) were adjusted. Free bacteria were the only predator of DOC. There was only enough DOC biomass to provide 35% of its diet. For this reason, a DOC import of 65% was included to reduce the EE of DOC to less than one (Figure 42). In EWE, an import was considered consumption of a prey not part of the system (Christensen et al. 2004); for the EWE-ICM 90%R run, free bacteria are consuming DOC outside the system. In the same vein, Hagy had to import organic matter in the form of sediment POC and/or DOC for his EWE base run and 1950s restored bay run to get a balanced model. He identified his carbon source as resuspension of the spring algal bloom (Hagy 2002).

Getting a net phytoplankton EE < 1 proved to be more complicated than what had been done previously for the EWE-ICM base run. It was complicated in that many more iterations had to be made because of the complex interactions from changing the diets of so many predator groups (Figure 35). All of the predators came from the lower trophic levels of I, II, or III. The diet composition of each predator of net phytoplankton was shifted from net phytoplankton to other groups that were preyed on. Changes to diet compositions of all net phytoplankton predators are illustrated in Figure 41, which shows that of the predators, the menhaden diet composition changed the most. Originally 90% of menhaden's diet came from net phytoplankton but was modified to 40% with most of remaining diet being consumed from POC.

The value of TST for the EWE-ICM 90%R run is 10,417 mg C m^{-2} day^{-1}. This value is about 38% less than the EWE base run and about 10% more than the EWE 1950s restored bay run. The difference between TST values for the EWE base run and the EWE-ICM 90%R run was expected because the primary producer biomasses were reduced by about half in the EWE-ICM 90%R run and the net primary production rate was also lower. As a result, the sum of all production is also less than 50% (Figure 37). It was surprising to see that the TST was quite similar between the EWE 1950s restored bay run and the EWE-ICM 90%R run, since the total biomass (excluding detritus) for the EWE restored bay run was almost double that of the EWE–ICM 90%R run (Table 13). The difference in total biomass was attributed to EWE 1950s values for bottom dwellers [i.e., see in Figure 39, DFB and suspension feeding benthos (SFB)] and SAVs (see Figure 37) being set to very high concentrations compared to the EWE-

ICM 90%R run and even the EWE base run. In Hagy's EWE 1950s restored bay run, most other group values were set lower (some more so than others) than the EWE-ICM 90%R run or remained the same (Figure 39) with the exception of a few higher trophic level groups. They included menhaden, spot, and croaker. After Hagy made changes to the lower trophic level groups, he made changes to these groups by allowing EWE to solve for biomass rather than EEs.

Hagy set the SAVs biomass to the high value because the bay in the 1950s was clearer with more light penetration, thus stimulating more SAV growth. In addition, he points out that during this period there is more activity in the benthic community and, based on biomass measurements from similar regional areas, he set these groups' biomasses accordingly.

EWE Base Run with Menhaden Increased 20%

This EWE run was different from the others. There was no substitution of ICM values in EWE, only an increase in the original menhaden biomass in the EWE base run by 20%. All other group values remained the same. The same procedure was followed to balance the model; the new menhaden biomass was substituted into the input data, and EWE was reparameterized. By increasing menhaden biomass a slight imbalance of the system occurred. This was demonstrated by values of EEs being slightly greater than one for DOC and sediment POC. Their values were 1.01 and 1.002, respectively. With more menhaden preying on net phytoplankton, there is less of this group going to DOC and POC as detritus (Figure 39). Ultimately, there is less POC that goes to sediment POC and DOC. These groups seem to be sensitive to system changes since their EEs were greater than one in all modified EWE runs. This is probably because the original EEs were very close to 1 in the EWE base run; any small change to groups that interact with these groups produces EE > 1. Predator biomasses of DOC and sediment POC were reduced—free bacteria by 10% and benthic bacteria by 5% (Figure 43). Both predators are in the lower trophic level II as calculated by EWE. DOC and sediment POC EE values were so close to one that only one iteration was necessary to attain mass balance.

Increasing the menhaden biomass causes slight changes to the TST compared to the value from the EWE base run (Figure 37). The TST value for this run is 16,482 mgC/m^2/day, compared to 16,822 mg C m^{-2} day^{-1}. All values of parameters that make up TST have been reduced 3–5%

except total exports. The value of total export changed from approximately 9 to 80 mg C m^{-2} day^{-1}. Increased menhaden biomass seemed to have produced this change since menhaden are predators of net phytoplankton.

ICM 20% Increase in Predation Primary Production Replaced in EWE Base Run

For this run, ICM-generated values of primary producers and P/B ratios replaced values for these groups in the EWE base run. Increasing the predators by 20% in this ICM run was a way to imitate the EWE-M20% discussed previously, since higher trophic levels such as menhaden are not actually modeled in ICM. Increasing predation would be equivalent to increasing predator biomasses in EWE. Biomasses from this ICM run for the primary producers were slightly less for all groups when compared to the primary producer biomasses in the EWE base, EWE-M20%, and EWE-ICM base runs (Figure 33). As discussed above, the primary producer biomasses and P/B ratios of the EWE base and EWE-M20% were the same; thus the blue bar in Figure 33 represents both. In terms of biomass, net phytoplankton was again the most important primary producer. Differences in P/B ratios for primary producers of this run (Figure 34) were also noticeable when compared to values set in the EWE base/EWE-M20% and EWE-ICM base runs. Values of net primary production rate except for microphytobenthos used to calculate P/B ratios were higher for this ICM run (even though biomasses were lower) than the other ICM runs conducted. The reason for this could be because, with less net phytoplankton, picoplankton, and SAV biomasses, more nutrients become available, creating faster growth resulting in increased net production of these groups.

Substituting ICM's primary producer biomasses and P/B ratios in for the EWE values and reparameterizing EWE produced some initial EEs > 1 for microphytobenthos, DOC, and sediment POC. Their EE values were 5.45, 1.32, and 1.15, respectively, and were very similar to the initial EE values from the EWE-ICM base run. This being the case, predator values were initially reduced by the same amount (Figure 36) as the EWE-ICM base run. This was enough to produce EE < 1 for the sediment POC but not the DOC. Thus, free bacteria biomass (i.e., predator of DOC; see network interactions in Figure 35) was reduced slightly from this initial value to produce an EE value for DOC of less than one.

As discussed for the EWE-ICM base run, microphytobenthos predator biomasses of meiofauna and DFB could only be reduced so much before they started affecting the EEs of other groups. Following the procedure to reduce EE, the diet composition of microphytobenthos predators was modified as shown in Figure 37. For each predator it was set to values used in the EWE-ICM base run. Only the diet composition of meiofauna had to be modified slightly from these values; the diet composition of DFB was the same. By comparison, the diet composition of the meiofauna changed the most of the two predators. Originally 50% of meiofauna's diet came from microphytobenthos, but it was modified to 12.5%, with more of its diet coming from benthic bacteria and sediment POC.

Substitution of primary producers and P/B ratios from the ICM run with predation increased 20% into EWE results in a TST value that is quite different than the TST value resulting from the EWE-M20% run (Figure 38). The TST value for this run was 11,883 mg C m^{-2} day^{-1}, compared to 16,482 mg C m^{-2} day^{-1} for the EWE-M20% run. All values of variables making up TST are different as well. Most variables are less than those produced by the EWE-M20% run except for the total exports (142 versus 80 mg C m^{-2} day^{-1}, respectively). The results from this run most resemble the results from the EWE-ICM base run. With primary producer biomasses being slightly less for the EWE-ICM 20%P run compared to the EWE-ICM base run, it seems logical that they would produce similar results. The sum of all production (identified as Total Production in Figure 38) is also less for this run compared to the EWE-M20% run, but it is slightly more than the EWE-ICM base run. This occurs because nutrient availability increases the net production of the primary producers.

Conclusions

In general, the results from the three modified EWE-ICM runs indicate that some higher trophic level groups (i.e., blue crab, white perch, spot, croaker, hogchoker, and catfish) cannot be supported without adjustments to their prey biomasses and diet compositions. Although these higher trophic level groups have reasonable EEs, groups that provide some of their diet do not. Of the groups with EE greater than one, net phytoplankton, picoplankton, and sediment POC affected higher trophic level groups while microphytobenthos and DOC affected lower trophic level groups. The imbalance of the system for the three modified EWE runs was attributed to lower ICM primary producer biomass values (especially for net phytoplankton and microphytobenthos) and lower

values of ICM net primary production rates for all primary producers except for the EWE-ICM 20%P run.

Results from the EWE-M20% run do not indicate direct problems with higher trophic levels, but to maintain mass balance, changes to predator biomasses of lower tropic level groups were made. Adjustments to the diet composition of the predators were not necessary for this run. However, instead of changing predator biomasses, perhaps mass balance could have been achieved simply through diet modification of the predators.

When biomasses of the upper and lower trophic groups of the EWE 1950s restored bay run were compared to values from the EWE-ICM 90%R run, similar biomass reductions in the lower trophic level groups had been made (e.g., the values for free bacteria were 587 mg C m^{-2} from the EWE base run compared to 294 mg C m^{-2} for the EWE restored bay run and 256 mg C m^{-2} for the EWE-ICM 90%R run). However, changes in some lower trophic level group biomasses (i.e., SAVs, DFB, and SFB) for the EWE 1950s restored bay run were much greater than for the EWE-ICM 90%R run. This was attributed to Hagy assuming that the 1950s bay was cleaner with a much more active benthic community. This was based on data and observations in the literature from similar regional areas. From this, Hagy set values of SAVs and bottom dweller biomasses to reflect this difference from those that exist today. Although the biomasses for these groups from the EWE-ICM 90%R run were different, this run could represent what could happen if nutrients were reduced for present-day conditions in the mid CB.

7 Menhaden Scenarios

Introduction

One objective of this investigation is to compare ICM and Ecopath representations of conditions in Chesapeake Bay resulting from increased grazing on phytoplankton by menhaden. Procedures for the model runs were described in the preceding chapter. The present chapter provides a detailed examination of results from these runs and draws preliminary conclusions about the role of menhaden grazing on phytoplankton in Chesapeake Bay.

The ICM Response

The Predation Term

Predation on phytoplankton is the sum of activity from four predator groups: microzooplankton, mesozooplankton, other planktivores, and benthic invertebrates. Within the water column, predation is modeled by the equation:

$$PR = \frac{B}{KHsz + B} \times RMsz \times SZ + \frac{B}{KHlz + B} \times RMlz \times LZ + Phtl \times B^2 \quad (28)$$

in which:

PR = quantity of phytoplankton grazed (g C m^{-3} d^{-1})
B = algal biomass (g C m^{-3})
$RMsz$ = microzooplankton maximum ration (g algal C g^{-1} zoo C d^{-1})
SZ = microzooplankton biomass (g C m^{-3})
$KHsz$ = half saturation concentration for carbon uptake by microzooplankton (g C m^{-3})
$RMlz$ = mesozooplankton maximum ration (g algal C g^{-1} zoo C d^{-1})
LZ = mesozooplankton biomass (g C m^{-3})
$KHlz$ = half saturation concentration for carbon uptake by mesozooplankton (g C m^{-3})
$Phtl$ = rate of predation by other planktivores (m^3 g^{-1} C d^{-1}).

During the study, little information was available to quantify menhaden grazing, and no projections were available as to the amount by which

grazing may be increased. To simulate the effect of increased menhaden grazing, the parameter *Phtl* was increased by 20% over the base value used in model calibration. This increase was employed for "proof of concept." In a model of carrying capacity, Luo et al. (2001) assumed that menhaden consume 10% of primary production. Examination of the complete 12,000-cell ICM model indicated that 60–90% of computed predation was represented by other planktivores (Cerco and Noel 2004a). The ICM model, no doubt, assigns excess predation to the other planktivores at the expense of zooplankton. A 20% increase in predation by other planktivores in ICM is a large quantity relative to Luo et al.'s 10% estimate of production consumed by menhaden. Although the 20% increase is arbitrary, best evidence suggests that it represents a substantial increase in the grazing by menhaden.

Carbon Stocks

ICM results are first examined for the carbon stocks that are common between ICM and Ecopath (Table 14, Figure 44). As expected, phytoplankton decline in all regions of the bay, from less than 2% to nearly 8%. Other primary producers change as well. The greatest change is a 10% decrease in benthic algae in the mid and lower bay. This decrease appears to be related to increased light attenuation effected by increased particulate carbon in the water column, which is produced by increased grazing on phytoplankton. SAV declines in these regions, as well, apparently for the same reason, although the change is less than 1%. Alterations in light attenuation also influence benthic algae in the upper bay, although the change is in the opposite direction. Diminished particulate organic carbon leads to reduced attenuation and enhanced benthic algal biomass, ≈ 2%.

Table 14. ICM carbon stocks computed for two grazing rates.

	Upper Bay		Mid Bay		Lower Bay	
	Base ($g\ C\ m^{-2}$)	Increased Predation ($g\ C\ m^{-2}$)	Base ($g\ C\ m^{-2}$)	Increased Predation ($g\ C\ m^{-2}$)	Base ($g\ C\ m^{-2}$)	Increased Predation ($g\ C\ m^{-2}$)
Phytoplankton	3.13	2.88	2.93	2.88	2.41	2.374
Benthic Algae	0.25	0.252	0.21	0.19	0.19	0.172
SAV	3.89	3.868	1.94	1.927	3.16	3.149
Microzooplankton	0.12	0.111	0.35	0.363	0.27	0.28
Mesozoplankton	0.21	0.20	0.28	0.281	0.11	0.124
Deposit Feeders	0.42	0.423	0.31	0.303	0.34	0.335
Filter Feeders	2.98	2.818	0.75	0.793	0.00	0.00
DOC	18.95	19.24	14.47	15.7	10.55	11.25
POC	11.60	11.24	15.04	15.7	7.94	8.51
Sediments	971.00	1122	433.60	518	226.00	261.3

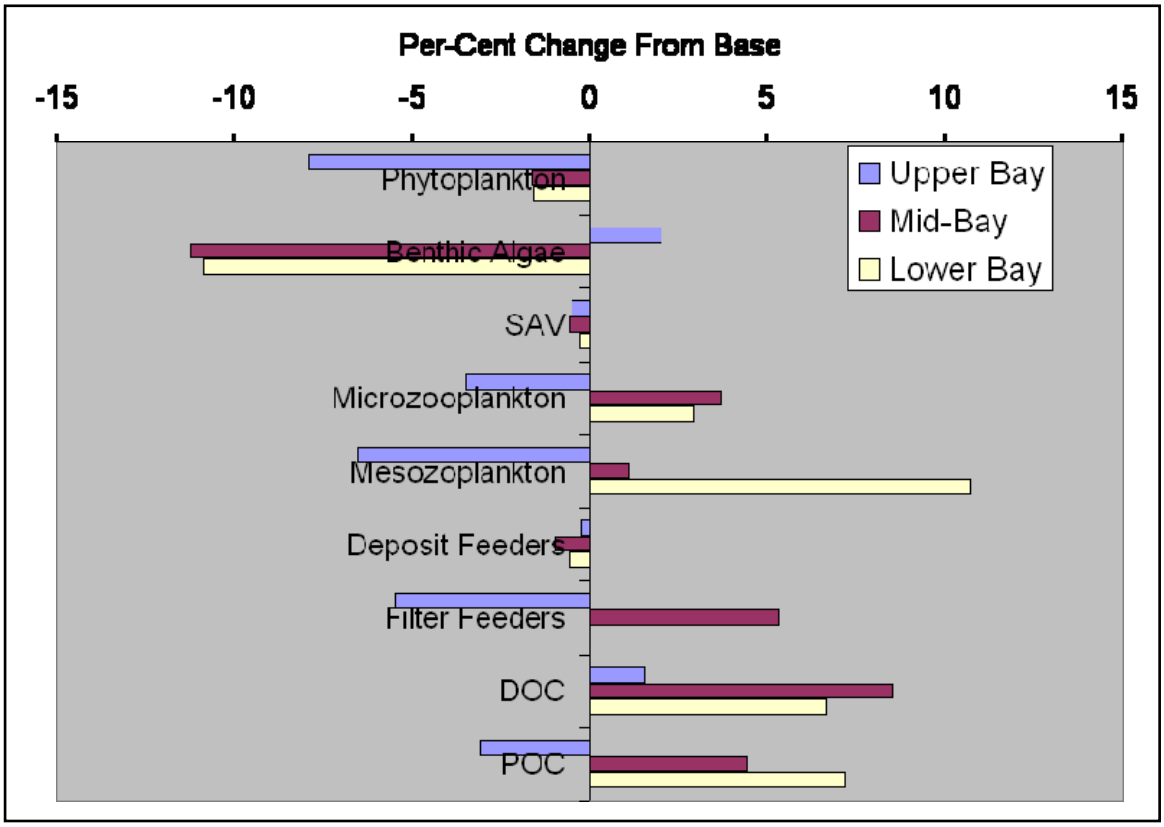

Figure 44. Percent changes in ICM carbon stocks resulting from 20% increase in grazing rate by other herbivores.

Production

The phytoplankton production-to-biomass ratio (P/B), or growth rate, increases when menhaden grazing is increased by 20% (Table 15). This response to alterations in the quadratic predation term has been noted previously (Cerco and Noel 2004a). Enhanced grazing releases nutrients and relaxes nutrient limitation on algal growth. Net carbon production, the product of growth rate and biomass, may increase or decrease as a function of grazing, depending on the changes in both growth rate and biomass (Table 16, Figure 45). In the upper bay, net phytoplankton production decreases; in the mid and lower bay, net phytoplankton production increases.

Changes in net production lend clarity to several of the changes in carbon stocks. Increased phytoplankton production, coupled with increased grazing, produces more detrital carbon in the mid and lower bay, resulting in increased light attenuation and detrimental effects on other primary producers. In the upper bay, diminished production produces less detrital carbon and decreased light attenuation, resulting in a small increase in benthic algal biomass. Despite the enhanced light environment, SAV biomass in the upper bay declines by a small amount, less than 1%. This decline can be explained by enhanced epiphyte production stimulated by greater nutrient availability, which is, in turn, stimulated by enhanced grazing on phytoplankton.

Table 15. ICM production/biomass ratios computed for two grazing rates.

	Upper Bay		Mid Bay		Lower Bay	
	Base (d^{-1})	Increased Predation (d^{-1})	Base (d^{-1})	Increased Predation (d^{-1})	Base (d^{-1})	Increased Predation (d^{-1})
Phytoplankton	0.603	0.629	0.480	0.523	0.295	0.32
Benthic Algae	0.222	0.223	0.193	0.184	0.145	0.128
SAV	0.032	0.032	0.010	0.01	0.006	0.006
Microzooplankton	0.017	0.018	0.003	0.006	0.001	0.001
Mesozoplankton	0.117	0.11	0.072	0.071	0.001	0.001
Deposit Feeders	0.084	0.084	0.065	0.067	0.046	0.047
Filter Feeders	0.001	0.001	0.001	0.001	0.000	0

Table 16. ICM production rates computed for two grazing rates.

	Upper Bay		Mid Bay		Lower Bay	
	Base ($g\ C\ m^{-2}\ d^{-1}$)	Increased Predation ($g\ C\ m^{-2}\ d^{-1}$)	Base ($g\ C\ m^{-2}\ d^{-1}$)	Increased Predation ($g\ C\ m^{-2}\ d^{-1}$)	Base ($g\ C\ m^{-2}\ d^{-1}$)	Increased Predation ($g\ C\ m^{-2}\ d^{-1}$)
Phytoplankton	1.885	1.812	1.405	1.506	0.712	0.760
Benthic Algae	0.055	0.056	0.041	0.035	0.028	0.022
SAV	0.124	0.124	0.019	0.019	0.019	0.019
Microzooplankton	0.002	0.002	0.001	0.002	0.000	0.000
Mesozoplankton	0.025	0.022	0.020	0.020	0.000	0.000
Deposit Feeders	0.036	0.036	0.020	0.020	0.016	0.016
Filter Feeders	0.003	0.003	0.001	0.001	0.000	0.000

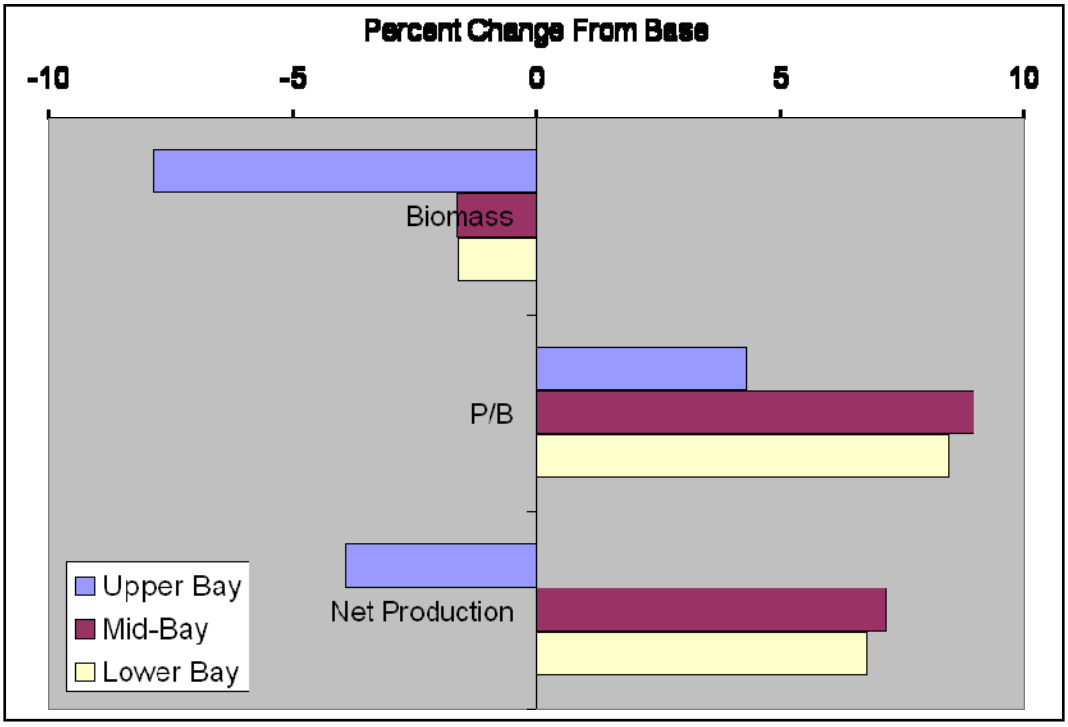

Figure 45. Percent changes in ICM algal biomass, production-to-biomass ratio, and net production resulting from a 20% increase in grazing rate by other herbivores.

In the mid and lower bays, grazer biomass (zooplankton and filter feeders) increases when menhaden grazing is increased (Table 14, Figure 44). The loss of phytoplankton prey to these grazers is more than compensated for by the availability of detrital carbon. Grazer biomass is related more to carbon production than to phytoplankton biomass. In the upper bay, the loss of both phytoplankton and particulate carbon results in diminished biomass of grazers. Deposit feeder biomass declines by a small amount,

less than 1%, bay-wide. This phenomenon has not been completely investigated. One hypothesis is that deposit feeders decline in response to diminished carbon production by benthic algae. This hypothesis does not explain diminished deposit feeders in the upper bay. There, however, the decline is the smallest in any region and is difficult to distinguish from numerical round-off in the computations and tabulations.

The Ecopath Response

A 20% increase in menhaden grazing was effected in Ecopath by increasing menhaden biomass in the representations of the bay's existing conditions. The system was then re-balanced as necessary, as described in the preceding chapter. The resulting biomasses show no change from existing conditions (Table 17). This result appears paradoxical. How can grazing increase with no resulting change in prey biomass? The result can be understood by noting that biomass is one of the basic inputs to Ecopath; biomass is not a computed output. When an increase in menhaden biomass is input, the computed Ecotrophic Efficiency must change, but the algal biomass will not change since this is an input constant. The increased menhaden biomass is compensated for by diminished computed flow from algae to detritus (Figure 46), which necessitates adjustments to the input biomass of detritivores in order to maintain Ecotrophic Efficiencies less than unity for all state variables (Table 18). These results indicate that the steady-state Ecopath model, alone, is not suited for addressing the issue of enhanced grazing by menhaden.

Table 17. Mid-bay ecopath carbon stocks for two menhaden biomasses.

	Ecopath Base (g C m^{-2})	Increased Menhaden (g C m^{-2})
Phytoplankton	3.91	3.91
Benthic Algae	0.27	0.27
SAV	0.53	0.53
Microzooplankton	0.19	0.19
Mesozoplankton	0.53	0.53
Deposit Feeders	1.52	1.52
Filter Feeders	0.42	0.42
DOC	28.20	28.20
POC	10.30	10.30
Sediments	201.70	201.70

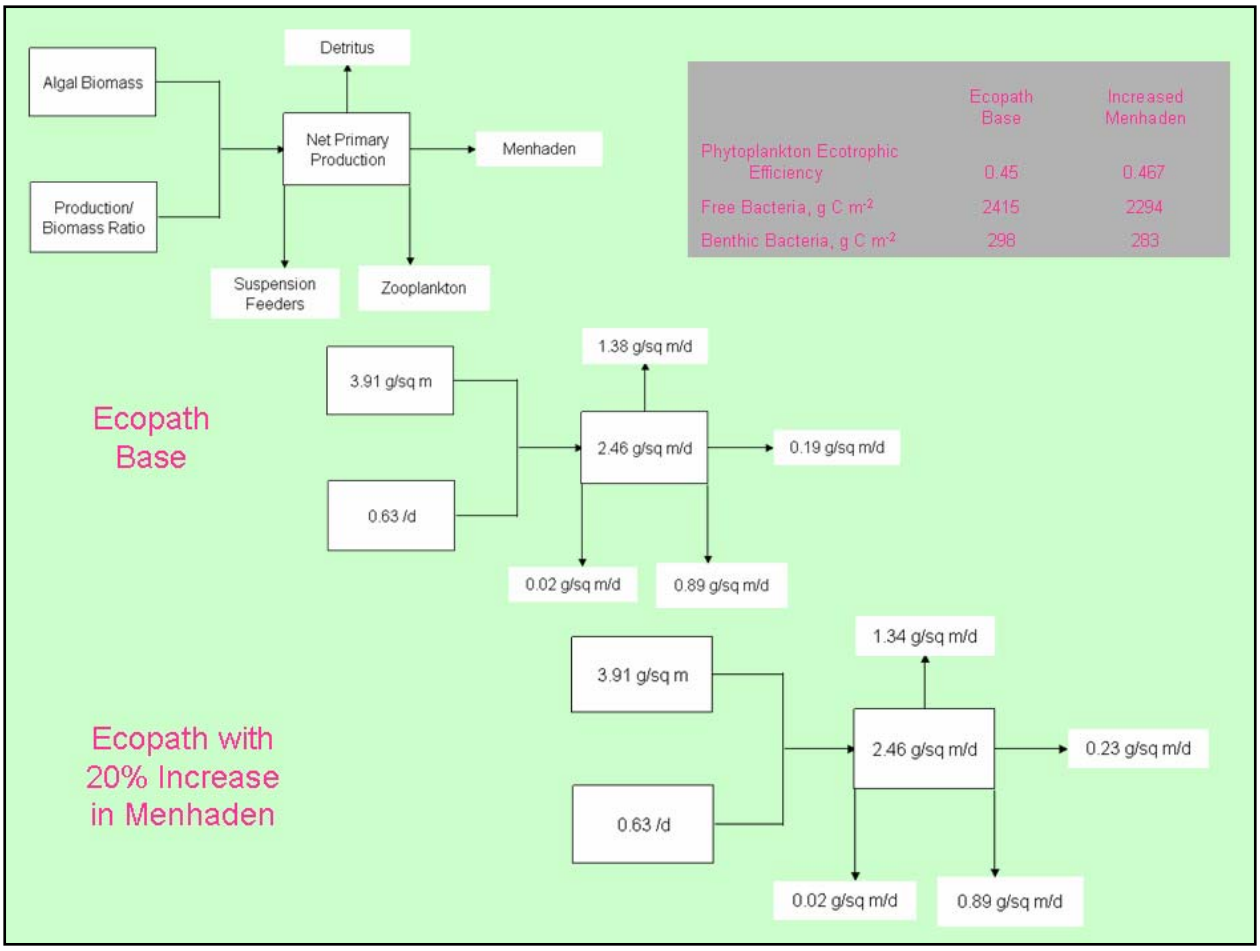

Figure 46. Distribution of algal production for two Ecopath applications to mid bay.

Table 18. Ecopath alterations required to accommodate increased menhaden biomass in the mid bay.

	Ecopath Base	Increased Menhaden
Phytoplankton Ecotrophic Efficiency	0.45	0.467
Free Bacteria (g C m^{-2})	2415	2294
Benthic Bacteria (g C m^{-2})	298	283

Combined Ecopath – ICM Approach

We propose an approach that combines Ecopath and ICM to address the issue of menhaden grazing. ICM is used to compute biomass and production rate of the primary producers and associated grazers for two scenarios: base and increased menhaden grazing. These values (Table 19) are input to Ecopath, which is used to examine the effects on living resources not computed in ICM. Ecopath models of the mid bay based on the two ICM runs show very little difference. In fact, the only parameter

that requires change is the "meiofauna diet fraction," forced by diminished benthic algae. In the face of diminished benthic algae, meiofauna obtain a greater fraction of their diet from sediment particulate organic carbon (Table 20).

Table 19. Mid-bay ICM carbon stocks input to Ecopath.

	ICM Base (g C m^{-2})	ICM Increased Predation (g C m^{-2})
Phytoplankton	3.56	3.42
Benthic Algae	0.11	0.103
SAV	1.28	1.255
Microzooplankton	0.14	0.137
Mesozoplankton	0.53	0.526
Deposit Feeders	1.10	1.095
Filter Feeders	0.42	0.421
DOC	28.20	28.20
POC	10.30	10.30
Sediments	201.70	201.70

Table 20. Alterations in mid-bay Ecopath model required to accommodate increased grazing in ICM.

	Base	Increased Predation
Meiofauna diet fraction from benthic algae	0.175	0.125
Meiofauna diet fraction from sediment POC	0.425	0.475

Conclusions

The steady-state Ecopath model, alone, is not suited to address the issue of increased grazing by menhaden. The major difficulty is that biomasses are input to Ecopath; they do not generally result from Ecopath computations.[1] Consequently Ecopath, alone, can be utilized only if the algal biomass resulting from enhanced grazing is known. Ecopath, alone, is also unsuited because it cannot compute effects such as altered nutrient recycling or light attenuation and the secondary effects from alterations in these primary forcing functions.

We have proposed a way in which ICM and Ecopath can be combined to address the issue of enhanced menhaden grazing. An Ecopath model was

[1] Biomass can be calculated if Ecotrophic Efficiency is input but this alternative is of no use in addressing this issue.

constructed using production rates and biomasses of primary producers and their grazers from ICM. A second Ecopath model was next constructed using ICM variables with enhanced grazing. Comparison of the two Ecopath models indicated changes in living resources not computed by ICM. In retrospect, detritus computed by ICM should have been input both Ecopath computations as well. This revision can be readily incorporated into future investigations of this issue.

Multiple lines of evidence from this preliminary investigation indicate that the environmental impacts of enhanced menhaden grazing are likely to be minor. Ecopath, alone, suggests minor impacts, although the resulting algal biomass cannot be estimated. Menhaden grazing, as represented in Ecopath, is a relatively small sink of algal biomass. A 20% increase in grazing represents a small increase in an already small number. ICM suggests that desirable decreases in phytoplankton, 2–8%, may be accompanied by increases in algal production due to enhanced nutrient recycling. Effects on nutrient cycling and light attenuation are computed that affect other ecosystem components. These alterations are on the order of a few percent and will be difficult to detect against the normal range of environmental variability. When Ecopath and ICM are coupled, the only resulting change, beyond those computed in ICM, is an alteration in meiofauna diet fraction. No changes are required in biomass of any higher trophic levels.

The effects described above may best be regarded as hypotheses, subject to further investigation, rather than conclusions. Comprehensive investigation of this issue requires:

- Quantitative evaluation of current menhaden biomass and grazing rates
- Projection of increased menhaden biomass
- Realistic representation of menhaden spatial and temporal distribution in ICM.

8 Summary and Conclusions

Study Objectives

The study reported here had the following objectives:

- Compare ICM and Ecopath representations of contemporary conditions in three regions of Chesapeake Bay.
- Compare ICM and Ecopath representations of conditions in mid Chesapeake Bay following nutrient load reductions to levels consistent with the 1950s.
- Compare ICM and Ecopath representations of conditions in three regions of Chesapeake Bay resulting from increased grazing on phytoplankton by menhaden.

CE-QUAL-ICM

The Corps of Engineers Integrated Compartment Water Quality Model (CE-QUAL-ICM, or simply ICM) was designed to be a flexible, widely applicable eutrophication model. The model incorporates 24 state variables in the water column that form groups or cycles, including a physical group, phytoplankton and zooplankton groups, and carbon, nitrogen, phosphorus, silica, and oxygen cycles. Multiple living resource groups are incorporated as well, including benthic algae, submerged aquatic vegetation (SAV), and filter-feeding and deposit-feeding benthos.

Ecopath with Ecosim

Ecopath with Ecosim (EWE) is a freely distributed network model supported by the Fisheries Centre, University of British Columbia. One existing application is of particular interest and forms the basis for this study. Ecopath was employed to represent summer conditions for three regions of Chesapeake Bay characteristic of the period 1985–1999. The model was next used to illustrate conditions in the mid bay consistent with nutrient loads of the 1950s to early 1960s. The application incorporated 34 state variables, including various forms of detritus, bacteria, primary producers, zooplankton, fish, and benthic invertebrates.

Linkage

ICM and Ecopath differ in their model currencies, nomenclature, and approach. The first step in coupling the two was to find variables and processes common to the two models. ICM code was created to transform quantities computed in ICM into quantities utilized in Ecopath. These were written to a unique file, which was subsequently post-processed to produced spatially and temporally aggregated quantities directly comparable to Ecopath.

Model Comparisons

Contemporary conditions in Chesapeake Bay, as represented by the two models, were first compared. Several distinct differences were noted:

- Phytoplankton primary production computed in ICM is highest in the upper bay and declines in the downstream direction away from the nutrient source. Planktonic production input to Ecopath is highest in mid bay and lower in both the upper and lower bay.
- Ecopath incorporates enormous biomass of benthic bivalve filter feeders in the upper bay, with lower concentrations in the mid bay. Ecopath includes the polychaeate *Chaetopterus* in the filter-feeding biomass of the lower bay. ICM computes higher bivalves in the upper bay than in the mid bay, but the disparity between the two regions is not as great as in Ecopath. ICM does not include *Chaetopterus* in the lower bay.
- Carbon flux across the sediment-water interface is a two-way process in Ecopath. Portions of organic carbon produced by benthic algae and excreted by invertebrates are returned to the water column. In contrast, carbon flux at the ICM sediment-water interface is in one direction only, to the sediments. No carbon is released to the water column from benthic primary production or excretion.

The ICM/Ecopath comparisons provide excellent guidance for revisions of processes in ICM. Complete consistency between the two models is unlikely to be attained, however. One barrier is that quantities input to Ecopath, such as primary production, must be computed from first principles in ICM. A second problem is that models such as ICM provide comprehensive, system-wide representations. Arbitrary, local variations in formulation or parameterization are avoided to the greatest extent possible. In contrast, the present Ecopath application is three independent

model applications. No unity is sought between the regions, so large differences can occur in parameter values and mass fluxes. Still the comparisons between the eutrophication model and the network model are most worthwhile and are recommended whenever an independent network model is available.

Ecosystem Projections

Two ICM scenarios were conducted for comparison with Ecopath. A 90% nutrient-reduction scenario was conducted for comparison with the Ecopath representation of the 1950s bay. Predation by higher trophic levels in ICM was increased by 20% and compared to Ecopath with menhaden biomass increased 20%. The comparisons were performed by substituting the ICM computed primary production into the Ecopath representations of the bay. The main concern in both scenarios was the impact on higher trophic levels of changes in computed primary production.

In general, the results from the ICM 90% nutrient reductions indicate that some higher trophic level groups (i.e., blue crab, white perch, spot, croaker, hogchoker, and catfish) cannot be supported without adjustments to their prey biomasses and diet compositions. The imbalance of the system was attributed to lower ICM primary producer biomass values (especially for the net phytoplankton and microphytobenthos groups) and the lower values of ICM net primary production rates.

The results from the menhaden scenario do not indicate a reduction in the biomasses of higher trophic levels. Changes were limited to biomass and diet composition of detritivores.

Menhaden Scenarios

Alternate approaches to the issue of menhaden grazing were considered, and results of the scenarios were examined in detail. We have proposed a way in which ICM and Ecopath can be combined to address the issue of enhanced menhaden grazing. An Ecopath model was constructed using production rates and biomasses of primary producers and their grazers from ICM. A second Ecopath model was next constructed using ICM variables with enhanced grazing. Comparison of the two Ecopath models indicated changes in living resources not computed by ICM. This preliminary investigation indicates that the environmental impacts of

enhanced menhaden grazing are likely to be minor. Substantial additional investigation is required to affirm this preliminary result, however.

Conclusions

This study was motivated by the lack of a single, comprehensive ecosystem model that encompasses trophic levels and organisms starting with primary producers and extending to the highest levels of predation. In the absence of a comprehensive model, management questions concerning the effects of nutrient load reductions on fisheries and the effects of fisheries management on primary producers cannot be answered. We have developed a process for combining the ICM eutrophication model and the Ecopath fisheries model that can be used to address these issues.

Perhaps the most valuable result of the present study was the comparison of the two model representations of the contemporary bay. Several disparities were noted, especially in benthic invertebrate biomass and sediment-water carbon fluxes. Adjustments to ICM to bring its representation closer to Ecopath will certainly lead to an improved ICM capability for predictive modeling of the bay.

Problems were noted as well, some originating with the nature of the comparisons and others originating in the Ecopath formulation. The largest problem originates with comparison of the time-variable ICM model with the steady state Ecopath model. Several seasonal trends in ICM could not be treated by Ecopath, notably negative accumulation of a state variable. ICM computed a decline in zooplankton biomass that was not accepted as Ecopath input. Other minor problems were that we could not input negative production (to produce a decline in biomass) nor were imports of any variables except detritus allowed. These problems did not have major detrimental impact on the study results, but they did cause difficulties until their exact nature was determined and solutions were derived.

The study has one more year to completion. The following efforts are recommended:

- At the start of this study, the Ecopath code was not distributed. The code is now available. The interface between ICM and Ecopath can now be fully automated in place of the present awkward combination of post-processing and data entry by hand.

- An Ecosim model of Chesapeake Bay is available. This multi-year time-variable product is much more suited to comparison with the time-variable ICM. We should obtain this model, master it, and commence interfacing with ICM.
- ICM was applied on a 4,000-cell grid created long ago to facilitate code development. Application on this grid is limited to hydrodynamics and loads that were available at the time it was created. The ICM application should be moved to a newer grid for which more extensive years of simulation are available.

References

Campbell, N.A. 1987. *Biology*. Redwood City, CA: The Benjamin/Cummings Publishing Company, Inc.

Cerco, C., and T. Cole. 1994. *Three-dimensional eutrophication model of Chesapeake Bay*. Technical Report EL-94-4. Vicksburg, MS: U.S. Army Engineer Waterways Experiment Station, Environmental Laboratory.

Cerco, C., and M. Noel. 2004a. Process-based primary production modeling in Chesapeake Bay. *Marine Ecology Progress Series* 282: 45–58.

Cerco, C., and M. Noel. 2004b. *The 2002 Chesapeake Bay eutrophication model*. EPA 903-R-04-004. Annapolis, MD: U.S. Environmental Protection Agency, Chesapeake Bay Program Office.

Cerco, C., and M. Noel. 2005. *Assessing a ten-fold increase in the Chesapeake Bay native oyster population*. Annapolis, MD: U.S. Environmental Protection Agency, Chesapeake Bay Program Office. www.chesapeakebay.net/modsc.htm.

Christensen, V., C. Walters, and D. Pauly. 2000. *Ecopath with Ecosim: A user's guide*. Vancouver, BC: University of British Columbia, Fisheries Centre.

DiToro, D., and J. Fitzpatrick. 1993. *Chesapeake Bay sediment flux model*. Contract Report EL-93-2. Vicksburg, MS: U.S. Army Engineer Waterways Experiment Station, Environmental Laboratory.

Hagy, J.D., III. 2002. *Eutrophication, hypoxia and trophic transfer efficiency in Chesapeake Bay*. Ph.D. diss. College Park, MD: University of Maryland.

HydroQual. 2000. *Development of a suspension feeding and deposit feeding benthos model for Chesapeake Bay*. Project No. USCE0410. Mahwah, NJ: HydroQual Inc. www.chesapeakebay.net/modsc.htm

Kavanagh, P., N. Newlands, V. Christensen, and D. Pauly. 2004. Automated parameter optimization for Ecopath ecosystem models. *Ecological Modelling* 172: 141–149.

Kemp, W., E. Smith, M. DiPasquale, and W. Boynton. 1997. Organic carbon balance and net ecosystem metabolism in Chesapeake Bay. *Marine Ecology Progress Series* 150: 229–248.

Kiely, G. 1997. *Environmental Engineering*. London, England: McGraw-Hill.

Leonard, B. 1979. A stable and accurate convection modeling procedure based on quadratic upstream interpolation. *Computer Methods in Applied Mechanics and Engineering* 19: 59–98.

Luo, J., K. Hartman, S. Brandt, C. Cerco, and T. Rippetoe. 2001. A spatially-explicit approach for estimating carrying capacity: An application for the Atlantic menhaden (*Brevoortia tyrannus*) in Chesapeake Bay. *Estuaries* 24(4): 545–556.

Ortiz, M., and M. Wolff. 2002. Trophic models of four benthic communities in Tongoy Bay (Chile): Comparative analysis and preliminary assessment of management strategies. *Journal of Experimental Marine Biology and Ecology* 268: 205–235.

Thompson, M., and L. Schaffner. 2001. Population biology and secondary production of the suspension feedeing polychaete *Chaetopterus* cf. *variopedatus*: Implications for benthic-pelagic coupling in lower Chesapeake Bay. *Limnology and Oceanography* 46(8): 1899–1907.

Tillman, D., C. Cerco, and M. Noel. 2006. Conceptual processes for linking eutrophication and network models. TN-SWWRP-05-x. Vicksburg, MS: U.S. Army Engineer Research and Development Center, Environmental Laboratory.

Westrich, J., and R. Berner. 1984. The role of sedimentary organic matter in bacterial sulfate reduction: The G model tested. *Limnology and Oceanography* 29: 236–249.

REPORT DOCUMENTATION PAGE

Form Approved
OMB No. 0704-0188

1. REPORT DATE *(DD-MM-YYYY)*	2. REPORT TYPE	3. DATES COVERED *(From - To)*
March 2008	Final report	

4. TITLE AND SUBTITLE

Use of Coupled Eutrophication and Network Models for Examination of Fisheries and Eutrophication Processes

5a. CONTRACT NUMBER

5b. GRANT NUMBER

5c. PROGRAM ELEMENT NUMBER

6. AUTHOR(S)

Carl F. Cerco and Dorothy H. Tillman

5d. PROJECT NUMBER

5e. TASK NUMBER

5f. WORK UNIT NUMBER

7. PERFORMING ORGANIZATION NAME(S) AND ADDRESS(ES)

Environmental Laboratory
U.S. Army Engineer Research and Development Center
3909 Halls Ferry Road
Vicksburg, MS 39180-6199

8. PERFORMING ORGANIZATION REPORT NUMBER

ERDC/EL TR-08-10

9. SPONSORING / MONITORING AGENCY NAME(S) AND ADDRESS(ES)

U.S. Army Corps of Engineers
Washington, DC 20314-1000

10. SPONSOR/MONITOR'S ACRONYM(S)

11. SPONSOR/MONITOR'S REPORT NUMBER(S)

12. DISTRIBUTION / AVAILABILITY STATEMENT

Approved for public release; distribution is unlimited.

13. SUPPLEMENTARY NOTES

14. ABSTRACT

The Corps of Engineers Integrated Compartment Water Quality Model (CE-QUAL-ICM or simply ICM) was designed to be a flexible, widely applicable eutrophication model. Ecopath with Ecosim (EWE) is a freely distributed network model supported by the Fisheries Centre, University of British Columbia. This study aimed to develop a coupling between the two models so that they could be used, in combination, to address management questions concerning the effects of nutrient load reductions on fisheries and the effects of fisheries management on primary producers. Specific objectives included: 1) comparing ICM and Ecopath representations of contemporary conditions in three regions of Chesapeake Bay; 2) comparing ICM and Ecopath representations of conditions in mid Chesapeake Bay following nutrient load reductions to levels consistent with the 1950s; and 3) comparing ICM and Ecopath representations of conditions in three regions of Chesapeake Bay resulting from increased grazing on phytoplankton by menhaden. Corresponding quantities in the two models were identified, and an ICM postprocessor was developed to facilitate the exchange of information between the two models. Significant differences were noted between the two model representations of contemporary primary production, benthic invertebrate biomass, and sediment-water organic carbon exchange. Substitution of ICM computed primary production from a 90% nutrient reduction scenario, intended to simulate loads in the 1950s, into Ecopath indicated that some higher trophic level groups (i.e., blue crab, white perch, spot, croaker, hogchoker, and catfish) cannot be supported without adjustments to their prey biomasses and diet compositions. Results of a similar procedure, intended to simulate enhanced menhaden grazing, did not require a reduction in biomasses of higher trophic levels.

15. SUBJECT TERMS

CE-QUAL-ICM
Chesapeake Bay
Coupled models
Ecopath
Ecosystem modeling
Eutrophication modeling
Menhaden

16. SECURITY CLASSIFICATION OF:			17. LIMITATION OF ABSTRACT	18. NUMBER OF PAGES	19a. NAME OF RESPONSIBLE PERSON
a. REPORT	b. ABSTRACT	c. THIS PAGE			19b. TELEPHONE NUMBER *(include area code)*
UNCLASSIFIED	UNCLASSIFIED	UNCLASSIFIED		116	